ELUCIDATING THE ROLE OF THE DUF 828 GENE FAMILY OF *ARABIDOPSIS THALIANA* IN AUXIN TRANSPORT

NEEMA PRABHAKARAN MARIYAMMA
Master of Science, Kerala Agricultural University, 2008
Bachelor of Science, Kerala Agricultural University, 2004

A Thesis
Submitted to the School of Graduate Studies
of the University of Lethbridge
in Partial Fulfilment of the
Requirements for the Degree

DOCTOR OF PHILOSOPHY

Biological Sciences
University of Lethbridge
LETHBRIDGE, ALBERTA, CANADA

© Neema Prabhakaran Mariyamma, 2015

ELUCIDATING THE ROLE OF THE DUF 828 GENE FAMILY OF *ARABIDOPSIS THALIANA* IN AUXIN TRANSPORT

NEEMA PRABHAKARAN MARIYAMMA

Date of Defense: December 15, 2015

Dr. Elizabeth Schultz Supervisor	Associate Professor	Ph.D.
Dr. James Thomas Thesis Examination committee member	Professor	Ph.D.
Dr. Steven Mosimann Thesis Examination committee member	Associate Professor	Ph.D.
Dr. Theresa Burg Thesis Examination committee member	Associate Professor	Ph.D.
Dr. Igor Kovalchuk Internal Examiner	Professor	Ph.D.
Dr. Ann Lacey Samuels External Examiner University of British Columbia British Columbia	Professor	Ph.D.
Dr. Roy Golsteyn Chair, Thesis Examination Committee member	Associate Professor	Ph.D.

DEDICATION

In the loving memory of my mother

ABSTRACT

The FORKED1 (FKD1) gene encodes a protein with a Domain of Unknown Function (DUF828) and a Pleckstrin Like Domain. The *Arabidopsis thaliana* genome contains 9 genes with a DUF828 domain whose function has never been characterized. FKD1 localizes to various BFA insensitive post-Golgi compartments and also forms a component of ARF mediated vesicle trafficking, supported by the colocalization of FKD1 with SFC/VAN3 (ARF-GAP) and ARF1 proteins. FKD1 colocalization with PIN1 suggests its role in PIN1 protein trafficking. Several DUF828 family members show colocalization with FKD1 suggesting their possible redundancy in vesicle trafficking pathway. I have identified four genes in the DUF828 family that act redundantly to establish vein meeting in root elongation and root gravitropism in Arabidopsis. PIN1 localization in the developing veins of triple mutants is highly defective indicating the role of the DUF828 family in establishing PIN1 polarity.

ACKNOWLEDGMENTS

Words fail to express my gratitude to Dr. Elizabeth Schultz, for her expertize, consistent guidance, patience and care she had for me during the period of my study and above all for offering me an opportunity to do research under her. I could not have imagined having a better advisor and mentor for my Ph.D. study. I would like to thank rest of my thesis committee members, Dr. James Thomas, Dr. Steven Mosimann and Dr. Theresa Burg for the insightful comments, valuable suggestions and encouragement.

Thanks to University of Lethbridge, Alberta Innovates Technology Future, School of Graduate Studies and Dept. of Biological sciences for giving me an opportunity to be a grad student and for the financial support. Thanks to Doug Bray, Grant Duke and Valerie for all the advise with confocal microscope. I would like to extend my heartfelt gratitude and appreciation to the people in Schultz lab, Ryan, Shankar, Jessica, Beadke, Chen, Chahat, Bianca, Emily, Vanessa, Houlin and everyone else who has helped me bring this study into reality. Thanks to everyone in Hepler Hall for being cooperative during the period of my study. Thanks to all the friends I have made in grad school for making grad life easy.

All appreciation and love to Lida for being there for me as a sister during my tough times. Thanks to all my friends Mohi, Lucy, Rachael, Brittany, Patrick, Alice, Aki, Corrine, Saabi and Lisiane for all the help, support and fun times. Thanks to Eddie for all the support, care and willingness to help me. Special thanks to Nunu

and Anas for giving me constant support, encouragement and good food. Thanks to Abhijt and family, Raja and family and Shankar and family for being there for me always. With boundless love and appreciation, my whole hearted gratitude to my best friend Sharma for moral support, precious friendship and for always standing by me. I could not thank enough my parents for the constant love and support. Finally, I would like to thank all people who contributed in some way or other during my grad life.

TABLE OF CONTENTS

APPROVAL/Signature Page....ii
DEDICATION....iii
ABSTRACT....iv
ACKNOWLEDGEMENTS....v
TABLE OF CONTENTS....vii
LIST OF TABLES....x
LIST OF FIGURES....xi
LIST OF ABBREVIATIONS....xiii
LIST OF GENE SYNONYMS....xv
CHAPTER 1: LITERATURE REVIEW....1
1. 1 Evolution of leaf vein architecture....1
1.2 Functional importance of leaf venation system....2
1.3 Auxin....2
1.3.1. Auxin biosynthesis....3
1.3.2 Auxin signaling....4
1.3.3 Auxin transport....6
1.3.3.1 Chemiosmotic model for polar auxin transport....6
1.3.3.2 Auxin efflux carriers....8
1.3.3.3 PIN proteins and their localization in different plant developmental processes....9
1.3.3.4 PIN1 localization during leaf vein formation....10
1.4 Vesicle trafficking mechanisms in plants....13
1.4.1. Transport from ER to GA....15
1.4.2 Transport from GA to other organelles....15
1.4.3 Trans-Golgi Network (TGN)/Early Endosome (EE)....16
1.5 Coat proteins in vesicle trafficking mechanisms....18
1.5.1 Role of coat GTPases in formation of a vesicle....19
1.5.2 Rab GTPase proteins and SNAREs in regulation of vesicle trafficking....21
1.5.3 GEFs and GAPs in vesicle formation and fusion....22
1.5.4 Phospholipids in regulation of vesicle trafficking....23
1.5.5 ARF-GEFs in PIN protein trafficking mechanisms....26
1.5.6 ARFs in PIN trafficking....30
1.5.7 ARF-GAPs in PIN protein trafficking....30
1.6 Regulation of PIN polarity by phosphorylation of PIN1 proteins....33
1.7 FORKED1 (FKD1)/VAN3-BINDING PROTEIN (VAB) gene....34
CHAPTER 2: MATERIALS AND METHODS....39
2.1 Seeds....39
2.2 Growth Conditions of *Arabidopsis thaliana* and *Nicotiana tabacum*....39
2.3 Bacterial constructs....40
2.4 Preparation of competent *Escherichia coli* and *Agrobacterium tumifaciens*....42
2.5 Transformation into *Escherichia coli* or *Agrobacterium tumifaciens*....43

2.6 Transient transgene expression in *N. tabacum* 44
2.7 Transformation of *Arabidopsis* by floral spray method 45
2.8 Generation lines expressing compartment specific markers 46
2.9 Introduction of FKD1-GFP into mutant lines 47
2.10 Identifying DUF828 domain evolution in plant kingdom 47
2.11 Identification of plants homozygous for T-DNA insertions 48
2.12 Generation of multiple mutant lines between members of DUF828 gene family 49
2.13 Generation of stable transgenic mutant lines expressing PIN1GFP 49
2.14 Confocal imaging and analysis 50
2.15 BFA, FM4-64 treatment and plasmolysis experiments 51
2.16 Leaf vein characterization of T-DNA insertion mutants 51
2.17 Analysis of epidermal cell shape and polarity 52
2.18 Root and shoot phenotypic analysis of mutant lines 53
2.19 Statistical analysis 54
CHAPTER 3: RESULTS 58
3.1 FKD1 localization pattern changes during development stages 58
3.2 FKD1-GFP localization is altered in *cvp2cvl1* mutants 59
3.3 FKD1 colocalizes with PM markers 60
3.4 FKD1 colocalizes with multiple endosomal markers 61
3.4.1 FKD1-GFP colocalizes with endocytic marker FM4-64 at the PM 62
3.5 FKD1 colocalizes with SFC/VAN3 (ARF-GAP) 63
3.6 SFC colocalizes with makers of endomembrane compartments 63
3.7 FKD1 and SFC punctae are partially insensitive to BFA 65
3.8 FKD1 colocalizes strongly with ARF1 proteins 66
3.9 FKD1 and SFC/VAN3 colcalize with PIN 68
CHAPTER 4:RESULTS 86
4.1 Evolution of Pleckstrin –Like/DUF 828 family in the plant kingdom 86
4.2 Phylogenetic analysis of Arabidopsis DUF828 gene family 88
4.3 DUF828 gene family members show variable localization to Golgi 89
4.4 DUF 828 gene family members colocalize with FKD1 91
4.5 Mutations to DUF 828 gene family members enhance the *fkd1* leaf vein pattern phenotype 92
4.5.1 PIN1: GFP expression and localization is defective in triple (*fkd1/fl2/ fl3)* mutants 94
4.6 General defects in plant development 98
4.6.1 DUF 828 gene family alters leaf number and flowering time 98
4.6.2 DUF 828 gene family bract affects leaf and bract architecture 99
4.6.2.1 DUF 828 gene family affects epidermal cell morphogenesis 100
4.6.2.1.1 Cell area and dimensions 100
4.6.2.1.2 Cell shape and elongation 101
4.6.2.1.3 DUF 828 gene family influences polarity of epidermal pavement cells 102
4.7 DUF 828 gene family affects the growth rate of primary roots 103
4.8 PIN1 localization is not defective in the root tissues of triple mutants 104
CHAPTER 5: DISCUSSION 137
5.1 FKD1 localizes to the PM and throughout the post-Golgi endosome 137

5.2 FKD1 localizes to SFC/VAN3 (ARF-GAP) and ARF proteins 140
5.3 FKD1 and SFC play a role in vesicle trafficking of PIN1 proteins 143
5.4 FKD1 localization is influenced by PI(4)P 145
5.5 DUF828 gene family acts redundantly to control leaf vein patterning 147
5.6 FKD1 gene family affects root elongation processes 149
5.7 DUF 828 gene family controls leaf morphology through polarity specific elongation of cells 150
5.8 Evolution of DUF 828 domain containing proteins 152
CHAPTER 6: CONCLUSIONS AND FUTURE DIRECTIONS 156
REFERENCES 160
APPENDIX I 178

LIST OF TABLES

Table 2.1: Primers used in PCR reactions for identifying T-DNA insertions and sequencing of constructs with pnigel 7 55
Table 2.2: Gene name and position of T-DNA insertions in Salk lines 56
Table 3.1: Correlation of expression between the intensities of FKD1-GFP or SFC-YFP together with different proteins fused to YFP or RFP 70
Table 3.2: Correlation of expression between FKD1-GFP or SFC-YFP and FM4-64 labeled vesicles at different time interval 71
Table 4.1: Domain organization of of DUF 828 (IPR00856), Pleckstrin like domain (PL; IPR013666) and Pleckstrin Homology domain (PH; IPR001849) in the DUF828 gene family members. 106
Table 4.2: Correlation of expression between the intensities of members of DUF 828 gene family fused to YFP with ST-RFP or SYP61-CFP. 107
Table 4.3: Correlation of expression between the intensities of FKD1-GFP with members of FKD1 gene family fused to YFP. 108
Table 4.4: Area and vein characteristics of 14DAG cotyledons from various genotypes. 109
Table 4.5: Area and vein characteristics of 21DAG first leaves from various genotypes. 110
Table 4.6: Frequency of non-meeting secondary veins (second and third set) in wild type and triple mutant. 111
Table 4.7: Percentage of wide PIN1GFP expression domains (PED) at different developmental stages of second and third 2° veins in wild type and triple mutant first leaves. 112
Table 4.8: PIN1GFP localization at developmental stages of second and third set of 2° veins in wild type and triple mutant first leaves. 113
Table 4.9: Comparison of phenotypic characters between various genotypes 114
Table 4.10: Comparison of gravitropic response in different genotypes 115

LIST OF FIGURES

Figure 1.1: Schematic representation of PIN1 localization, auxin maxima and vein formation during successive stages of leaf vein development in *Arabidopsis thaliana*... 37
Figure 1.2: Schematic representation of phospholipid metabolism in plants 38
Figure 2.1: Genotyping of double mutants using PCR..... 57
Figure 3.1: Cellular FKD1-GFP localization differs at different stages of cotyledon development..... 72
Figure 3.2: Subcellular localization of FKD1-GFP in wild type and in *cvp2cvl1* and *PI4Kβ1β2* mutant cotyledons..... 73
Figure 3.3: Subcellular localization of FKD1-GFP with PM markers. 74
Figure 3.4: Subcellular localization of FKD1-GFP with Golgi and Trans-Golgi markers. 75
Figure 3.5: Subcellular localization of FKD1-GFP with endosome markers. 76
Figure 3.6: Colocalization of FKD1-GFP with FM4-64 at different time intervals. 77
Figure 3.7: Subcellular localization of FKD1-GFP or SFC-YFP with either ST-RFP or SYP61-CFP. 78
Figure 3.8: Colocalization of SFC-YFP with FM4-64 at different time intervals. 79
Figure 3.9: Subcellular localization of FKD1-GFP or SFC-YFP after BFA treatment..... 80
Figure 3.10: Subcellular localization of FKD1-GFP with SFC-YFP without and with BFA treatment. 81
Figure 3.11: Subcellular localization of FKD1-GFP with ARF1 proteins and ARFA1c with Golgi marker, ST-RFP. 82

Figure 3.12: Subcellular localization of FKD1-GFP or SFC-YFP with PIN1-RFP 84
Figure 3.13: Subcellular localization of FKD1 with PIN1 after BFA treatment 85
Figure 4.1: Phylogenetic tree of DUF 828-domain sequences from diverse species in plant kingdom and of DUF 828 encoding genes in *Arabidopsis thaliana*..... 116
Figure 4.2: Multiple sequence alignment of DUF 828 and PL/PH domain sequence of DUF 828 gene family. 118
Figure 4.3: Subcellular localization of FKD1 with DUF828 gene family members with ST-RFP in Nicotiana and of FL3 with SYP61-CFP in stably transformed Arabidopsis..... 120
Figure 4.4: Subcellular localization of FKD1 with DUF 828 gene family members in Nicotiana and of FL3 with FKD1 in stably transformed Arabidopsis. 122
Figure 4.5: Vascular patterns of cotyledons of various genotypes at 14DAG 124
Figure 4.6: Vascular patterns of first leaves of various genotypes at 21DAG 125
Figure 4.7: PIN1:GFP expression in the developing second set of secondary veins in wild type and triple mutant (*fkd1/ fl/2x fl/3*) 126
Figure 4.8: PIN1:GFP expression in the developing third set of secondary veins in wild type and triple mutant (*fkd1/ fl-2/ fl-3*) 127
Figure 4.9: PIN1 expression in LLD of 3rd secondary veins showing PIN1-GFP localization 128

Figure 4.10: Adult plant phenotype of various genotypes..... 129
Fig 4.11: Adaxial and abaxial view of entire fifth leaves and SEM micrographs of fifth leaf epidermal pavement cells of various genotypes. 130
Fig 4.12: Adaxial and abaxial view of entire second bracts and SEM micrographs of second bract epidermal pavement cells of various genotypes 131
Figure 4.13: Graphs representing the cell length of epidermal pavement cells on adaxial and abaxial sides of second bracts. 132
Figure 4.14: Cell polarity of epidermal pavement cells on abaxial and adaxial sides of second bracts..... 133
Figure 4.15: Primary root growth of Arabidopsis seedlings assessed over 24h..... 134
Figure 4.16: Gravitropic response showing the angle of root tip divergence from 0-6h of seedlings of various genotypes at 5DAG 135
Figure 4.17: PIN1 trafficking is not altered in wild type and triple mutant roots.... 136

LIST OF ABBREVIATIONS

A. tumifaciens = Agrobacterium tumefaciens
ABA = Abscisic Acid
ABCB/PGP = ATP binding cassette/P-glycoprotein (ABCB/PGP)
ABP1 = AUXIN BINDING PROTEIN1 (ABP1)
AFB = AUXIN SIGNALING F-BOX PROTEIN
AGD = Arf GAP domain proteins (AGD)
Arf = ADP- Ribosylation Factor
ARF = Auxin Response Factor
AUX1/LAX = Auxin Resistant1/Like Aux1
BAR = Bin Amphiphysin- Rvs
BEN1 = BFA- VISUALIZED ENDOCYTIC TRAFFICKING DEFECTIVE
BEX1 = BFA-VISUALIZED EXOCYTIC TRAFFICKING DEFECTIVE
BFA = Brefeldin A
BiFC = Bimolecular fluorescence complementation (BiFC)
CCV= clathrin coated vesicle
CFP = Cyan Fluorescent Protein
COP = Cytoplasmic Coat Protein
CVL1 = COTYLEDON VASCULAR PATTERN 2 LIKE1
CVP2 = COTYLEDON VASCULAR PATTERN 2
DAG = Days After Germination
DBD = DNA BINDING DOMAIN
DNA =Deoxyribonucleic acid
dNTP = deoxynucleotide triphosphates
DUF828 = Domain of Unknown function
DV = Dense vesicle
E.coli = Escherichia coli
ECM = extra cellular matrix
EE = Early Endosomes
FKD1 = FORKED1
FL1 = FORKED LIKE1
FLS2 = FLAGELLAR SENSING 2
FM4-64= (*N*-(3-Triethylammoniumpropyl)-4-(6-(4-(Diethylamino) Phenyl) Hexatrienyl) Pyridinium Dibromide
GA = Golgi Apparatus
GAP = GTPase-activating protein
GBF = Golgi BFA Resistance factor
GEF = Guanine nucleotide exchange factors
GFP = Green Fluorescent Protein
GGG = Gea/GBF/GNOM
GNL1= GNOM LIKE1
GUS = β-GLUCORONIDASE
HL = Hydrophilic loop
IAA = indole-3-acetic acid

IBA = indole butyric acid
LE = Late Endosomes
LLD = Lower Loop Domain
MVB = Multi-vesicular bodies
N. tabacum = Nicotiana tabacum
NPSN1 = NOVEL PLANT SNARE 12
OD = Optical Density
PA = phosphatidic acid
PAT= polar auxin transport
PC = pavement cells
PCC = Pearson's coefficient of correlation
PEDs = PIN1 Expression Domains
PH = Pleckstrin Homology
PL = Pleckstrin Like
PI = Phosphoinositides
PID = PINOID
PIN = PIN FORMED
PIP = phosphorylated phosphatidylinositols
PIP1;4 = Plasma membrane Intinsic Protein 1
PM = Plasma membrane
PP2AA = protein phosphatase 2AA
PVC= Prevacoular compartments
Ras = Ras related Nuclear
RE = Recycling Endosome
RFP = Red Fluorescent Protein
ROPs = Rho of plants
SAR1 = Secretion-Associated Ras1
SCF = SKP1/CULLIN/F-BOX PROTEIN
SEM = Scanning electron microscope
SFC = SCARFACE
SNAREs = Soluble *N*-ethylamide-sensitive factor Attachment protein Receptors
SNX = Sorting Nexin
ST = sialyl transferase
SYP = Syntaxin of Plants
T-DNA = Transfer -DNA
TGN = Trans Golgi Network
TIR = Transport Inhibitor Response
UI = Undulation Index
ULD = upper loop domain
VI = Vascular Islands
VTI12 = VESICLE TRANSPORT V-SNARE 12
WT = wild type
YFP = Yellow Fluorescent Protein

LIST OF GENE SYNONYMS

ARF1 = ARF1A1c/BEX1
BIG5=MIN7
FKD1=VAB
FKD2=SFC/VAN3
RabF2b = ARA7

CHAPTER 1: LITERATURE REVIEW

1. 1 Evolution of leaf vein architecture

In plants, leaves are the major organs that are involved in the perception of light and conversion of solar energy into organic carbon. During the process of evolution, plants have developed leaves of certain shapes and forms in order to adapt to various environmental factors and to maximize life strategies and propagation (Malinowski, 2013). In the Devonian and early Carboniferous periods, plants with fern-like leaves (ferns, progymnosperms and gymnosperms) appear to have had an open venation pattern, characterized by the bifurcation of veins. This primitive architecture of open venation served as a base for the evolution of modern network-like venation patterns across different lineages (Roth-Nebelsick et al., 2001). In Angiosperms, dicots exhibit a characteristic hierarchical network pattern with small veins emerging from larger veins and small veins forming a closed reticulum. On the other hand, monocots exhibit a parallel venation with vein connections occurring near the leaf blade base and apex and small commissural veins forming a reticulum (Dengler and Kang, 2001). The evolution of multiple vein orders might have occurred to i) increase the efficiency of structural support ii) distribute water potential more evenly throughout the leaves and iii) create redundancy of transport pathways thus reducing the deleterious effects caused by insects and other damage (Feugier and Iwasa, 2006; Zwieniecki, et al., 2002).

1.2 Functional importance of the leaf venation system

The architectural properties of leaf venation can be correlated with its two main functional aspects: transport of water and solutes and mechanical stabilization. The two primary vascular tissues in leaf veins are xylem and phloem. Xylem is mainly involved in the transport and storage of water, nutrients and hormones from the root to the above ground tissues. The hormones transported by xylem are abscisic acid (ABA), cytokinins and strigolactones (Robert and Friml, 2009). Carbohydrates, produced in the assimilating tissue of a leaf, are transported through phloem. Phloem is also involved in the transport of mRNA, proteins and hormones like ABA and cytokinins. (Sack and Scoffoni, 2013). The other function, mechanical stabilization, based on the lignified xylem and sclereid elements, is associated with the conducting bundle system of a leaf (Roth-Nebelsick et al., 2001). Although the molecular mechanisms responsible for the patterning of leaf venation are not fully understood, the role of the phytohormone auxin in vascular differentiation has been well documented.

1.3 Auxin

The phytohormone auxin plays a significant role in plant growth and development. In plants, the predominant active form of auxin is Indole Acetic Acid (IAA). Auxin regulates diverse cellular and developmental processes in plants including cell division, cell polarity and morphogenesis (Friml et al., 2003), cell expansion, cell differentiation (Fukuda, 2004), cytoskeletal organization,

intracellular membrane trafficking (Paciorek et al., 2005), pattern formation, organogenesis (Weijers et al., 2006), apical dominance and tropic response to light and gravity (Reed et al., 2001; Woodward and Bartel, 2005). Auxin possesses highly efficient self-organizing and self-regulating properties, which characterize auxin action at a cellular, tissue and whole plant level (Benjamins and Scheres, 2008). Auxin mediated plant development is mainly orchestrated by the concerted action of three components: i) sites of auxin biosynthesis to create a source ii) auxin transport to generate gradients and iii) auxin perception or response to effect developmental processes (Chandler, 2009).

1.3.1. Auxin biosynthesis

Auxin pools are mainly composed of conjugated auxin, free auxin, the inactive auxin precursor Indole Butyric acid (IBA) and the inactive methyl form of IBA. Auxin conjugates are considered as temporary reservoirs of inactive auxin. Auxin conjugates are grouped into two classes; a low molecular weight group consisting of sugar esters and amide conjugates to amino acids and a high molecular weight group comprising amide conjugates to peptides and proteins (Bajguz and Piotrowska, 2009). The conjugate forms of auxin are usually inactive and are converted into active forms by their hydrolysis. The composition of IAA conjugates varies between plant species. IAA is primarily stored as amide-linked amino acid conjugates in *Arabidopsis* and most of the dicot species (Korasick et al., 2013).

Auxin biosynthesis in plants is extremely complex and multiple pathways contribute to its production, which is supported by the identification of genes and

enzymes involved in the pathway. The production of auxin is highly localized and auxin biosynthesis plays a significant role in shaping local auxin gradients (Stepanova et al., 2008). Traditionally, it was considered that auxin biosynthesis is located in the aerial plant parts like young developing leaves and meristems (Ljung et al., 2001), but it has been demonstrated that local auxin biosynthesis also occurs in other tissues like the meristematic region of the primary root and tips of the emerged lateral root (Ljung et al., 2005).

Auxin biosynthesis occurs mainly by a tryptophan dependent pathway and a tryptophan independent pathway (Chandler, 2009). In the tryptophan dependent pathway, tryptophan is the precursor for IAA biosynthesis. Tryptophan is synthesized in the chloroplasts from chorismate via indole-3-glycerol phosphate. The molecular components of Trp-independent pathway have not been identified, however, indole-3-glycerol phosphate or indole serves as the precursor in that pathway (Zhao, 2012).

1.3.2 Auxin signaling

Auxin, both transcriptionally and non-transcriptionally,,is capable of controlling the physiological auxin response of specific cells. Auxin regulates the transcription of auxin response genes through the action of TRANSPORT INHIBITOR RESPONSE1 (TIR1)/ AUXIN SIGNALING F-BOX PROTEIN (AFB) (F-box proteins), Auxin/INDOLE-3-ACETIC ACID (Aux/IAA) transcription repressors and auxin response factors (ARFs). One of the best-studied molecular pathways for auxin signaling involves the targeted degradation of transcriptional repressors within the

Aux/IAA family (Chapman and Estelle, 2009).

Aux/IAA proteins can alter ARF-regulated gene expression by interacting with ARF proteins and altering their activity. Under low auxin concentrations, AUX/IAA repressors heterodimerize with ARFs and act as transcriptional repressors, thereby blocking the transcriptional activation of auxin–responsive genes (Hayashi, 2012). Auxin relieves ARF repression by promoting degradation of Aux/IAA transcriptional repressors via the proteasomal pathway, thereby promoting the ubiquitination of Aux/IAA proteins (Hayashi, 2012). Intracellular auxin is perceived by the TIR1 protein or closely related proteins, the AFB receptors. Auxin acts as molecular glue and stabilizes the interaction between TIR1/AFB and Aux/IAA proteins. TIR1/AFB is an integral component of the SKP1/CULLIN/F-BOX PROTEIN (SCF) ^{TIR1} complex that eventually mediates the ubiquitination of AUX/IAAs and thereby destines them for 26S proteasome-dependent degradation (Abel, 2007). The degradation of Aux/IAAs directly or indirectly changes the transcription of thousands of genes. The direct targets are genes with Auxin Response Elements in their promoters that are bound by the ARFs. Upon their auxin-induced degradation, ARFs are freed to form ARF-ARF dimers, which can activate or repress transcription and thereby regulate the expression of auxin-responsive genes.

In addition to the Aux/IAA-AFB auxin-signaling pathway, one additional route for auxin signaling is the transcription independent pathway, which involves auxin perception by AUXIN BINDING PROTEIN1 (ABP1). ABP1 functions as a

receptor for auxin perception at the plasma membrane (PM) or extracellular matrix (ECM) and is involved in auxin responses like cell elongation (Badescu and Napier, 2006).

1.3.3 Auxin transport

Long-range and short-range auxin transport occurs through different mechanisms. Long-range, source to sink, auxin transport occurs from biosynthetically active young shoot tissues towards sink tissues. Auxin is synthesized in young apical regions like leaf primordia and floral buds (Ljung et al., 2001) and can passively migrate into phloem vessels along with other metabolites (Rozov et al., 2013). This type of non-polar transport occurs through the mature phloem vessels in the vascular tissue and through it auxin is passively distributed throughout the whole plant and then unloaded in sink tissues, such as the root (Marchant et al., 2002). The direction and velocity of long-range auxin transport is dependent on factors regulating phloem currents (Morris et al., 2010). Short-range auxin transport occurs between adjacent cells in a cell-to-cell manner and is dependent on specific auxin influx and efflux carrier proteins (Vanneste and Friml, 2009).

1.3.3.1 Chemiosmotic model for polar auxin transport

Auxin is distributed through tissues in a short range, cell-to-cell directional transport mechanism known as polar auxin transport (PAT) (Vieten et al., 2005). The polar cell-to-cell auxin transport is the major determinant for the spatio-temporal auxin distribution within the tissue (Tanaka et al., 2006). PAT, which leads

to the establishment of auxin maxima and gradients, occurs according to the chemiosmotic theory, which involves auxin influx and efflux carrier proteins (Chandler, 2009). The auxin gradients are regulated by the expression and subcellular re-localization of transport proteins in response to environmental and developmental cues (Friml, 2010).

Auxin is capable of moving across the plasma membrane based on the physical-chemical nature of auxin molecules. Auxin is a weak acid and its ability to cross the plasma membrane is dependent on the pH. At the apoplastic pH of 5.5, IAA exists in both dissociated, anionic (IAA-) and protonated (IAAH) forms. Auxin influx can occur either by passive lipophilic diffusion of the protonated form of IAA (IAAH) across the cell membrane or by active transport of the anionic form (IAA-) with the help of auxin influx carrier proteins. AUXIN RESISTANT 1/LIKE AUX1 (AUX1/LAX) family of proteins represents the major auxin influx carriers. In the cytoplasm where pH is around 7, IAAH is dissociated into its anionic (IAA-) form. The anionic auxin molecules cannot diffuse across the plasma membrane and require efflux transporters to exit the cell. Two classes of auxin efflux carriers exist: a) PIN-FORMED PROTEIN (PIN) family of trans-membrane proteins and b) ATP dependent transporters belonging to B subclass of the large superfamily of ATP binding cassette/P-glycoprotein (ABCB/PGP) transporters (Petrášek and Friml, 2009). ABCB transporters reside at the PM and are mostly non-polar. It has been found that ABCBs and PIN proteins act in concert to maintain auxin efflux. For example, ABCB19 and PIN1 can associate together and ABCB is capable of stabilizing PIN1 at PM microdomains thereby mediating auxin transport in some tissues under specific

developmental conditions (Blakeslee et al., 2007; Mravec et al., 2009). The asymmetrical localization of transporters provide directional cellular auxin efflux and the coupled asymmetries in adjacent cells establish polar flows (Zažímalová et al., 2010).

1.3.3.2 Auxin efflux carriers

PIN proteins represent a family of plant specific trans-membrane proteins, which function as auxin efflux carriers. The first identification of PIN family proteins as auxin efflux carriers was done in the model plant *Arabidopsis thaliana* (Gälweiler et al., 1998). Polar auxin transport (PAT) depends on the asymmetric localization of PIN proteins. The polar distribution of PIN proteins mediates directional auxin transport across the membranes thereby generating auxin maxima and gradients that influence development (Vieten et al., 2007, van Berkel et al., 2013).

The *PIN* gene family consists of eight members (*PIN1-PIN8*) in *Arabidopsis thaliana*. PIN proteins comprise of two hydrophobic regions separated by a short or a long hydrophilic loop (Habets and Offringa, 2014). PIN proteins are classified into two major groups (long PINs and short PINs) based on the difference in the length of the hydrophilic loop in the middle of their polypeptide chain (Křeček et al., 2009). The long PINs (comprising of PIN1-4 and PIN7) are defined as auxin efflux carriers and exhibit polar PM localization (Petrášek et al., 2006). The main characteristic feature of the long PINs is the presence of a central hydrophilic loop separating two hydrophobic domains of about five transmembrane regions each. The central hydrophilic loop contains several conserved phosphorylation motifs that are

targeted by certain kinases to modulate PIN trafficking and sub cellular polarity (Ganguly et al., 2012). The short PINs (comprise of PIN5, PIN6 and PIN8) have a partly reduced (PIN6) or dramatically reduced (PIN5 and PIN8) central hydrophilic loop (Rosquete et al., 2012). They are localized to the endoplasmic reticulum where they mediate auxin flow between the cytoplasm and ER lumen to regulate subcellular auxin homeostasis (Křeček et al., 2009).

1.3.3.3 PIN proteins and their localization in different plant developmental processes

Plant growth responses require dynamic redirection of auxin fluxes. The polar localization of PIN proteins on the plasma membrane controls the direction of auxin flow (Wiśniewska et al., 2006) thereby influencing various developmental processes like embryogenesis (Friml et al., 2003), organogenesis (Benkova et al., 2003), vascular development (Scarpella et al., 2006) and gravitropism (Friml et al., 2002). Processes regulated by PIN proteins include organogenesis and embryogenesis (PIN1, PIN4 and to a lesser extent by PIN7) (Friml et al., 2003; Benkova et al., 2003; Reinhardt et al., 2003), vascular differentiation (PIN1 (Scarpella et al., 2004) and to a lesser extent, PIN5, PIN6 and PIN8 (Sawchuk et al., 2013), gravitropism (PIN2, PIN3) (Swarup et al., 2005; Blilou et al., 2005) and phototropism (PIN1, PIN3) (Papanov et al., 2005).

PIN2, *PIN3* and *PIN4* are mainly expressed in root tips where they mediate auxin flow and auxin redistribution for root elongation and gravitropism (Friml et al., 2002). PIN2 proteins are involved in mediating polar auxin flux in the root tip

and root gravitropism (Friml et al., 2004). PIN2 localizes to the apical PM of the epidermal cells and lateral root cap cells and to the basal PM of cortical cells. Additionally, the sub-cellular distribution of PIN2 is redefined in response to light and gravity to modulate directional growth (Laxmi et al., 2008). PIN3 shows no pronounced polarity in columella cells, but shows localization to the basal side of vascular cells and to the lateral sides of pericycle cells in the elongation zone of roots. PIN3 is responsible for lateral auxin movement in both shoots and roots leading to phototropic and gravitropic responses (Keuskamp et al., 2010). In the root cap columella cells, PIN3 has an even distribution throughout the plasma membrane. Upon gravistimulation PIN3 relocalizes to the lateral side of columella cells, creating a differential auxin gradient across the root cap (Friml et al., 2002). PIN4 is mainly found in the quiescent centre and localizes to the basal side of the PM vascular cells.

1.3.3.4 PIN1 localization during leaf vein formation

Auxin is responsible for triggering vascular differentiation. Auxin canalization is proposed to drive vascular strand formation and leaf vein patterning as hypothesized by Sachs (1981). According to this model, a cell's capability to transport auxin increases with auxin flux. As auxin moves through plant tissues, it up regulates and polarizes its own transport, gradually resulting in a file of cells with very high auxin flux away from auxin sources. These high auxin flux cells serve as the precursors of veins and differentiate to form vasculature. The new vasculature develops towards and unites with the existing vasculature resulting in a connected

vascular network (Sachs, 1981). In molecular terms the direction of auxin flux is controlled by the polar localization of PIN1 and its dynamic relocalization, which in turn enhances the auxin flux (Bayer et al., 2009).

The process of leaf initiation is closely associated with the formation of the midvein, which in turn is specified before the primordium begins to bulge from the surface of the meristem. In the bulging leaf primordia, PIN1 is strongly expressed in developing vasculature with a basal PIN1 localization (Benkova et al., 2003; Bayer et al., 2009). The epidermal cells of the young leaf primordium have PIN1 localized to the apical side resulting in a convergence point and creating an auxin maximum at the leaf apex (Reinhardt et al., 2003). Cells at the convergence point acquire basal PIN1 localization and pump auxin into the inner layers (Figure 1.1.A). PIN1 expression is turned on in these layers in a triangular expression domain, gradually resolving into a narrow canal of cells characterized by high auxin concentration and basal PIN1 localization. In the adjacent cells, PIN1 polarizes laterally towards the midvein, thereby draining auxin from the surrounding areas and focusing the midvein to a narrow file of cells (Bayer et al., 2009).

The formation of second-order veins reiterates the process of midvein formation. After the formation of the midvein, PIN1 proteins within the epidermal cells in the distal margin of the leaf shift their localization from apical to basal, thereby directing auxin flow downwards in the leaf margin and creating epidermal convergence points on each side of the leaf (Figure 1.1.B). The epidermal convergence point thus created initiate a triangular PIN expression domain (PED) in

the inner cell layers, that resembles that formed early in midvein development (Figure 1.1.C). The formation of the second-order vein can be divided into two stages: stage I in which the formation of a lower loop domain (LLD) occurs and stage II in which formation of the upper loop domain (ULD) occurs. In second-order veins, PEDs associated with the epidermal convergence point extend and eventually connect to the PED of the midvein. These early second-order PEDs, referred to as the LLD are composed of a transient wide distal section near the marginal convergence point and a persistent narrow proximal section near the midvein. PIN1 localization is both basal and lateral in the distal section and basal in the proximal section. After the LLD is fully connected to the midvein PED, initiation of the ULD occurs which gradually extends from the LLD toward the distal midvein to become a "connected" PED (Figure 1.1 D). Once the ULD connects to the midvein, the transient wide section of the LLD near the epidermal marginal convergence point disappears. Thus, each second order vein consists of two segments, LLD where PIN1 localization is basal and ULDs in which PIN1 localization is basal (towards the LLD) and apical (towards the midvein). The two segments in the ULD with opposite polarity are bridged by a single bipolar cell (Scarpella et al., 2006; Wenzel et al., 2007).

It is evident that PIN1 protein changes its localization dynamically during different stages of vein development, ranging from apical to basal to lateral localization. The ability of PIN proteins to maintain polarity and quickly redistribute is dependent on cellular signaling events occurring at the polar PM site where PIN proteins are localized (Gao et al., 2008). PIN proteins are internalized by clathrin mediated endocytosis and are constitutively recycled between the endosome and

the PM, a process which is required for maintenance of PIN polarity. The targeting of PIN1 proteins to specific compartments is mediated by a wide variety of proteins involved in the vesicle trafficking mechanism. Before going into detail about the maintenance of PIN1 polarity by membrane trafficking process, I will explain the vesicle trafficking mechanisms in plants in general.

1.4 Vesicle trafficking mechanisms in plants

The plant endomembrane system consists of distinct membrane bound organelles such as the endoplasmic reticulum (ER), the golgi apparatus (GA), endosomes and vacuoles, each of which maintain a unique composition of membranes and cargo proteins (Bonifacino and Glick, 2004). This network of independent organelles functions in a sequential manner to mediate protein secretion to the PM, extracellular matrix or transport to the vacoule for degradation (Lee et al., 2004a). The membrane bound organelles are highly dynamic and membrane synthesis is a highly regulated process. The structural and functional identity of each organelle is determined by various factors such as the membrane composition, the continuous exchange of membranes between various organelles and recycling processes (Brandizzi et al., 2002).

The endomembrane system mediates bidirectional flow of secretory molecules through the secretory system. The endomembrane protein trafficking consists of molecular machineries involved in packing cargo proteins into the vesicles as well as formation, recognition, tethering and fusion of vesicles (Bonifacino and Glick, 2004). The cytoskeleton is also involved, as vesicle budding

and movement occurs along actin cables either through the association of actin based motor proteins or actin polymerization to generate vectoral force (Eitzen, 2003). Two default pathways exist for the transport of secretory molecules, the secretory pathway and the endocytic pathway. The secretory pathway (anterograde traffic) transports newly synthesized proteins targeted to the PM or ECM or to the vacuole via the ER and the GA. The endocytic pathway refers to the transport of materials endocytosed from the PM or ECM to destined organelles. The endocytic pathway consists of early/sorting endosomes that are involved in sorting and recycling of PM proteins and late endosome or pre vacuolar compartments (PVC) that are involved in Golgi to vacuole trafficking (Tse et al., 2004; Jürgens, 2004). The retrograde trafficking pathway functions as a recycling mechanism to retrieve material from later steps and also to direct newly synthesized cargo vesicles destined for the vacuole from the default secretory pathway (Bassham et al., 2008).

The transfer of luminal macromolecules (proteins, glycoproteins, and polysaccharides) and trans-membrane proteins between different organelles in the cell is facilitated by vesicle transport. Transport vesicles with a protein coat on their cytoplasmic surface and containing specific cargo bud off from the donor compartment and are transported to a specific destination. Prior to the fusion of a vesicle with the target membrane, the protein coat is removed from the vesicle. Precise regulation of vesicle trafficking is essential to prevent mistargeting to an incorrect compartment. The trafficking machinery works precisely for delivering proteins from one compartment to another (Alberts, 2002). Among these, small GTPases, SNAREs, phosphatidylinositols and cargo receptors are main players in

protein trafficking. I will discuss the role of some of these factors in detail later.

1.4.1. Transport from ER to GA

The ER is the entry point for newly synthesized proteins, where they undergo folding and assembly. The ER is entrusted with varied functions such as secretory and membrane protein biosynthesis, quality control, folding and modification of proteins, synthesis of phospholipids and steroids, and storage of calcium ions and their regulated release into the cytosol (Voeltz et al., 2002). The proteins enter the ER through translocation across the ER membrane either during co-translational or post-translational processes (Hanton et al., 2005). Once inside the ER lumen, the newly synthesized proteins interact with ER resident proteins known as chaperones, which help in the correct and efficient folding of the proteins. After processing in the ER, membrane proteins that are destined for secretion accumulate in transport vesicles, are coated with COPII coat components and bud from ER exit sites (Popescu, 2012).

1.4.2 Transport from GA to other organelles

The common destination for most secretory proteins once they depart the ER is the GA. The GA acts as a complex carbohydrate factory in the cell. The important functions of the GA are modification and glycosylation of glycoproteins. In plants, the GA has additional functions such as *de novo* synthesis of complex cell wall polysaccharides such as hemicellulose and pectins. In addition, protein trafficking and sorting of proteins to specific destinations are important roles of the GA (Nebenführ, 2001). In plant cells, Golgi bodies are highly mobile, scattered in the

cytoplasm and within the trans-vacuolar strands of the cytoplasm as numerous cisternal stacks, produced by stacking of 5-20 individual cisternae (Saint-Jore et al., 2002). The cisternae possess a defined polarity, cis Golgi facing the ER, medial Golgi in between and trans-Golgi facing the opposite side. The functional subdivision of the Golgi into different stacks is based upon the enzymatic activities within each stack.

After leaving the ER, vesicles with cargo first encounter the cis-Golgi. COPII coat vesicles fuse with cis-Golgi and deliver their contents to the lumen/limiting membrane. Inside the cis-stack, proteins undergo N-glycosylation, making substrates for other enzymatic reactions in subsequent stacks (Neumann et al., 2003). ER resident proteins, which are associated with the processing of newly synthesized proteins, might escape the ER due to accidental incorporation errors (Phillipson et al., 2001). Resident proteins involved in export machinery need to be recycled from the Golgi back to the ER for reuse in subsequent cycles of vesicle formation. Cis-Golgi also deals with the recapture of escaped ER resident proteins. The KDEL receptor recognizes the C- terminal K/HDEL motif within the ER- resident proteins, recruits COP1 machinery and returns them to the ER.

1.4.3 Trans-Golgi Network (TGN)/Early Endosome (EE)

In plants, the TGN compartment merges endocytic and secretory pathways and serves as a sorting station to traffic proteins directly to the plasma membrane or lytic vacoule, transport of proteins from the PM to the lytic vacuole, and recycling of proteins back to the PM. In general, the early endosome (EE) is defined as the first

endosomal compartment that receives endocytosed cargo from the PM (Otegui and Spitzer, 2008). Application of molecular markers tagged with GFP along with the styrl dye FM4-64, which when exogenously applied is incorporated into the PM and passes through various endosomal compartments *en route* to the vacuole, has allowed the characterization of different endosomal compartments and visualization of endocytic trafficking routes (Ueda et al., 2004). Whereas in animal cells and yeasts, EE is distinctively separate from the TGN (Hwang, 2008), in plants the TGN functions as an early endosome (EE), since FM4-64 was transported to the TGN immediately after internalization from the PM. EE are the first site for the delivery of endocytosed cargo. Thus, the TGN serves as a major hub, receiving endocytosed cargo from PM and also sorting biosynthetic cargo from Golgi targeted to vacuole, PM, cell wall or cell plate (Lam et al., 2007; Reyes et al., 2011).

For a long time, the TGN was seen as an appendage of trans-side of the Golgi (Hawes et al., 2010). When observed under electron tomography, the TGN appears as a tubule-vesiculated mesh of heterogeneously sized membranes and was suggested to be morphologically and functionally distinct from the Golgi (Staehelin and Kang, 2008; Kang et al., 2011). The TGN is a distinct organelle that can either associate with Golgi or can exist as an independent organelle in the cytosol (Viotti et al., 2010; Contento and Bassham, 2012). Golgi associated TGN (GA-TGN) is suggested to generate from trans-most Golgi cisternae by maturation and is released to become a freestanding TGN (Staehelin and Kang, 2008). Confocal studies have revealed that TGNs are not only highly mobile but are able to fuse to one another and temporarily interact closely with a Golgi stack (Viotti et al., 2010).

The transport of cargo carrying vesicles in the endomembrane system is mediated a by a wide variety of factors like coat proteins, dynamin, SNARE molecules, Rab proteins and SNARE proteins. Coat proteins are responsible for the deformation of the membrane that allows vesicle budding and are also involved in cargo selection. The fission of transport vesicle from the membrane is regulated by dynamin-like GTPases (Nebenführ, 2002). Fusion of the cargo vesicle to the target membrane is regulated by SNARE molecules present in the vesicle (v-SNARE) and target (t-SNARE) membrane. The targeting and tethering of transport vesicles to the target membrane is regulated by Rab proteins (Saito and Ueda, 2009). I will briefly explain some of these factors and their relevance to PIN1 protein trafficking.

1.5 Coat proteins in vesicle trafficking mechanisms

The process of formation of a transport vesicle requires selection of both cargo and site of formation. During generation of a vesicle, localized curvature of the membrane sculpts a vesicle out of the donor compartment, a process mediated by the cytoplasmic coat protein complexes (Lee et al., 2004a). Each type of coat protein is distinct and responsible for vesicle formation at a particular type of organelle (Bassham et al., 2008). The three types of coat proteins (Clathrin, Coat protein complex (COP) I and II) interact with different adaptor proteins and small GTPases to generate a new vesicle (Pizarro and Norambuena, 2014). Coat protein complex II (COPII) is involved in the formation of vesicles or cargo at the ER-Golgi interface. The sorting of cargo from the Golgi to ER and intra-Golgi trafficking is mediated by COPI. Clathrin based complexes are involved in multiple steps in post-Golgi

trafficking (McMahon and Mills, 2004).

1.5.1 Role of coat GTPases in formation of a vesicle

The coating process is mediated by coat GTPases which vary depending on the particular coat proteins. Small GTP binding proteins (G proteins) represent the largest family of signaling proteins in eukaryotes and are involved in regulation of a wide variety of processes such as cell proliferation, cytoskeletal assembly and intracellular membrane trafficking (Takai et al., 2001). In *Arabidopsis thaliana*, there are four main families of G proteins: i) ARF/SAR; (ii) RAB (Rab-like GTPases); (iii) ROP (Rho-like proteins in plants); and (iv) RAN (Ras related Nuclear) proteins. Among these G proteins, ARF/SAR and RAB proteins are involved in coat protein formation and tethering of vesicles respectively.

As in other eukaryotes (McMahon and Boucrot, 2011), clathrin coat proteins play an important role in the endocytic processes in plants. Clathrin coats are composed of the protein clathrin (comprising clathrin heavy chain and clathrin light chain), adaptor protein 2 (AP2) complex along with other accessory factors. Following clathrin and cargo recruitment for CCV formation, dynamin, a large GTPase regulates membrane scission which results in pinching of endocytic vesicles from the membrane (Lusching and Vert, 2014).

COPII coat protein recruitment is mediated by a specific subset of the Arf GTPase family known as SECRETION-ASSOCIATED AND RAS-RELATED 1 (SAR1) Sar1p GTPase (Vernoud et al., 2003). In Arabidopsis, multiple homologues of SAR

(AtSARA1a, AtSARA1b, AtSARA1c and AtSARA1d) are present (Yorimitsu et al., 2014).

The ARF-family of G proteins mediate COPI and clathrin coat formation (Luschnig and Vert, 2014), In Arabidopsis, there are 12 ARF proteins of which ARF subgroups A to D are plant specific (Jürgens and Geldner, 2002; Vernoud et al., 2003), suggesting that functional specificity has occurred in the plant ARF family. Arabidopsis ARF proteins are classified into different subgroups. The ARFA1 subgroup consists of 6 members (ARFA1a, AtARFA1b, AtARFA1c (ARF1A/BEX1), AtARFA1d, AtARFA1e, AtARFA1f). The ARFB group consists of three members (AtARFB1a, AtARFB1b and AtARFB1c); ARFC consists of one member (AtARFC1) and ARFD consists of two members (AtARFD1a and AtARFD1b). The large number and potential for redundancy has made it quite difficult to elucidate the function of plant ARF proteins (Yorimitsu et al., 2014).

The role of the ARF1A subclass of proteins in developmental processes is not known at a whole plant or tissue level (Yorimitsu et al., 2014), since the six proteins are ubiquitously expressed and single loss of function mutants in these genes have revealed no obvious developmental phenotype (Xu and Scheres, 2005). Nevertheless, this group is one of the best-characterized groups of *AtArfs* in terms of function and localization. The evolutionarily conserved ARF1 was known to regulate intracellular trafficking at the GA and endosomal compartments in humans (Gillingham and Munro, 2007), and also to mediate the recruitment of COP1 components to the GA during retrograde trafficking from the GA to the ER (Lee et al.,

2004a). Plant ARFs have been shown to localize to various subcellular compartments like GA, post Golgi organelles and PM (Stefano et al., 2006; Matheson et al., 2007). In plants, ARF1A1c is distributed to the Golgi and post-Golgi compartments that bud from the Golgi apparatus (Xu and Scheres, 2005) and localizes with the Rab5 homolog, ARA7 (Ueda et al., 2004). ARF1A1c (ARF1p) is thought to be required for post Golgi trafficking of vacuolar proteins to lytic vacuoles (Pimpl et al., 2003), suggesting a possible interaction with clathrin coat components. In tobacco epidermal cells, ArfA1F-YFP was shown to localize to punctate structures of heterogeneous size, the largest ones being Golgi stacks and the smallest ones being TGN (Robinson et al., 2011; Renna et al., 2013).

1.5.2 Rab GTPase proteins and SNAREs in regulation of vesicle trafficking

Regulation of tethering and fusion of cargo carriers with the target membrane in vesicle trafficking mechanisms involves conserved key molecules including RAB-GTPases, Soluble N-ethylmaleimide sensitive factor adaptor receptor protein (SNARE) molecules and tethers. This set of proteins controls specificity of directional targeting and ensures membrane fusion with the correct organelles (Ueda et al., 2004). Rab GTPases and their effector proteins act to tether vesicles to the target membrane (Whyte and Munro, 2002). During vesicle tethering and fusion, a Rab GTPase on the vesicle membrane interacts with a tethering protein complex on the target membrane. Once the membrane carriers are tethered to the target membrane, another group of conserved molecules known as SNAREs mediates fusion. SNARE proteins regulate membrane fusion of the uncoated vesicle to the

target membrane through their highly conserved SNARE domains (Jahn and Scheller, 2006). SNAREs are classified into vesicle SNAREs (v-SNAREs) and target SNAREs (t-SNAREs). A vesicle buds from a donor compartment carrying a particular SNARE (Vesicle or v- SNARE), which then finds the target membrane, marked by a t-SNARE and their interaction leads to fusion. Fusion between t-SNAREs and v-SNARE occurs via conserved coiled-coil domains, where one helical domain wraps around another, forming a trans-SNARE complex, thereby triggering membrane fusion (Ungermann and Langosch, 2005).

1.5.3 GEFs and GAPs in vesicle formation and fusion

During vesicle formation, GEFs embedded in the membrane mediate the recruitment of coat-GTPase to the donor membrane, and activate the coat-GTPase by triggering the exchange of bound GDP for GTP. All ARF-GEFs possess a sec7 domain that is necessary for catalyzing the exchange of GDP for GTP (Donaldson and Jackson, 2000). Once the coat–GTPases are activated at the budding site of the donor membrane, they recruit effector molecules and “cargo-selective” subunits of the coat complexes from the cytoplasm. The effector molecules can either recruit other factors (SNAREs or Rab-GTPases) into the budding vesicle or alter the lipid characteristics of the budding site. Once the coat subunits are assembled on the bud site, they serve as machinery to drive membrane deformation (Stagg et al., 2006). Excision of vesicle from the donor membrane is mediated by the coat, by the special lipid composition of the vesicle neck, or by molecular machines like dynamin of GTPases or by some combination of the three (Takei and Haucke, 2001).

Once detached from the donor membrane, the coat proteins are removed and the uncoated vesicle is trafficked along the endomembrane trafficking system and it finally reaches the.target membrane (McMahon and Boucrut, 2011). The uncoating of vesicle is triggered by GTP hydrolysis, converting active GTP to inactive GDP bound form thereby altering the conformation of the GTPase (Hanton et al., 2005). The conversion to the inactive GDP bound form from the active form occurs by GTP hydrolysis, either by intrinsic G-protein activity or through the action of GAPs, which stimulates the hydrolytic activity of G proteins. Once in the inactive form, the G protein is ready to begin the cycle again (Vernoud et al., 2003). The targeting of the vesicle carrying cargo to the specific correct compartment and the membrane fusion of the vesicle to the target membrane is mediated by tethering complexes and SNARE proteins. By these mechanisms, the vesicle docks to the specific compartment, fuses with the membrane and releases cargo into the compartment.

1.5.4 Phospholipids in regulation of vesicle trafficking

Tethering of a vesicle to the target membrane is mediated by the specific signals present on the membrane of which phospholipids and phosphoinositides (PI) play a significant role. PI are membrane lipids consisting of phosphatidylinositol and its phosphorylated counterparts. Following biosynthesis in the ER, Phosphatidylinositol (PtdIns) is distributed to subcellular locations either by lipid transfer proteins or vesicle trafficking or a combination of both. PIs are generated from PtdIns through the phosphorylation at one or more hydroxyl positions on the lipid head group (Figure 1.2). Phosphorylation may occur in the ER, nucleus, Golgi,

endosomes or at the plasma membrane (Lofke et al., 2008) by specific kinases differentially localized within the cells to create different intracellular pools of phosphoinositides (de Matties et al., 2002). As well, in an opposing reaction, inositol polyphosphates can be dephosphorylated by inositol polyphosphate phosphatases (Xue et al., 2009) (Figure 1.2).

The inositol ring of phosphatidylinositol can be phosphorylated at the D-3, D-4 or D-5 position by specific phoshpohinositide kinases PI3Ks (phosphoinositide 3-kinases), PI4Ks (phosphoinositide 4-kinases) and PI5Ks (phosphoinositide 5-kinases) to produce PI(3)P, PI(4)P or PI(5)P respectively. PI(4)P and PI(3)P serve as substrates for further phosphorylation by Phosphatidylinositol-monophosphate-kinase (PIPkinase). Sequential phosphorylation of PI(4)P or PI(5)P leads to production of PI(4,5)P_2 and this phosphorylation is mediated by phosphoinositide 4-phosphate 5-kinase phosphoinositide 5-phosphate 4-kinase.

PI (4,5)P_2 can be hydrolysed by PLC resulting in production of Ins (1,4,5)P_3 and DAG (diacylglycerol) (Figure 1.2). Phosphoinositides possess their own distinctive subcellular localization and define organelle identity. PI(3)P is mainly found on early endosomes and multi-vesicular bodies (MVBs), PI(4)Ps on Golgi bodies and PI(3,5)P_2 on late endosomes. PtdIns(4,5)P_2 is enriched in the PM where it regulates endocytosis, exocytosis, generation of second messengers and reorganization of actin cytoskeleton (Saarikangas et al., 2010).

Arabidopsis thaliana encodes 12 PI3/4 domain-containing proteins predicted to be PI4K genes, 15 isoforms of PIP5Ks (phosphoinositide phosphate 5-kinases), 15

isoforms of 5PTases (inositol polyphosphate 5-phosphatases) and 12 PI4K isoforms (Mueller-Roeber et al., 2002, Berdy et al., 2001, Meijer and Munnik, 2003 and Xue et al., 2009). PI4Ks are divided into two types based on the size and substrate affinity. i) type II PI4Ks and ii) type III PI4Ks. Type III PI4Ks are subdivided into two distinct subfamilies PI4KIIIα and PI4KIIIβ. In Arabidopsis, two PI4KIIIα and two PI4KIIIβ (PI4KIIIβ1 and PI4KIIIβ2) genes have been identified (Mueller-Roeber and Pical, 2002). At the protein level, PI4KIIIβ2 is 83% identical to PI4KIIIβ1 (Preuss et al., 2006). The root hairs of PI4Kβ1β2 double mutants are shorter and abnormal in comparison to the WT (Preuss et al., 2006). PI4KIIIβ1 and PI4KIIIβ2 were shown to interact with RabA4b GTPase, which specifically labels TGN like compartments (Preuss et al., 2004). The loss of PI4Kβ1β2 results in changes to the morphology of RabA4b labeled TGN compartments and altered root hair tip growth, suggesting that the product of PI4KIIIβ1 and PI4KIIIβ2, PI(4)P might be involved in polarized secretion (Thole and Nielsen, 2008).

The Arabidopsis genome contains PIPKs, and based on the substrate specificity PIPKs are divided into three families: Type I are PI(4)P 5-kinases, type II are PI(5)P4-kinases and type III are PI(3)P5-kinases. In Arabidopsis, *PIP5K1K2* double mutants exhibit defects in endocytic recycling of PIN1 and PIN2, indicating that clathrin mediated endocytosis might be impaired in plants with defects in formation of PtdIns(4,5)P_2 (Ischebeck et al., 2008). The knock out mutants of PIP5K1K2 exhibited apolar or random PIN1 localization in roots, abnormally strong lateral localization of PIN2 in root cortex cells and lack of coordinated PIN polarization during vascular strand formation. It has been proposed that the two

PI(4)P 5-Kinases, PIP5K1 and PIP5K2, are required for polar localization of PIN proteins (Tejos et al., 2014). Alterations to PtdIns(4,5)P_2 biosynthesis affects actin remodeling at sites of tip growth such as root hairs and pollen tubes. Arabidopsis PIP5K1 interacts directly with actin and recruits PI4KB1 to the actin cytoskeleton (Davis et al., 2007). Even though the exact molecular role of PtdIns(4,5)P_2 remains unclear, these results suggest a possible role in clathrin mediated endocytosis.

1.5.5 ARF-GEFs in PIN protein trafficking mechanisms

As mentioned in the earlier sections, various developmental processes in plants, including leaf vein formation, are mediated by dynamic relocalization of PIN proteins to particular sides of the cell, which in turn directs auxin transport. These PIN vesicle trafficking mechanisms are proposed to be regulated by the concerted action of ARF-GTPases, ARF-GEFs and ARF-GAPs, which co-operate to regulate PAT by mediating the proper localization of auxin influx and efflux carriers.

It has been suggested that plant developmental processes are tightly correlated with ARF-GEF mediated vesicle trafficking processes (Du et al., 2013). Plants contain two ARF-GEF subfamilies i) the GBF subfamily that comprises GNOM, GNOM LIKE1 (GNL1) and GNL2 and ii) the BIG subfamily that comprises of five members, BIG1-5 (Richter et al., 2007). Bredfeldin A (BFA) is a fungal toxin that specifically inhibits the action of certain ARF-GEFs by inhibiting the activation of ARF-GTPases (Geldner, 2004) and is a useful diagnostic tool in ARF-GEF characterization. Of the eight ARF-GEFs, GNOM, GNL2 and BIG (1,2, and 4) are BFA sensitive whereas GNL1, BIG3 and BIG5/MIN7/BEN1 are BFA insensitive (Geldner

et al., 2003, Du et al., 2013). Since BFA inhibits the action of five ARF-GEFs simultaneously, it is still not clear how many ARF-GEFs are involved in vesicle trafficking mechanisms.

GNOM belongs to the Gea/GBF/GNOM (GGG) subfamily of ARF-GEF proteins (Jackson and Casanova, 2000). In animals and yeasts, GGG type ARF-GEFs have been implicated in ER-Golgi or inter Golgi traffic. In *Arabidopsis thaliana*, GNOM (GN)/EMB30 gene was identified as a loss of function mutant displaying defects in establishing the apical-basal axis of the embryo (Steinmann et al., 1999). Different alleles resulted in various defects during different developmental stages including perturbed division of the zygote, variable fusion or deletion of cotyledons and hypocotyls, irregular cell division and elongation patterns, lack of embryonic root, reduced apical structures, defective alignment of vascular cells and irregular and discontinuous venation (Mayer et al., 1993; Geldner et al., 2003). The pleiotropic defects are associated with mislocalization of PIN1 protein. For example, whereas in the provascular tissue of wild type embryos, PIN1 is localized to the basal side, in *gnom* mutant embryos PIN1 is not localized to the basal side. BFA treatment phenocopies loss of gnom function; in both basal PIN1 localization is reduced and instead PIN1 is recruited to the apical side of the PM (Prasad and Dhonukshe, 2013).

GNOM is proposed to be required for basal PIN1 localization by regulating endocytosis and recycling pathways (Geldner et al., 2003). PIN1 is normally localized to the PM, but upon BFA treatment PIN1 disappears from the basal PM and accumulates in intracellular compartments (BFA compartments), the core of which

accumulate PM and endosomal markers which partially overlap with trans-Golgi markers (Geldner et al., 2003). In plants expressing GNOM engineered to be BFA resistant, PIN1 recycling is not inhibited (Geldner et al., 2003). These results show that steady state polar localization of PIN1 involves the regulation of vesicle trafficking mechanisms by BFA sensitive ARF-GEFs. GNOM has been shown to colocalize with compartments of early FM4-64 accumulation in the presence of BFA (Geldner et al., 2003). Complete co-localization of GNOM with FM4-64 and also with PIN1 was observed after BFA treatment (Geldner et al., 2003). Together these data led to the conclusion that GNOM functions at the RE (Geldner et al., 2003). More recently, a minor portion of GNOM was found to localize at the PM, and co-localization with clathrin suggested GNOM regulates endocytosis (Naramoto et al., 2010).

Even though it had been believed that GNOM localizes to RE, new methods that allow visualization of GNOM in the absence of BFA treatment indicates that GNOM primarily localizes to GA instead of RE (Naramoto et al., 2014). BFA treatment initially stabilizes GNOM at the GA, followed by a gradual translocation of GNOM from the Golgi to the TGN, which also indicates that prolonged BFA treatment causes GNOM mislocalization and explains the earlier interpretations (Naramoto et al., 2014). According to the new model, GNOM is localized primarily at the GA, maintains TGN structure and function, and thus indirectly regulates recycling of PIN and other proteins to the PM, an idea supported by the fact that TGN/EE seems to be highly vesiculated in *gnom* mutants (Naramoto et al., 2014). While GNOM has been extensively studied, the function of other ARF-GEFs is not well known. GNOM Like 1

(GNL1), the closest homologue of GNOM, is a BFA resistant ARF-GEF that is localized to the GA and regulates COP1 mediated trafficking of ER resident proteins from Golgi back to ER (Richter et al., 2007). GNL1 has been suggested to be involved in regulation of internalization of PIN2 proteins and redundancy of function is suggested by the result that GNOM can take over function of GNL1 when it is mis-localized to the Golgi (Teh and Moore, 2007). It had been suggested that both GNOM and GNL1 are involved in an early secretory pathway, mediating PIN1 targeting to the basal side of the cell (Doyle et al., 2015). GNOM LIKE 2 (GNL2) is a pollen specific ARF-GEF, which is highly expressed in pollen grains and pollen tubes. When ectopically expressed in seedling roots, GNL2 has been shown to mediate polar recycling of PIN1 (Richter et al., 2012). The defects in pollen tube germination shown by *gnl2* mutants indicates the role of GNL2 in secretion mechanisms associated with pollen tube germination (Jia et al., 2009)

The BIG ARF-GEF clade comprises of five members, BIG1-BIG5. BIG1-4 proteins have been suggested to play a role in non-polar delivery of newly synthesized proteins to PM (Richter et al., 2014). BIG3 has been shown to activate the nucleotide exchange of ARF1 in a BFA insensitive manner in vitro (Nielsen et al., 2008). BIG5/MIN7/BEN1 (BFA-VISUALIZED ENDOCYTIC TRAFFICKING DEFECTIVE 1) is required for PIN2 accumulation in BFA compartments (Tanaka et al., 2006). The mutants of *ben1* showed cotyledons with disconnected vasculature and primary roots with aberrant lateral PIN1 localization (Tanaka et al., 2009; Tanaka et al., 2013). BEN1 has been shown to localize to early endosomes (Tanaka et al., 2009) and affects PIN1/PIN2 endocytic trafficking by localization at TGN (Reyes et al.,

2011).

1.5.6 ARFs in PIN trafficking

BFA-VISUALIZED EXOCYTIC TRAFFICKING DEFECTIVE (BEX1) encodes ARF-GTPase ARF1A1c and is essential for recycling of PIN transporters. Interference with BEX function impacted PIN1 PM distribution, vacuolar targeting of PIN2 and caused defects in auxin dependent developmental processes like embryogenesis and root gravitropic responses (Tanaka et al., 2014). In root epidermal cells of *A. thaliana*, ARF1A1c colocalizes with TGN/EE/GA markers (Xu and Scheres, 2005; Tanaka et al., 2009). ARF1A1c was found to partially localize with the ARF-GEFs GNOM, GNL1 and BEN1/MIN7, suggesting that ARFA1c might be regulated by different ARFs in distinct compartments to affect different vesicle trafficking processes (Tanaka et al., 2014).

1.5.7 ARF-GAPs in PIN protein trafficking

In Arabidopsis, 15 proteins with ARF-GAP domains have been identified, and have been named Arf GAP domain (AGD) proteins. The ratio of ARF/ARF like proteins to AGDs is 18:15 (Stefano et al., 2010) suggesting that the AGDs must be promiscuous and work in multiple compartments to satisfy GTPase activation in distinct membranes. Based on phylogenetic analysis and overall domain organization, they have been placed into four different classes, Class 1 (AtAGD1-AtAGD4), Class 2 (AtAGD5-AtAGD10), Class3 (AtAGD11-AtAGD13) and Class 4 (AtAGD14 and AtAGD15) (Vernoud et al., 2003). Class 1 AtAGD proteins represent a novel plant specific family of putative Arf-GAP proteins. The ARF-GAP proteins

(except for class 4 AGDs) comprise of AGD, Pleckstrin Homology (PH), BIN/Amphiphysin/Rvs (BAR) domain, and 2-3 ankryin repeats. Ankyrin repeats modulate protein-protein interactions by associating to form a higher order structure. The BAR domain senses membrane curvature, binds to the lipid plasma membrane and sculpts it into desired shapes. The BAR and F-BAR domains of yeast endocytic proteins have been found to promote $PI(4,5)P_2$ clustering and induce the formation of lipid micro domains (Zhao et al., 2013). The PH domain is a lipid-binding domain found in numerous proteins involved in PI signaling (Lemmon, 2003). PH domains can be distinguished based on their binding preferences for different PIs and they are capable of binding to different partner proteins.

SCARFACE (also known as Vascular Network Defective 3-VAN3) is an ARF-GAP protein belonging to the class 1 (AGD3) of AGD protein (Sieburth et al., 2006) *SFC/VAN3* gene is required for the normal continuous vein pattern formation in leaves and cotyledons, since mutants of SFC/VAN3 produce isolated fragments of vascular tissue called vascular islands (VI) in place of continuous and interconnected secondary and higher-order leaf and cotyledon veins (Deyholos et al., 2000). In *van3* mutants, although PIN1 polarity is established, it fails to be maintained in pre-procambial cells, which results in the discontinuous vein formation in leaves (Scarpella et al., 2006). Based on the nearly opposite vascular phenotypes of the single mutants, and the mutual suppression of both phenotypes within the *gnsfc* double mutant, it had been suggested that SFC/VAN3 and GNOM might be acting in opposing pathways (Sieburth et al., 2006). *sfc* mutants have few cotyledon veins, that are often disconnected to form vascular islands (VI), whereas *gn* mutants have

more veins with increased connections. In double mutants, the *sfc* phenotype is moderately suppressed with fewer VI in double mutants, and *gn* phenotype is moderately suppressed with a reduction in vein width. When *sfc* mutant roots are treated with BFA, PIN1:GFP is localized to smaller organelles than in the wild type (Sieburth et al., 2006). In addition, GNOM and SFC/VAN3 have been shown to colocalize at the PM thereby suggesting their role in endocytosis at the PM (Naramoto et al., 2010).

SFC/VAN3 has been shown to colocalize with SYP41 suggesting its localization to the TGN (Koizumi et al., 2005). SFC/VAN3 binds with higher affinity to PI(4)P than to PI or PI(4,5)P (Koizumi et al., 2005). Analysis of truncated versions of GFP-tagged SFC/VAN3 showed that BAR and PH domains are minimal requirements for subcellular localization of SFC/VAN3 to the TGN (Naramoto et al., 2009). A mutation to the PH domain resulted in the mislocalization of VAN3. Together, the data suggest that SFC/VAN3 might be recruited to PI(4)P rich domains of the TGN by the specific binding ability of PH domain to PI(4)P and that this binding might stimulate its activity (Naramoto et al., 2009). CVP2 and CVL1 genes encode a type I inositol polyphosphate 5-phosphatase 6 (At5PTase6) which is required for vein continuity. As mentioned earlier, 5PTases dephosphorylate the 5' position of the inositol ring of IPs and PIs (Carland and Nelson, 2009) thus generating PI(4)P from PI(4,5)P_2. In *cvp2cvl1* mutants, SFC/VAN3 localization becomes cytosolic, supporting the idea that recruitment of SFC/VAN3 to the TGN requires interaction with PI(4)P likely through the PH domain (Naramoto et al., 2009).

1.6 Regulation of PIN polarity by phosphorylation of PIN1 proteins

As described earlier, PIN proteins move between different sides on the PM under different cellular and environmental conditions. While the control of PIN localization to a particular membrane face is incompletely understood, the phosphorylation status of PIN proteins is a key factor in determining whether the protein is basally or apically localized. The AGC (named after the protein kinase A, G, and C families PKA, PKC, PKG) serine/ threonine protein kinases (PINOID, WAG1 and WAG2) and the protein phosphatase, PP2A, act at the PM (Gao et al., 2008, Michniewicz et al., 2007) to antagonistically regulate PIN proteins through reversible phosphorylation of serines within the hydrophilic loop (HL) (Dhonukshe et al., 2010).

Loss of function *PINOID* (PID) mutants or *pid wag1 wag2* triple mutants result in apical to basal PIN polarity shifts, which can be correlated to defects in embryo and shoot organogenesis and in primary roots (Benjamins et al., 2001, Michniewicz et al., 2007). Either PID gain-of-function or PP2A loss-of-function results in basal-to- apical shift in PIN polarity in embryos and roots. As well, these mutations reduce BFA sensitivity of PIN1 localization, which suggests the BFA resistance of the apical PIN localization mechanism (Dhonukshe et al., 2010; Kleine-Vehne et al., 2009). All these suggest that PP2A dependent PIN dephosphorylation results in PIN targeting to the basal side of the plasma membrane (Michniewicz et al., 2007; Möller and Weijers et al., 2009), whereas PID dependent PIN phosphorylation leads to removal of PIN from the basal membrane via endocytosis,

followed by apical delivery of PIN proteins via a GNOM independent, BFA resistant trafficking pathway (Kleine-Vehne et al., 2008).

1.7 FORKED1 (FKD1)/VAN3-BINDING PROTEIN (VAB) gene

The *FKD1* gene is crucial for the formation of the closed leaf vein pattern in Arabidopsis. The mutants of *fkd1* show an open leaf vein pattern in cotyledons and leaves, due to the lack of distal vein junctions between secondary, tertiary and quaternary veins (Steynen and Schultz, 2003). *FKD1* expression is controlled by auxin transport and response (Hou et al., 2010). PIN1 localization is defective in *fkd1* mutants during leaf vein formation, suggesting that the *FKD1* gene is required for PIN1-GFP membrane localization and narrowing of PIN1 expression domain (PED) (Hou et al., 2010). Within the LLD, the narrowing of PIN1-GFP to a single file of cells is delayed in *fkd1* mutants and the cells in the ULD do not show apical PIN1 localization (Hou et al., 2010). Furthermore, the establishment of a bipolar cell is not observed in *fkd1* mutants. Hence, it was suggested that FKD1 forms a component of an auto regulatory loop that enables auxin canalization, by recruiting PIN1 to the cell membrane (Hou et al., 2010). *FKD1* gene encodes a protein of 'Domain of Unknown function' (DUF828) a plant specific domain and a Pleckstrin like (PL) domain, which is similar to the PH domain (Hou et al., 2010). The DUF 828 domain is unique to the plant kingdom and the *Arabidopsis thaliana* genome includes 8 other genes which possess DUF828 genes whose function has never been studied.

VAB, which is the same locus as FKD1 (Hou et al., 2010), was identified as a plant specific VAN3 interacting protein by yeast two hybrid reactions and BiFC

confirmed that FKD1/VAB and SFC/VAN3 form a complex at the TGN (Naramoto et al., 2009). This was consistent with the idea that FKD1/VAB and SFC/VAN3 might be acting redundantly in regulating vascular differentiation which was evident from the more extreme phenotype exhibited by the double mutants between *fkd1* and *fkd2,* and allele of *SFC* (Steynen and Schultz, 2003). The abnormal PIN1 expression pattern of *sfc* and *sfcvab1* mutants were similar, suggesting that VAN3 and VAB function in the same pathway for continuous vascular formation (Naramoto et al., 2009). The PH domain of VAN3/SFC binds to PI(4)P and is necessary for localization of VAN3/SFC to TGN (Naramoto et al., 2009). The fact that the PH domain of SFC/VAN3 or FKD1 is required for proper targeting of the complex via phosphoinositide recognition (Naramoto et al., 2009) suggests that the PL domain of FKD1 might also be recognizing PI(4)P, generated by 5PTases like CVP2/CVL1. FKD1 and CVP2 have been suggested to have overlapping functions in promoting the continuity of lateral veins (Carland and Nelson, 2009), which was evident from the double mutant phenotype of *fkd1* and *cvp2* resulting in an open reticulation pattern, with open secondary and higher order veins (Carland et al., 1999; Steynen and Schultz, 2003). SFC/VAN3 is an ARF-GAP and was shown to localize with GNOM, an ARF-GEF in the PM (Naramoto et al., 2010). The results that FKD1 and SFC possess PH/PL domain, the proteins form a complex at the TGN and mutants display similar abnormal PIN1 localization patterns suggests that FKD1 and SFC/VAN3 might be associating, thereby regulating PIN1 protein trafficking. The mechanism by which the FKD1 gene mediates PIN1-GFP localization may be through its ability to interact

with SFC/VAN3 and bind to PtdIns(4)P enriched membranes in TGN (Naramoto et al., 2009).

In order to better understand the role of FKD1 in PIN1 localization and the function of DUF 828 genes, I sought to:

i) Determine the precise subcellular localization of FKD1 and the position of FKD1 in the vesicle trafficking mechanism.
ii) Determine the localization of FKD1-GFP in mutants that are defective in the phospholipid signaling pathway.
iii) Identify the possible interaction of FKD1 with members of the ARF-machinery, including ARFs and ARF-GEFs.
iv) Determine the role of FKD1 in the PIN1 protein trafficking mechanism.
v) Identify the subcellular localization of DUF 828 gene family members.
vi) Determine the biological role of the DUF828 gene family members in auxin transport related processes.

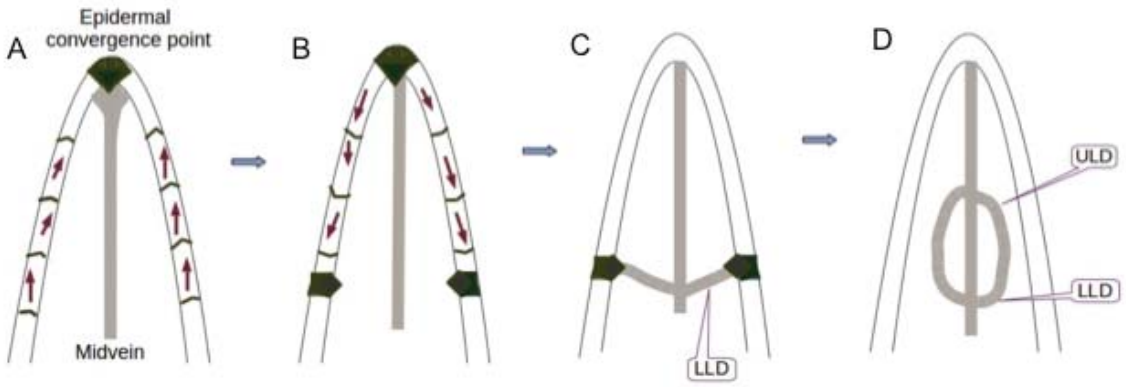

Figure 1.1: PIN1 localization, auxin maxima and vein formation during successive stages of leaf vein development in *Arabidopsis thaliana*. Apical PIN1 localization in the epidermal cells creating an epidermal convergence point (green) at the leaf apex (A). Auxin is pumped downwards through the inner tissue resulting in formation of a midvein(A). Shift in PIN1 localization from basal to apical along the margin of the leaf creates epidermal convergence points at two sides along the margin of the leaf (B). The epidermal convergence point at the margin initiates formation of the lower loop domain (LLD) (C). In the later stages, the upper loop domain (ULD) extends from the LLD and eventually connects to the midvein(D).

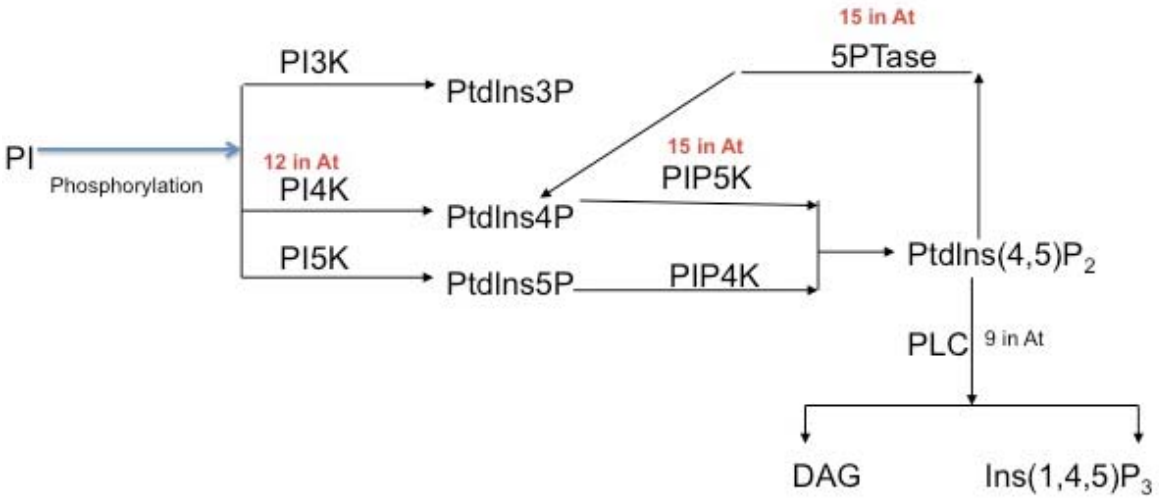

Figure 1.2: Schematic representation of phospholipid metabolism in plants (Modified from Xue et al., 2009). Isoforms in *Arabidopsis thaliana* are shown in red. Phosphorylation of PIES carried out by PI3K/PI4K/ PI5Ks producing PtdIns3*P*, PtdIns4*P* or PtdIns5*P* respectively. Sequential phosphorylation PIP5K or PIP4K will generate PtdIns(4,5)P_2, which is then hydrolysed by PLC generating Ins(1,4,5)P_3 and DAG.

CHAPTER 2: MATERIALS AND METHODS

2.1 Seeds

Arabidopsis thaliana, Columbia (Col-O) ecotype, was used as a wild type control in all experiments. *Nicotiana tabacum* seeds were obtained from Michigan State University (MSU), USA. PIN1-GFP seeds, T-DNA insertional lines (Salk lines) for the members of the FKD1 gene family and seeds of various organelle markers, Wave 13Y (YFP-VTI12; At1g26670), Wave34Y (YFP-RabA1e; At4g18430), Wave129Y (YFP-RabA1g; At3g15060), Wave2Y (YFP-RabF2b/ARA7; At4g19640) Wave131Y (YFP-NPSN12: At1g48240) and Wave138Y (YFP-PIP1;4; At1g48240), were obtained from the Arabidopsis Biological Resource Centre (ABRC) at Ohio State University, USA. SYP61pro:SYP61:CFP seeds were obtained from Dr. Marissa Otegui, University of Wisconsin, USA. Seeds of FKD1-GFP and SFC-YFP were generated by Dr. Elizabeth Schultz, University of Lethbridge, Canada. FKD1-GFP in *fkd1* background and SFC-YFP in *fkd2* background complemented the mutant phenotypes indicating that the fusion proteins are functional. PIN1:PIN1-mRFP seeds were obtained from Dr. Jiri Friml, Institute of Science and Technology, Austria. *cvp2cvl1* seeds were obtained from Dr. Francine Carland, Yale University, USA. *pi4kβ1β2* seeds were obtained from Dr. Erik Nielsen, University of Michigan, USA.

2.2 Growth Conditions of *Arabidopsis thaliana* and *Nicotiana tabacum*

Arabidopsis thaliana seeds were sown on a damp mixture of 3:1 Flora Compo Compost (Coaldale Nurseries, Coaldale, Alberta) to vermiculite (Coaldale Nurseries, Coaldale, Alberta) at the rate of 20-25 seeds per 100cm^2 pot. Pots were then covered

with saran wrap and incubated for 2-3 days at 4°C for stratification. The day of transfer to the growth chamber (Percival Scientific, Perry, IA) was considered as 0 DAG (days after germination). Plants were grown in growth chambers at 22°C with continuous light intensity of approximately 130 mmol photons per m^2 per sec from Sylvania Cool White, Grow Lux and 60W frosted incandescent bulbs (Osram Sylvania Inc, Danvers, MA). At 7 DAG, saran wrap was removed and plants were maintained at 60% humidity. Seedlings of *Arabidopsis thaliana* for root analysis or analysis by confocal microscopy were grown on petri dishes with *Arabidopsis thaliana* (AT) growth medium (Ruegger et al., 1998). *Nicotiana tabacum* seeds were sown on soil and treated in the same way as the Arabidopsis until 14 DAG. Seedlings were transplanted into pots at 14 DAG at the rate of one plant per pot, covered with saran wrap for 4 days, and grown at 16 h of light at 22°C and 8 h of dark at 18°C in 60% relative humidity. Approximately 4 weeks after germination plants were injected with Agrobacterium for transient gene expression.

2.3 Bacterial constructs

Vectors containing full-length cDNA were available for several members of the DUF 828 gene family, U87319 (At5g43870), U19780 (At4g14740), S67212 (At4g17350), S67215 (At5g47440), S69284 (At4g16670) and for four members of the ARF gene family, U09053 (ARF1A1a; At1g23490), U21558 (ARF1A1c: At2g47170), U09461 (ARFA1d; At1g70490) and U12397 (ARFA1e; At3g62290). These vectors and the pnigel 7 vector were obtained from ABRC. pVKH18-GFPN was obtained from Hugo Zheng (McGill University, QC, Canada). SYP61-YFP and ST-RFP

was obtained from Dr. Federica Brandizi, MSU, USA and GA-RB was obtained from Dr. Andreas Nebenführ, University of Tennessee, USA.

To generate the FKD1-GFP construct, FKD1 cDNA was amplified from U16276 and ligated into binary vector pVKH18-GFPC (Zheng et al., 2005) so that the fusion protein was driven by the constitutive 35S promoter (construct made by Dr. Hongwei Hou in our laboratory). To generate the SFC-YFP construct, SFC cDNA was amplified from full length cDNA, ligated into pCR 2.1-TOPO (Invitrogen), and recombined into the pEARLEYGATE101 vector (Earley et al., 2006) using LR Clonase (Invitrogen Cat. No. 11791020), according to the manufacturer's instructions (construct made by Elizabeth Schultz). The pEARLEYGATE101 vector places the fusion protein under control of the constitutive 35S promoter. Generation of constructs for transient expression in *N. tabacum* was done by recombining cDNAs from the DUF 828 and ARF1 gene families (U87319, U19780, S67212, S67215, S69284, U09053, U21558, U09461 and U12397) with the pnigel 7(YFP) vector using the Cre/lox system. The pnigel7 vector places the fusion protein under the control of P_{UBQ10} promoter. DNA was extracted from an overnight culture using a commercial mini-prep kit (Bio Basic Inc., Markham, ON). For the recombination reaction, 500 ng of pnigel 7 vector DNA was mixed with 500 ng of the cDNA vector and incubated with 1 unit of Cre recombinase enzyme and 1 µl Cre recombinase buffer in a 10 µl total reaction volume. After 30 min, the enzyme was heat inactivated by incubation at 70°C for 10 min and the reaction mix transformed into 100 µl Rubidium Chloride competent *Escherichia coli* cells.

2.4 Preparation of competent *Escherichia coli* and *Agrobacterium tumifaciens*

Escherichia coli cells were made competent using the following protocol. A starter culture was made by inoculating a single colony of *E. coli* strain DH5α into 20 ml SOC media and growing the culture overnight at 37°C with shaking at 250 rpm. A starter culture of 2.5 ml was used to inoculate 250 ml of 2XYT media (Appendix I) and this culture was incubated at 37°C with 250 rpm shaking until an OD_{600} of 0.5 was reached. The culture was chilled on ice for 15 min and then spun down at 4°C at 4500 rpm for 10 min. The pellet was resuspended in 100 ml of TFBI buffer (Appendix I) using a 10 ml serological pipette and incubated on ice for 5 min. Cells were again spun down at 4°C at 4500 rpm for 5 min. The pellet was resuspended in 10 ml of TFBII buffer (Appendix I) and incubated on ice for 60 min. Cells were dispensed as 100 µl aliquots into pre-chilled microcentrifuge tubes, snap frozen in liquid nitrogen and stored at -80°C for future use.

In order to transform the binary vectors into Agrobacterium, the *Agrobacterium* strain GV3101 was made electrocompetent. A starter culture was made by inoculating a single colony of *A. tumefaciens* strain GV3101 into 2 ml of YEP (Appendix I) media supplemented with antibiotics (25 mg/ml rifampicin and 25 mg/ml gentamycin) and incubated at 28°C with shaking at 250 rpm. An overnight starter culture of 2 ml was used to inoculate 200 ml of YEP (Appendix I) with proper antibiotics and shaken at 250 rpm at 28°C until an OD_{600} of 0.3 was reached. Cells were then spun down at 4°C at 5000 rpm for 10 min and the pellet was resuspended in 20 ml ice cold, filter sterilized 1 mM HEPES (pH 7); pelleting and resuspension was repeated three times. Finally, the pellet was resuspended in 2 ml of ice cold,

10% sterile glycerol and stored as 100 µl aliquots at -80°C for future use. For constructs with pnigel 7 (YFP) vector, Agrobacterium GV3101 cells were first transformed with helper plasmid Psoup (protocol described in section 2.5) and selected for transformants (25 mg/ml rifampicin, 25 mg/ml gentamycin and 10 mg/ml tetracyclin). A single colony of Agrobacterium harbouring Psoup was made competent as described above and transformed with pnigel vectors.

2.5 Transformation into *Escherichia coli or Agrobacterium tumifaciens*

The whole reaction mixture from the Cre-recombination reaction was transformed into Rubidium Chloride competent *Escherichia coli* strain DH5α according to the following protocol. For transformation, 50 ng of DNA was added into 40 µl of DH5a competent cells in a 1.5 ml Eppendorf tube and incubated on ice for 10 min. A heat shock of 42°C for 45 sec was given and the cell mixture was immediately incubated on ice for a further 5 min. After adding 1 ml of LB (Appendix I), the cell mixture was incubated at 37°C with shaking at 250 rpm for an hour. 200 µl of the cells were plated on LB media with proper antibiotics. The transformants were selected on LB media containing 50 mg/ml Kanamycin (selection for cDNA vector) and 100 mg/ml of Ampicillin (selection for pnigel 7 vector DNA). The presence of the insert was verified by PCR amplification using primers listed in Table 2.1. Components of PCR reaction mixture were 1X PCR buffer, 1.5 mM $MgSO_4$, 0.2 mM dNTPs, 0.5 µM each of forward and reverse primer, 40 ng/µl template DNA and 5U of Taq (Tru Taq) DNA polymerase. Conditions are an initial denaturation at 94°C for 3 min followed by 35 cycles of denaturation at 94°C for 30 sec, annealing at primer T_m for 30 sec and extension at 72°C for 1 min/ 1kb template. Incubation for

an additional 5 min at 72°C was done and the reaction was maintained at 4°C. The presence of inserts as confirmed by restriction digestion using *Sfi* enzyme and sequences were confirmed to be correct by sequencing using primers listed in Table 2.1. Sequencing was done at Nanuq, McGill University and Genome Quebec Innovation Centre, Montreal, QC.

The transformation of a binary vector into competent agrobacterium was done by electroporation as follows. Vector DNA (600 ng) was added to 80µl of thawed *Agrobacterium* cells and the mixture was chilled on ice for 5 min. The reaction mixture was transferred to an ice-chilled electroporation cuvette (2 mm) and pulsed at 2.5 kV in an electroporator (Eppendorf electroporator 2510). Ice cold SOC medium (500 µl) was immediately added to the electroporated cells in the cuvette and the cell mixture was transferred to a 1.5 ml Eppendorf tube and incubated with shaking (200 rpm) at 28°C for 4 hours. Transformed cells (200 µl) were plated onto LB media supplemented with appropriate antibiotics (25 mg/ml rifampicin and 25 mg/ml gentamycin to select for *Agrobacterium*, 50 mg/ml kanamycin to select for the plasmid and 10 mg/ml tetracyclin to select for Psoup) and incubated at 28°C for 48-72 hr for colonies to grow. The positive colonies were picked, restreaked and grown in liquid cultures.

2.6 Transient transgene expression in *N. tabacum*

The colocalization of the following constructs was analyzed by transient expression in *N. tabacum* a) FKD1-GFP with TGN marker SYP61-CFP b) FKD1-GFP with members of ARF1 gene family c) ARFA1c–YFP with ST-RFP d) members of

DUF828 gene family fused to YFP with Golgi marker ST-RFP and e) FKD1-GFP with members of DUF828 gene family fused to YFP. To assess localization to fluorescently tagged proteins through transient expression, *N. tabacum* plants were injected with various Agrobacterium strains harbouring appropriate binary vectors following the protocol of Batoko et al. (2000). Agrobacterium cultures were grown on antibiotics (50 mg/ml kanamycin, 25 mg/ml of rifampicilin, 25 mg/ml gentamycin) at 28°C overnight. 1 ml of each culture was centrifuged at 4000 rpm for 5 min at 20°C and the supernatant was discarded. The pellet was resuspended in 1 ml of infiltration buffer (Appendix I) and recentrifuged. The supernatant was discarded and the pellet was resuspended in 1 ml of infiltration buffer. Resuspended culture (200 µl) was mixed with 80 µl of infiltration buffer and OD at 600 nm was measured using an Ultraspec 1100 Amersham Pharmacia Biotech spectrophotometer. The diluted culture was then further diluted with infiltration buffer to give a final OD_{600} value of 0.05. The inoculum was injected using a 5 ml syringe into the *N. tabacum* leaves through the lower epidermis.

2.7 Transformation of *Arabidopsis* by the floral dip method

Stable transgenic plants of one member of the DUF 828 gene family (At4g14740) expressing YFP were created by transforming wild type *Arabidopsis thaliana* plants with the Agrobacterium strain harboring the binary vector (At4g14740-YFP). An overnight starter culture in 5 ml of LB with appropriate antibiotics was made by inoculating a single colony of the Agrobacterium strain harboring At4g14740-YFP and growing the culture at 28°C at 250 rpm. Next day, 5 ml of the overnight starter culture was used to inoculate 300 ml of LB with

antibiotics and the culture was grown at 28°C, at 250 rpm until the OD at 600 nm reached 1. The culture was centrifuged at 5000 rpm for 15 min at 4°C and the pellet was resuspended in 250 ml fresh LB media with 5% sucrose. Once the pellet was resuspended, 0.05% Silwet was added. The plants were dipped for 30 sec and wrapped in plastic wrap for 2 days. The sleeves were removed after two days and the plants were allowed to grow normally for 4-5 weeks. Seeds were harvested and primary transformants were selected by screening for Basta resistance.

2.8 Generation of lines expressing compartment specific markers

To analyze the co-localization of FKD1 with various organelle markers and other proteins (PIN1 and SFC), stable transgenic lines were made by crossing plants homozygous for FKD1-GFP with plants homozygous for YFP-VTI12, YFP-RabA1e, YFP-RabA1g, YFP-RaF2b/ARA7, YFP-NPSN12, YFP-PIP1;4, PIN1:PIN1-mRFP, SFC-CFP. To determine the co-localization of SFC with PIN1 and SYP61, stable transgenic lines were made by crossing plants homozygous for SFC-YFP with plants homozygous for PIN1-RFP or SYP61-CFP. The transformants were selected based on their resistance to specific herbicide: Hygromycin selects for FKD1-GFP, Basta selects for SFC-YFP, YFP-NPSN12, YFP-PIP1;4, and Kanamycin selects for Syp61-CFP and PIN1-RFP. The localization of FKD1-GFP with organelle markers YFP-VTI12, YFP-RabA1e, YFP-RabA1g and YFP-RabA2b/ARA7 was done in the F_1 generation. Homozygous lines of FKD1GFP with YFP-NPSN12, YFP-PIP1;4, PIN1-RFP, SFC-YFP or SYP61-YFP and SFC-YFP with PIN1-RFP or SYP61-CFP were identified in the F_3 generation.

2.9 Introduction of FKD1-GFP into mutant lines

In order to analyze localization of FKD1 in various mutants defective in phosphoinositide production, FKD1GFP was crossed to *cvp2cvl1* and *pi4kβ1β2* and the F_1 was backcrossed to the double mutant. Homozygous plants for FKD1-GFP with *cvp2cvl1* and FKD1-GFP with *pi4kβ1β2* were obtained in the F_3 generation by screening for the double mutant phenotype, resistance to hygromycin (FKD1-GFP), and fluorescence by confocal microscope. The localization of FKD1-GFP in these mutant lines (FKD1GFP-*cvp2cvl1* and FKD1-GFP- *pi4kβ1β2)* was assessed in the epidermal pavement cells of the cotyledon or in root cells at 2.5 DAG and compared with *fkd1* plants expressing FKD1-GFP.

2.10 Identifying DUF828 domain evolution in the plant kingdom

The *FKD1* gene encodes a protein with a 'Domain of Unknown function' (DUF828), a plant specific domain and PL domain (Hou et al., 2010). GreenPhylDB web resource for plant comparative and functional genomics was used to identify the presence of genes that encode conserved DUF828 domains in the plant kingdom. GreenPhylDB search retrieved genes that possess DUF 828 with or without a PH or P-like domain. A phylogenetic tree was constructed in GreenPhylDB choosing different representative species within the plant kingdom possessing DUF828 domain encoding genes. A second phylogenetic tree was created using nine sequences retrieved for *Arabidopsis thaliana* to understand the phylogenetic relationship of the DUF828 domain encoding genes in *Arabidopsis thaliana*. On the basis of their relation with the FKD1 gene (Hou et al., 2010), all of the other eight members were named FKD-Like (FL) 1-8. These eight genes along with FKD1 were

named the Arabidopsis DUF828 gene family, the details of which are given in Table 2.2.

2.11 Identification of plants homozygous for T-DNA insertions

DNA was isolated from leaf tissues of 16-day-old plants using the CTAB DNA extraction protocol. Two to three young leaves were ground in liquid nitrogen and incubated in 300 µl DNA total extraction buffer (Appendix I) for 1 hour at 65^{o}C. The supernatant was extracted by adding 300 µl of chloroform and phase separated by centrifugation at 12000 rpm for 5 min. DNA in the aqueous phase was precipitated by adding 2/3 volume of isopropanol, incubating for two hours at 4^{o}C and centrifuging at 12000 rpm for 10 min. The pellet was washed twice with 70% ethanol, air-dried and resuspended in 40 µl TE. Plants homozygous for insertions in *At5g43870/FL1* (Salk 124321; *fl1-1* and Salk 64024; *fl1-2*), *At3g22810/FL2* (Salk 26656; *fl2*), *At4g14740/FL3* (Salk 13371; *fl3*), *At4g16670/FL6* (Salk 63367; *fl6-1* and Salk 77717; *fl6-2*) and *At5g47440/FL7* (Salk 128544; *fl7*) were identified by PCR, using the primers listed in Table 2.1. PCR was done using a combination of forward and reverse gene specific primers and also the left border T-DNA primer. Wild type plants with no insertions should produce a product with forward and reverse gene specific primers (Figure 2.3). Homozygous lines with insertions in both chromosomes should give product only with the left border T-DNA and the gene specific primer (Figure 2.3).

2.12 Generation of multiple mutant lines between members of DUF828 gene family

Homozygous T-DNA insertions in *FL1*, *FL2*, *FL3*, *FL6*, *FL7* did not show any obvious phenotype. Hence I focused on creating multiple mutant lines between members of the DUF828 gene family. Plants homozygous for insertions in *FL1*, *FL2*, *FL3, FL6, and FL7* were crossed with *fkd1*. Homozygous double mutants of *fkd1/fl1-1*, *fkd1/fl1-2*, *fkd1/fl2* and *fkd1/fl3* were identified through phenotypic analysis to confirm the *fkd1* phenotype and PCR using specific primer combinations particular for each insertion to confirm the T-DNA insertion. Double mutants of *fkd1/fl2* and *fkd1/fl3* were crossed to produce an F_1 generation. Triple mutants were identified by checking for *fkd1* phenotype and identifying T-DNA insertions by PCR. Triple mutant (*fkd1/fl2/fl3*) was crossed with homozygous double mutants *fkd1/fl1-1* and *fkd1/fl1-2* and quadruple mutants (*fkd1/fl1-1/fl2/fl3*) and (*fkd1/fl1-2/fl2/fl3*) were identified by PCR in F_3 generations. Homozygous lines of *fkd1/fl6-1* were crossed with *fkd1/fl7* and a triple mutant *fkd1/fl6-1/fl7* was identified in the F_3 generation, by checking for homozygosity for the *fkd1* phenotype and T-DNA insertions by PCR. Homozygous lines of *fkd1/fl6-2* were crossed *with fkd1/fl7* and homozygous triple mutants *fkd1/fl6-2/fl7* were identified in the F_3 generation. Homozygous plants thus generated were used for further phenotypic analysis.

2.13 Generation of stable transgenic mutant lines expressing PIN1GFP

A stable transgenic line of the triple mutant expressing PIN1:GFP was generated by crossing plants homozygous for *fkd1*-PIN1:GFP with homozygous

triple mutant line (*fkd1/fl2/fl3)*. The F_1 was backcrossed to *fkd1/fl2/fl3* and a homozygous line was identified in F_2 generation by screening for *fkd1* phenotype, confirming the presence of T-DNA insertions by PCR and checking for PIN1:GFP expression. PIN1:GFP expression in wild type and mutant lines was compared at various development stages of first leaf vein development.

2.14 Confocal imaging and analysis

For transient expression analysis, pieces of *N.tabacum* leaves 48 h post injection were mounted in water. For stable expression systems, Arabidopsis root cells or cotyledons at 2.5 DAG were mounted in water. Tissue was viewed under a 20 X or a 40X oil-immersion objective using an Olympus Fluoview FV1000 confocal microscope. GFP/YFP with RFP were excited with 473 nm and 559 nm lasers, respectively. For colocalization experiments with combinations (GFP with YFP and CFP with YFP), GFP and YFP were excited with 488 nm and 515 nm lasers, respectively. For visualization of EGFP, the emission window was set at 500 to 530 nm and for visualization of EYFP, the emission window was set at 530 to 600 nm. All images used in comparisons were taken at the same confocal settings. For all co-localization analyses, an average of 15 cells were observed for each experiment. NIH Image J software with PSC colocalization plugin (French et al., 2008) was used to assess the colocalization of proteins tagged with GFP/YFP, GFP/RFP or CFP/YFP. Pearson's coefficient of correlation (PCC) values were obtained from PSC colocalization plugin in NIH Image J software, from a selected region of interest (ROI) so as to eliminate background noise. For example, in the cotyledon epidermis, the ROI selected was a single epidermal cell. As a standard for describing the results

of quantitative colocalization using PCC, the following terms were used for the respective value ranges; weak (0-0.3), moderate (0.3-0.5), strong (0.5-0.8) and very strong (0.8-1.0). Images shown in the figure are representative of average colocalization patterns for the samples whenever possible. Images were processed with Adobe Photoshop Elements version 5.0 software (Adobe Systems). In hypocotyledon cells, where autoflourescence of chloroplasts was seen in GFP and RFP channels, to eliminate colocalization associated with chloroplasts, quantification was done by manual counting of vesicles less than 2 μm in size.

2.15 BFA, FM4-64 treatment and plasmolysis experiments

BFA treatment was done by incubating 2.5 DAG seedlings expressing FKD1-GFP, FKD1-GFP and PIN1-RFP or FKD1-GFP and SFC-YFP in 50 mM BFA for 3 hours and viewing seedlings immediately by confocal microscope. A BFA wash out experiment was performed following the protocol of Geldner et al. (2001), in which seedlings were washed free of BFA and the root cells were imaged after 2 h. For FM4-64 treatment, seedlings of homozygous lines expressing FKD1-GFP or SFC-YFP at 2.5 DAG were treated with 16 μM FM4-64 for 15 min, rinsed in water and then viewed after a further 15, 30 and 45 min. For plasmolysis experiments, 2.5 DAG seedlings homozygous for FKD1-GFP and YFP-NPSN12 or FKD1-GFP and YFP-PIP1;4 were incubated in 5% NaCl for 20 min followed by 60 sec rinse with water before viewing under confocal microscope.

2.16 Leaf vein characterization of T-DNA insertion mutants

For analysis of cotyledon and leaf area, vein density and Vascular Islands (VI), cotyledons and first leaves were taken at 14 DAG and 21 DAG respectively from

wild type, *fkd1* mutants and homozygous T-DNA insertion lines. They were collected and kept in 70% ethanol overnight, followed by clearing in chloral hydrate (8 chloral hydrate: 2 glycerol: 1 water) for one week. When clear, they were mounted in 66% glycerol and images were taken using a Nikon Cool Pix 990 camera mounted on Leica MZ8 microscope. Image J software was used to analyze cotyledon and leaf characteristics such as leaf area, leaf vein density and vascular islands. Leaf area and vein length was obtained by tracing the whole leaf area and all the leaf veins. Leaf vein density was calculated by dividing the total length of veins by leaf area.

2.17 Analysis of epidermal cell shape and polarity

Epidermal cell shape was assessed in casts of fifth leaves and second bracts using the Scanning Electron Microscope (SEM). Fifth leaves were taken at 26 DAG and second bracts when the plants were at 2-3 flowers stage. A dental impression of each leaf or bract was made by applying a 1:1 mixture of Coltene catalyst and Coltene base (President light, ISO4823, Type 3) immediately following preparation onto the adaxial/abaxial side of leaves/bracts. The impressions were allowed to dry for 10 min, after which clear nail polish was applied and left to dry for 15 to 20 minutes. Once they were dry, nail varnish casts were taken from the dental impression peels casts and images were taken using SEM.

Random cells within an area of 250 mm^2 were chosen for cell area, Undulation Index (UI) and cell length and analysis was done using NIH Image J software. Undulation index represents the degree of cell wall undulation independent of cell area and measures the variation in cell shape (Thomas et al., 2003).

UI was calculated using the following formula (Minamisawa et al., 2011).

$$UI = \frac{Ce}{(2 \times \pi) \times \sqrt{Ae/\pi}}$$

Where UI (dimensionless) is the undulation index, Ce (mm/cm) is the cell perimeter, and Ae (mm^2/cm^2) is the cell area.

Within wild type leaves, elongated cells are normally oriented parallel to the midvein. To assess the direction of cell elongation in wild type and mutant lines, 30 elongated cells whose orientation deviated most from parallel to the midvein were chosen within an area of 504.78 mm^2 and their divergence in cell angle relative to mid vein was measured using NIH Image J software.

2.18 Root and shoot phenotypic analysis of mutant lines

Seedlings of wild type, *fkd1*, *fkd1/fl2/fl3* and *fkd1/fl1-2/fl2/fl3* were grown vertically on petri plates with AT media at a density of 10 plants per plate. Primary root length measurements were performed by photographing roots at 4DAG and 24h later. Images were merged in Photoshop and the root growth difference between the two images were measured in Image J. Analysis of root gravitropism was done by rotating 90° the 5 DAG seedling that had been growing vertically on AT medium. Images of the position of the root tips after 2, 4, and 6 hours were then captured. The change in the angle of root tip at each time point was measured by using Image J. To analyze shoot characteristics, genotypes were grown on soil under previously described conditions (Section 2.1). Flowering time was defined as the

time at which the inflorescence shoot was 5 cm long. The number of rosette leaves and bracts was counted at flowering time.

2.19 Statistical analysis

An analysis of variance (ANOVA) was carried out for all analyses with a sample size (n >30) using the PROC MIXED procedure of SAS (SAS Institute, 2005). Means were then compared using the least squares mean linear hypothesis test (LSMEANS/PDIFF). Treatment effects were declared significant at $P< 0.05$. Student's T-test (a value of $p<0.05$ represent significant difference) was conducted for sample size ($n<30$) to determine if the compared samples were significantly different ($p<0.05$) from each other. Fisher's test was carried out to determine the statistical difference between the genotypes for measurements (vascular islands, frequency of non meeting veins, FKD1-GFP expression in mutant lines, and PIN1 localization in developing veins) with a mean value of zero.

Table 2.1: Primers used in PCR reactions for identifying T-DNA insertions and sequencing of constructs with pnigel 7 (listed 5' to 3') and their optimal annealing temperatures.

Region amplified	Left Primer	Right Primer	T_m (°C)
At5g43870/fl1-1	GGCATAAGACTTTAGATGGTAGC	GCCATGATACGTTCCATGACC	58.0
At5g43870/fl1-2	GCTCATTCACCGACAGTCCTCCG	GGCTGTTGAGATAGACCGTTGTG	56.0
At3g22810/fl2	CACTGCAACAACTACACAGTCC	CGTGAAGGTCCCTCCTACATGC	59.5
At4g14740/fl3	GTATCACCAAGAACATCTGGTCGGC	CGTGAATCTGAGCGTTATGAGCCCG	58.0
At5g47440/fl6-1	GGCTGCTCAATGTGTGGAAG	GCCAAGAAATGGTTTTAAGCAGA	57.0
At5g47440/fl6-2	ACAGTGCACAAGTGATCGAA	TGGCAACTACTGAAAACGACA	56.5
At4g16670/fl7	CAAACAACACACCAACCCAAGC	CTCGCTTATTTCGCTGCAATC	55.0
pnigel7(YFP) inserts	GCTGGGGCACAAGCTGGAGTACAG	GGACAGTGGGAGTGGCACCTTCCG	59.5
T-DNA left border	CGTCCGCAATGTGTTATTAAG		

Table 2.2: Gene name and position of T-DNA insertions in Salk lines (TAIR website)

AG1 designation	FKD1-Like designation	Salk line	Allele name	Position of T-DNA insertion
At5g43870	FL1	124321	*fl1-1*	Promoter
	FL1	64024	*fl1-2*	Intron 2 of 6
At3g22810	FL2	026656	*fl2*	Exon 4 of 7
At4g14740	FL3	013371	*fl3*	Exon 2 of 7
At5g47440	FL6	63367	*fl6-1*	Exon 2 of 6
	FL6	128544	*fl6-2*	Exon 3 of 6
At4g16670	FL7	077717	*fl7*	Exon 1 of 6

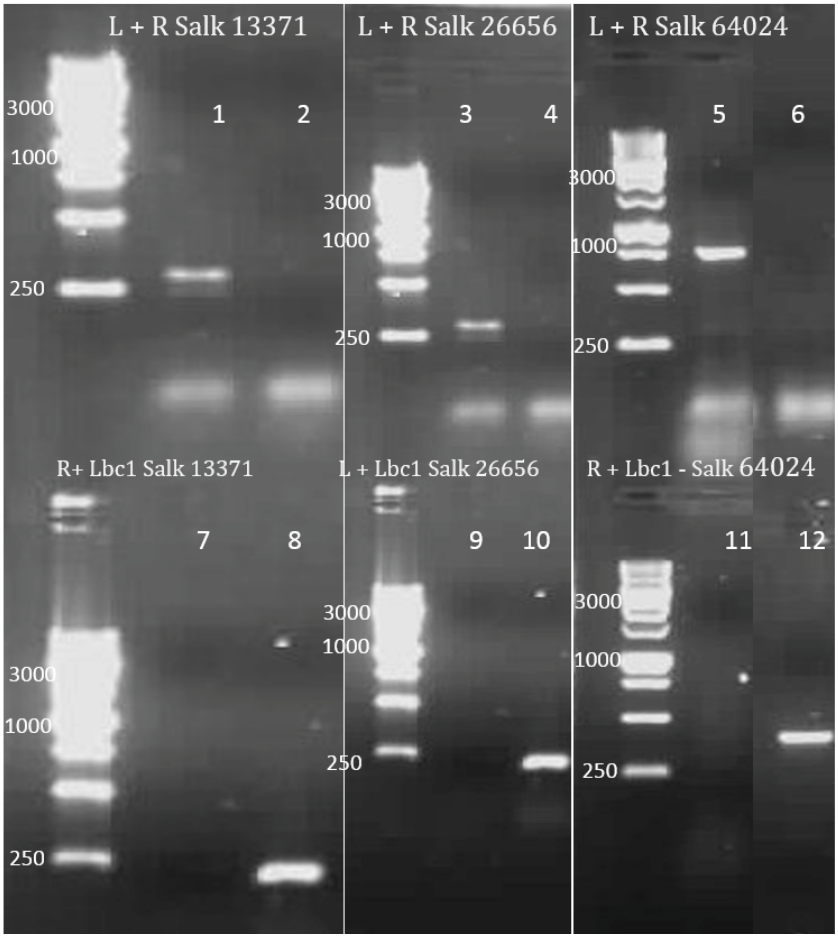

Figure 2.1: Genotyping of SALK T-DNA insertion lines using PCR

DNA from wild type and various genotypes (*fkd1/ fl1-2*, *fkd1/fl2* and *fkd1/fl3*) was amplified with six sets of primers (L+R SALK-13371C (1,2) and R+LBC$_1$ SALK-013371C) (7-8), (,4) and R+LBC$_1$ SALK-26656) (9-10) and (L+R SALK-64024 (5,6) and R+LBC$_1$ SALK-64024) (11-12). Wild type DNA (1, 3, 5, 7, 8, 9) generates a product when amplified with the gene specific primers: L+R SALK-13371C (1), L+R SALK-26656 (3) and L+R SALK-64024 (5) but not with gene specific and T-DNA primers: R+LBC$_1$ SALK-013371C (7), R+LBC$_1$ SALK-26656 (9) and R+LBC$_1$ SALK-64024 (11). DNA of plants homozygous for the T-DNA insertions generate a product with T-DNA primers R+LBC$_1$ SALK-013371C (7), R+LBC$_1$ SALK-26656 (9) and R+LBC$_1$ SALK-64024 (11) but not with gene specific primers: L+R SALK-13371C (2), L+R SALK-26656 (4) and L+R SALK-64024 (6) DNA electrophoresis on 0.8 % agarose gel at 80 volts for 0.5 hours. TECDNA-20R© 10000 bp ladder labelled in bp.

CHAPTER 3: RESULTS

The *FKD1* gene is required for PIN1-GFP membrane localization and narrowing of PIN1 expression domain (PED) (Hou et al., 2010). FKD/VAB1 and SFC/VAN3 (ARF-GAP) form a complex at the TGN (Naramoto et al., 2009). The defective PIN1:GFP expression in *sfc/van3* and *fkd1* mutants and the formation of a FKD1-SFC complex suggest that they might be involved in maintaining PIN1 expression within continuous cell file, thereby regulating vascular differentiation. Hence, to understand the precise subcellular localization of FKD1 and their potential interactors in vesicle trafficking pathways, I performed colocalization of FKD1 with markers for different endomembrane compartments, PIN1 and ARF proteins.

3.1 FKD1 localization pattern changes during development stages

FKD1 is essential for the auxin response that directs vascular differentiation in developing leaves (Steynen and Schultz, 2003). To determine the localization of FKD1-GFP in vascular tissues, localization of FKD1-GFP in the vascular tissues of 2.5 DAG cotyledons were analyzed. Motile punctae of FKD1-GFP are visible in developing vascular cells (Figure 3.1.F), but expression is too weak to provide sufficient samples for reliable comparison. Thus, cotyledon epidermal cells were used for further analysis. During the course of my analysis of FKD1-GFP, I noticed that FKD1 exhibited different cellular localization in cotyledons at different seedling ages. To describe the changes in detail, I undertook an analysis of FKD1 localization in cotyledon epidermal pavement cells at different days after germination (2DAG, 2.5DAG, 3DAG and 4DAG). The shape of pavement cells in cotyledons becomes more complex over time. At 2 DAG, pavement cells are more or less circular in shape. By

2.5 DAG, cells are at the expanding stage, with shallow lobes and alternating indentations and lobe initiation completes by 3 DAG. At 4 DAG cells are more expanded and appear as highly lobed, interlocking cells. The details of FKD1-GFP localization patterns at different days of cotyledon pavement cell development are given in Figure 3.1. At 2 DAG, FKD1 expression is more cytosolic (Figures 3.1.G). As the development progresses, by 2.5 DAG the number of cells with punctae FKD1GFP localization and cells with both PM and punctae localization are more compared to 2 DAG (Figures 3.1.H.I). At 3 DAG and 4 DAG, FKD1 localization is again more cytosolic. Thus, punctae and PM localization of FKD1-GFP corresponds to the stage in which cell polarity is being established. Because 2.5 DAG have high punctae and PM expression of FKD1-GFP, subsequent analyses were done at this stage.

3.2 FKD1-GFP localization is altered in *cvp2cvl1* mutants

VAN3/SFC and FKD1 form a complex which has been proposed to bind to PtdIns(4)P, a product generated by 5PTases like Cotyledon Vascular Pattern 2 (CVP2). FKD1 and SFC/VAN3 possess PH/PL domains respectively which are likely involved in recognizing PtdIns(4)P. In addition, it was also known that double knockout of *CVP2* and *CVL1* caused mislocalization of VAN3 from the TGN to the cytoplasm (Naramoto et al., 2009). With this background, to investigate whether FKD1-GFP localization is altered in *cvp2cvl1* mutants, FKD1-GFP was introduced into *cvp2cvl1* mutant background. FKD1-GFP localization was analyzed in cotyledons and compared with wild type and mutants. At 2.5 DAG, there was significant difference ($p<0.05$) in FKD1-GFP expression of mutants and wild type, in which FKD1-GFP

expression was more cytosolic in *cvp2cvl1* mutants (89%) compared to wild type (63%) (Figures 3.2.A,B,E).

The phospholipid signaling pathway of *Arabidopsis thaliana* includes three families of phosphoinositide kinases (more details in Section 1.5.4), of which PI4Ks (two types) can phosphorylate the D-4 position of the inositol ring of phosphatidyl insoxfcotol to yield PI4(P). In Arabidopsis, two PI4KIIIβ (PI4KIIIβ1 and PI4KIIIβ2) genes have been identified (Mueller-Roeber and Pical, 2002). Since the PL domain of FKD1 is believed to bind to PI(4)P, I asked whether FKD1 localization or expression is altered in mutants defective in two members of PI4K family (*PI4Kβ1β2)*. FKD1-GFP was introduced into *PI4Kβ1β2* mutants, and cotyledons of homozygous lines at 2.5 DAG were analyzed for FKD1-GFP expression and compared with wild type plants. No significant difference ($p>0.05$) was observed in FKD1-GFP expression between wild type and mutant lines and both had similar percentage of cells with cytosolic or punctae FKD1-GFP localization (Figure 3.2.E).

3.3 FKD1 colocalizes with PM markers

As mentioned in Section 3.1, my initial analysis indicated that FKD1 labels punctae and seems to be associated with the PM I focused on establishing that FKD1 is localized at the PM and understanding the nature of the punctae by determining the localization of FKD1 with a set of markers specific for the plant endomembrane system. The localization of FKD1 with these markers was assessed using both stable (*Arabidopsis thaliana*) and transient expression (*Nicotiana tabacum*) systems. Tobacco epidermal pavement cells were used in the transient system, whereas

cotyledons (pavement cells), hypocotyledons and roots were used in the stable expression system. Quantification of different proteins with various markers are given in Table 3.1.

My initial analysis (Section 3.1) suggested that a proportion of FKD1-GFP is localized to the PM and this was supported by subsequent plasmolysis analysis. FKD1-GFP showed weak association with PM markers, YFP-NPSN12 (PCC = 0.16 ± 0.25, n=26) and YFP-PIP1;4 (PCC = 0.32 ± 0.20, n=16 (Geldner et al., 2009; Alassimone et al., 2010) (Figures 3.3 C,K and Table 3.1). In order to confirm that FKD1 colocalizes with the PM, plasmolysis of homozygous lines of Arabidopsis seedlings expressing FKD1-GFP and YFP-NPSN12 or FKD1-GFP and YFP-PIP1;4 was performed by treating seedlings with 5% NaCl for 20min. After plasmolysis, the majority of the FKD1-GFP signal remained associated with the shrunken PM (Figures 3.3 G,O), which suggests that a proportion of FKD1 resides in the PM.

3.4 FKD1 colocalizes with multiple endosomal markers

Analysis of the precise localization of FKD1-GFP in the vesicle trafficking pathway using different markers of endomembrane compartments suggests that FKD1 is localized to motile punctae throughout post-Golgi compartments. Various markers of endosomal compartments were used: for Golgi apparatus, ST:RFP (Wee et al., 1998; Kim et al., 2001); for TGN/EE, YFP–VTI12 (Wave 13Y) (Geldner et al., 2009) and SYP61-YFP (Bassham et al., 2000; Sanderfoot et al., 2001, Drakakaki et al., 2012); for RE, YFP-RabA1e and YFP-RabA1g (Geldner et al., 2009; Liljegren et al., 2009; Ganguly et al., 2014) and for LE/PVC, YFP-RabF2b/ARA7 (Geldner et al., 2009; Ueda et al., 2004; Ebine et al., 2011).

Co-localization of FKD1-GFP with ST-RFP revealed that FKD1 is negatively associated with the Golgi (PCC = -0.30 ± 0.12, n = 17) (Table 3.1 and Figure 3.4 C), whereas FKD1-GFP is moderately co-localization with TGN/EE markers YFP-VTI12 (PCC = 0.37 ± 0.10, n = 32) and SYP61-YFP (PCC = 0.39 ± 0.20, n = 30) (Figures 3.4 G,K, and Table 3.1). FKD1 was shown to colocalize strongly with markers of the RE and late endosomal compartments, YFP-RabA1e (PCC = 0.60 ± 0.18, n = 42), YFP-RabF2b (PCC = 0.68 ± 0.17, n = 19) and YFP-RabA1g (PCC = 0.85 ± 0.17, n = 20) (Figure 3.5 C, G, K). Taken together, my results suggest that a large proportion of FKD1 is acting in the post-Golgi compartments followed by a smaller proportion of FKD1 acting at the TGN/EE and residing within the PM. Together, these results suggest a possible role of FKD1 in regulating endomembrane trafficking processes, which could include either trafficking of proteins from the TGN to the PM and/or recycling of proteins from the RE to the PM.

3.4.1 FKD1-GFP colocalizes with endocytic marker FM4-64 at the PM

To gain further insights into the subcellular dynamics of FKD1 and its role in the endocytic pathway, homozygous lines of *Arabidopsis* seedlings expressing FKD1-GFP were treated with the fluorescent endocytic tracer FM4-64. FM4-64, a lipophilic styryl dye, is a common probe used for detection of membrane endocytosis (Jochum et al., 2002) and is internalized via a clathrin dependent process (Dhonukshe et al., 2007). FM4-64 labels the PM and is then taken into the cell interior only by endocytosis after which it gradually labels the entire endosomal pathway, which includes endosomal, prevacuolar and vacuolar compartments, over 1 to 2h (Ueda et al., 2004; Bolte et al., 2004; Tse et al., 2004; Dettmer et al., 2006; Geldner et al., 2003;

Paciorek et al., 2005, Yamada et al., 2005). Following the protocol of Geldner et al. (2003), seedlings were treated with FM4-64 for 15 minutes, rinsed with water and then observed under the microscope after 15, 30 and 45 minutes. The details of quantification of colocalization of FKD1-GFP with FM4-64 are given in Table 3.2. Fifteen min after FM4-64 treatment, FKD1 showed moderate association (PCC = 0.27 ± 0.30, n = 15), and remained similar through subsequent time intervals (Table 3.2). Throughout, most of the colocalization was seen at the PM and only a very small percentage (2% of punctae at 15 min, 4% of punctae at 30 min and 6% of punctae at 45 min in 15 cells) of FKD1 punctae was labeled with FM4-64 (Figures 3.6 C,F,I). The low level of FKD1 punctae localizing with FM4-64 suggests that FKD1 is not involved in endocytosis.

3.5 FKD1 colocalizes with SFC/VAN3 (ARF-GAP)

Previous experiments using transient expression in the leaf epidermis of *Nicotiana bethamiana* showed that FKD1/VAB-YFP and SFC/VAN3-GFP colocalized to dot-like structures (Naramoto et al., 2009). To confirm that FKD1 and SFC colocalize in Arabidopsis, I created stable transgenic lines expressing FKD1-GFP and SFC-YFP and analyzed their localization patterns. FKD1-GFP was shown to colocalize strongly with SFC-YFP in cotyledon epidermal cells (PCC = 0.69 ± 0.21, n = 36) and root epidermal cells (PCC = 0.73 ± 0.15, n = 10) (Figure 3.7 C and Table 3.1), providing further evidence that SFC may be acting with FKD1.

3.6 SFC colocalizes with makers of endomembrane compartments

The results mentioned in section 3.5 indicate that, as in *Nicotiana bethamiana*, FKD1 colocalizes with SFC in *Arabidopsis*. SFC/VAN3 has been shown to

localize to the PM (Naramoto et al., 2010) as well co-localizing with SYP41, suggesting that it also resides in the TGN/EE (Koizumi et al., 2005; Naramoto et al 2009). It had been suggested that SFC (ARF-GAP) and GN/EMB30 (ARF-GEF) might be acting in opposing pathways (Sieburth et al., 2006). GNOM (ARF-GEF) is localized at the GA, indirectly regulating recycling of PIN and other proteins to PM (Naramoto et al., 2014). Hence, to confirm the subcellular localization, I analyzed the colocalization pattern of SFC-YFP with ST-RFP (Golgi marker) in the transient system and observed negative association of SFC-YFP and ST-RFP (PCC = -0.26 ± 0.14, n = 16) The stable expression system was used to analyze the colocalization of SFC-YFP and SYP61-CFP (TGN marker), which showed moderate association (PCC = 0.69 ± 0.21, n = 33) (Figure 3.7 K), confirming previous studies. To gain further insights about the role of SFC in the endocytic pathway, homozygous lines of *Arabidopsis* seedlings expressing SFC-YFP were treated with the fluorescent endocytic tracer FM4-64. Like FKD1-GFP, SFC/VAN3 showed moderate association with FM4-64 after 15 (PCC = 0.20 ± 0.11, n = 15) of FM4-64 treatment. However, VAN3/SFC showed strong association with FM4-64 labeled vesicles after 30 min (PCC = 0.48 ± 0.23, n = 15) and 45 min (PCC = 0.50 ± 0.14, n = 15).(Figures 3.8 C,F,G). Similar to FM4-64 localization with FKD1, much of the localization of SFC with FM4-64 was seen at the PM, and few vesicles were seen associated with FM4-64 labeled vesicles at early time points (at 15 min, 7% of punctae in 15 cells). The higher colocalization at later time points (at 45min 23% of punctae in 15 cells) suggests that VAN3/SFC may localize to late endosomes as well as TGN/EE.

3.7 FKD1 and SFC punctae are partially insensitive to BFA

BFA is an excellent tool to study protein trafficking as it inhibits intracellular trafficking. BFA specifically targets certain ARF-GEFs, including GNOM, thus inhibiting the function of ARF-GTPases and thereby affecting trafficking processes. BFA blocks trafficking from endosomes to PM,, but not the first internalization steps in endocytosis (Šamaj, et al., 2004). BFA causes the accumulation of PM proteins into large aggregates known as BFA compartments or BFA bodies (Geldner et al., 2001). Of eight ARF-GEFs in plants, BFA inhibits the action of five ARF-GEFs simultaneously. Genetic evidence from the opposing vascular phenotypes produced by *sfc* and *gn* mutants (Sieburth et al., 2006) suggests that SFC/VAN3 (ARF-GAP) might be functioning in a pathway opposing the GN/EMB30 (ARF-GEF). SFC/VAN3 and GNOM have been shown to colocalize at endocytic sites at the PM (Naramoto et al., 2010). Hence, it had been suggested that SFC/VAN3 might negatively regulate the same ARF that is regulated by GN/EMB30, while no molecular evidence for that regulation exists.

Since I have shown that FKD1 associates with SFC/VAN3, an ARF-GAP, and ARF1 proteins being the likely substrates of SFC action, it seems that FKD1 might associate with an ARF-GEF and hence might show BFA sensitivity. The epidermal pavement cells (cotyledons) of FKD1-GFP when treated with BFA (50 mM for 3 h) resulted in slightly larger FKD1 vesicles in comparison to the untreated cells. BFA treated cells have 32% FKD1 punctae greater than 2 μm size (Figure 3.9.B) compared to untreated samples, which have only 12% cells with FKD1-GFP punctae

of the same size (Figure 3.9.A). Although their morphology changes somewhat, FKD1 vesicles do not aggregate into typical BFA compartments and thus can be considered BFA resistant.

Comparison of untreated and BFA treated seedlings expressing FKD1-GFP indicates no difference in localization of FKD1-GFP and in morphology of FKD1-GFP compartments in the root tissues, which suggests that FKD1 compartments are insensitive to BFA treatment in root tissues (Figures 3.9.C,D). BFA treatment of seedlings expressing SFC-YFP did not change the localization or the morphology of SFC labeled vesicles in the root tissues (Figures 3.9.E,F). To further determine whether the FKD1-SFC complex is sensitive to BFA, seedlings expressing FKD1-GFP and SFC-YFP were treated with BFA and compared with untreated ones. No difference was observed either in the morphology of vesicles labeled with both FKD1 and SFC or in the colocalization pattern of the two proteins (Table 3.1 and Figures 3.10.G,H). These results suggest that FKD1 and SFC compartments are insensitive to BFA. GNOM (ARF-GEF) being one of the most sensitive targets, the insensitivity of BFA and FKD1 and SFC to BFA suggests that they might be involved in trafficking pathways that do not involve GNOM.

3.8 FKD1 colocalizes strongly with ARF1 proteins

Supporting prior interaction of FKD1/VAB-YFP and VAN3/SFC-GFP in *Nicotiana benthamiana* leaf epidermis by Bimolecular fluorescence complementation (BiFC) in Arabidopsis protoplasts (Naramoto et al., 2009), I have shown that a proportion of FKD1 colocalizes with SFC. SFC/VAN3 is an ACAP-type

ARF-GAP, and ARF proteins are potential substrates of ARF-GAPs. However, the ARF proteins on which SFC acts is not known. To assess if FKD1, which forms a complex with SFC, might associate with ARF1 proteins, the potential substrates of SFC, transient expression of FKD1-GFP with four members of the ARF gene family (ARFA1a, ARFA1c, ARFA1d and ARFA1e)-YFP was done in *Nicotiana tabacum*. FKD1 shows strong colocalization with ARFA1a, ARFA1c and ARFA1d, and moderate localization with ARFA1e (Table 3.1 and Figures 3.11C,G,K,O). At-ARFA1c-glutathione S-transferase fusion protein localizes to Golgi as evident by immunogold electron microscopy (Pimpl et al., 2000) and immunofluorescence (Stierhof and El-Kasmi, 2010; Ritzenthaler et al., 2002). ARF1A1c was suggested to be required for clathrin coated vesicle formation at TGN (Pimpl et al., 2003) and is known to localize with TGN markers, SYP61-CFP and VHA-a1-GFP (Paciorek et al., 2005; Stefano et al., 2006; Tanaka et al., 2009). Hence, to understand the site of action of the most studied ARF1 member in Arabidopsis and due to the lack of availability of appropriate fluorophore for TGN markers in transient analysis, I analyzed the subcellular localization of ARF1A1c with ST-RFP. Co-localization of ARFA1c-YFP with ST-RFP revealed only weak association to Golgi (Figure 3.11.S), which is consistent with ARF1A1c predominantly localizing to TGN. The fact that FKD1 and SFC complex forms at the TGN and the strong association of FKD1 with ARF1 proteins, fits with the idea that FKD1 protein might be acting together with SFC (ARFGAP) and could influence the interaction of SFC with ARF1.

3.9 FKD1 and SFC/VAN3 colocalize with PIN1

FKD1 is important to establish the asymmetrical basal PIN1-GFP membrane localization in provascular cells which allows narrowing of PIN1-GFP expression domains (Hou et al., 2010). Similarly, it has been reported that SFC/VAN3 is involved in the maintenance of continuous PIN1 expression domains in the leaf primordia (Scarpella et al., 2006) through the polar localization of PIN1 proteins. The increased discontinuities in leaf vein patterning of *fkd1sfc* compared to single mutants (Steynen and Schultz, 2003; Naramoto et al., 2009) and the similarly abnormal PIN1 expression in *sfc* and *sfcvab* mutants suggest FKD1/VAB and SFC/VAN3 act at the same point of the pathway, an idea supported by the finding that FKD1 and SFC interact (BIFC) (Naramoto et al., 2009). Based on defective PIN1 protein localization in *fkd1* mutants, I speculated that FKD1 and SFC/VAN3 might function in intracellular trafficking of PIN1 proteins and hence might colocalize with PIN1 in endosomal compartments. In order to investigate this, stable transgenic lines of Arabidopsis expressing FKD1-GFP and PIN1-RFP or SFC-YFP and PIN1-RFP were created and localization was analyzed in root tissues and hypocotyledons. For quantification of colocalization in roots, Pearson's coefficient of correlation (PCC) was measured over the entire image, to take into account both punctate and membrane localization. In hypocotyls, chloroplast autofluoresence appears in both GFP and RFP channels (arrowheads in Figure 3.12). To eliminate chloroplasts in hypocotyeldon cells, quantification of colocalization was done by manual counting of vesicles less than 2 μm in size. In roots, FKD1-GFP associates moderately with PIN1-RFP (Figures 3.12 C,F and Table 3.1), whereas SFC-YFP shows weak association with

PIN1-RFP (Figure 3.12 I and Table 3.1). The results from manual counting in hypocotyls indicate that over half the proportion of FKD1 and SFC in punctae colocalizes with PIN1 proteins. The colocalization of both FKD1 and SFC with PIN1 proteins, together with the defects in PIN1 localization in mutants are consistent with the idea that these proteins act within the endomembrane system to appropriately traffic PIN1 proteins.

To investigate the role of FKD1 in PIN1 endocytosis, stable lines expressing FKD1-GFP and PIN1-RFP were treated with BFA. Long-term treatment of plants expressing FKD1-GFP and PIN1-RFP with BFA (mM for 3hr) resulted in association of PIN1 in BFA compartments (Figure 3.13.C). Quantification of colocalization (PCC=-0.17) showed negative association of FKD1-GFP and PIN1-RFP, however results from manual counting suggests that a small subset of FKD1-GFP (18%) labeled vesicles remained associated with PIN1 proteins outside the BFA compartments. Quantification (manual counting) of FKD1 vesicles associating with PIN1-RFP in root tissues before and after BFA treatment showed a significant difference (Table 3.1). These results suggest that a proportion of PIN1 proteins might be associating with FKD1 and that FKD1 may traffic PIN1 through both BFA-sensitive and BFA insensitive pathways.

Table 3.1: Correlation of expression between the intensities of A) FKD1-GFP or B) SFC-YFP together with different proteins fused to YFP or RFP in various tissues of stably transformed leaf epidermis (Arabidopsis seedling at 2.5 DAG) or in transiently transformed (*N. tabacum*) leaf epidermis. PCC is the mean of PCC from all merged images and determined using colocalization plugin in NIH image J, while % punctae colocalizing was counted manually in hypocotyledons or root.

A) Colocalization of FKD1-GFP with	Sample size (n)	Tissue type	Mean PCC	% puncta
SFC-YFP	36	Arabidopsis cotyledon	0.69 ± 0.21	93.18
SFC-YFP (BFA untreated)	10	Arabidopsis root	0.73 ± 0.15	
SFC-YFP (BFA treated)	10	Arabidopsis root	0.63± 0.14	
ST-RFP	17	*N. tabacum*	-0.30± 0.12	60.07
SYP61-YFP	32	*N. tabacum*	0.37± 0.10	54.99
VTI12-YFP	30	Arabidopsis cotyledon	0.39 ± 0.20	37.47
YFP-RabA1e	42	Arabidopsis cotyledon	0.60 ± 0.18[b]	39.26
YFP-RabA1g	20	Arabidopsis cotyledon	0.85± 0.17[a]	
YFP-RabF2b	19	Arabidopsis cotyledon	0.68 ± 0.17[b]	
YFP-NPSN12	26	Arabidopsis cotyledon	0.16 ± 0.25	100
YFP-NPSN12 after plasmolysis	26	Arabidopsis cotyledon	0.15 ± 0.35	
YFP-PIP1;4	16	Arabidopsis cotyledon	0.32 ± 0.20	
YFP-PIP1;4 after plasmolysis	16		0.16 ± 0.40	
ARFA1a-YFP	24	*N. tabacum*	0.66 ± 0.25	100
ARFA1c-YFP	23	*N. tabacum*	0.63 ± 0.13	100
ARFA1d-YFP	23	*N. tabacum*	0.76 ± 0.15	100
ARFA1e-YFP	30	*N. tabacum*	0.43 ± 0.29	100
PIN1-RFP	30	Arabidopsis root	0.50 ± 0.17[c]	67.30[c]
	18	Arabidopsis hypocotyledons		68.85
PIN1-RFP (BFA treatment)	15	Arabidopsis root	-0.017± 0.18[d]	18[d]
B) Colocalization of SFC-YFP with				
ST-RFP	16	*N. tabacum*	-0.26± 0.14	
SYP61-CFP	33	Arabidopsis cotyledon	0.69 ± 0.21	67.13
PIN1-RFP	27	Arabidopsis root	0.11 ± 0.34	55.19
PIN1-RFP	17	Arabidopsis hypocotyledon		65.30

[a] is significantly different from [b], [c] is significant differently from [d] (Fisher's test on raw data, $p<0.05$).

Table 3.2: Correlation of expression between FKD1-GFP or SFC-YFP and FM4-64 labeled vesicles at different time intervals. PCC is the mean of PCC from all merged images and determined using colocalization plugin in NIH image J. Percentage FKD1-GFP punctae or SFC-YFP punctae colocalizing with FM4-64 labeled vesicles were counted manually. The same images (n=15) were used for PCC and % measurements.

Constructs	FM4-64 (15 min)	FM4-64 (30 min)	FM4-64 (45 min)
FKD1-GFP	0.27 ± 0.30	0.27 ± 0.29	0.26 ± 0.30
SFC-YFP	0.20 ± 0.11	0.48 ± 0.23	0.50± 0. 14
FKD1-GFP	2.36%	4.31%	6.07%
SFC-YFP	7.09%	21.32%	23.25%

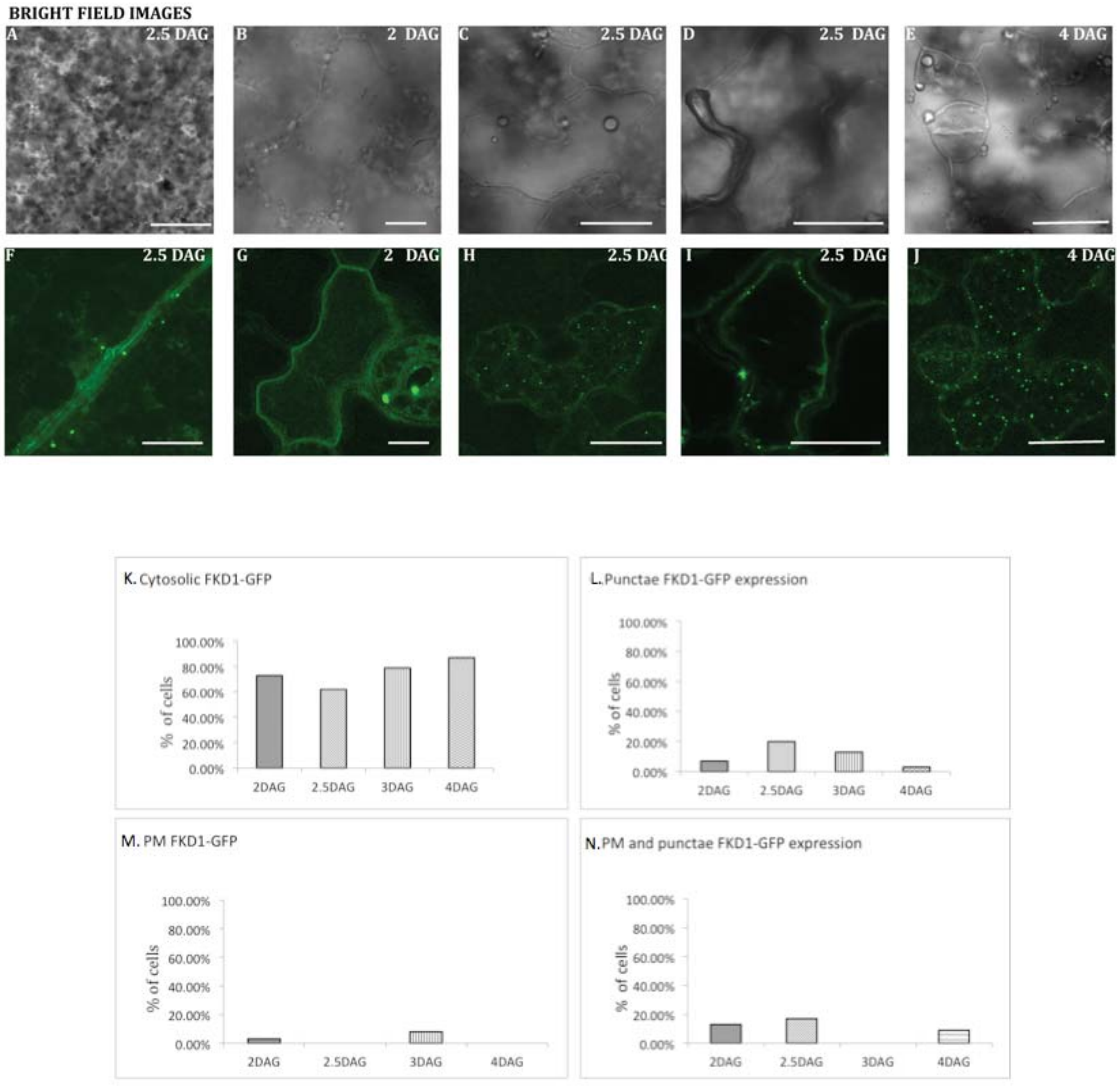

Figure 3.1: Cellular FKD1-GFP localization differs at different stages of cotyledon development.

Bright field with corresponding confocal images below(A-F), FKD1-GFP expression in root vascular tissue (F), FKD1-GFP cytosolic expression (G), FKD1-GFP punctae expression (H), FKD1-GFP PM localization (I) and FKD1GFP PM and punctae localization (J). (K-N) Graphs showing % of cells with cytosolic (K), punctae (L), PM(M) and PM and punctae (N) respectively. Scale bar 10 µm. Sample size for 2 DAG (n=22), 2.5 DAG (n=20) and for 3 and 4 DAG (n=16).

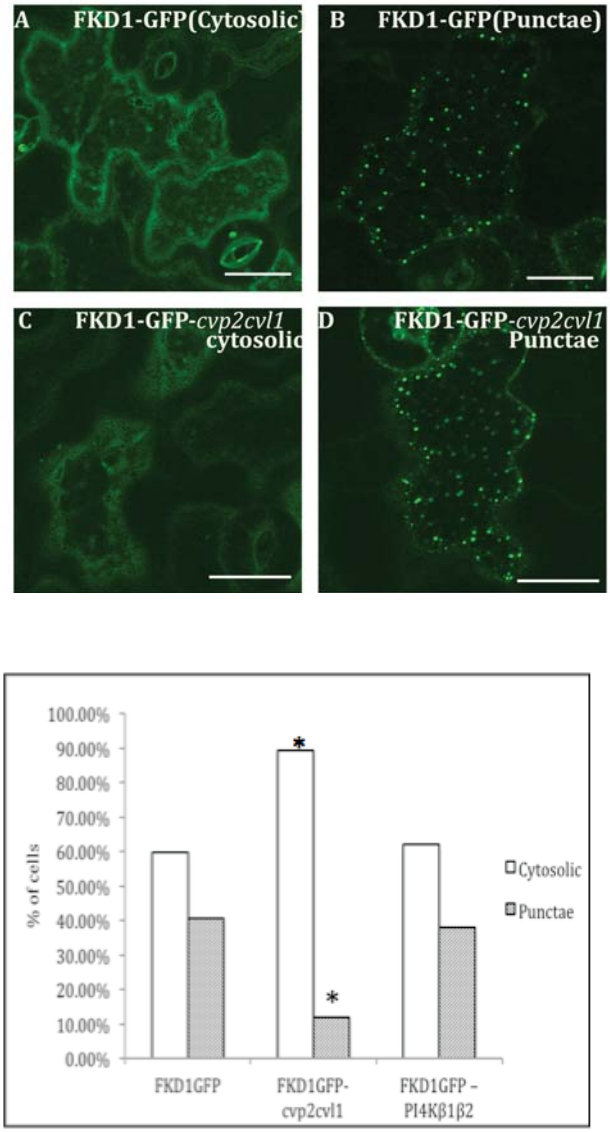

Figure 3.2: Subcellular localization of FKD1-GFP in wild type and in *cvp2cvl1* and *PI4Kβ1β2* mutant cotyledons.

Cytosolic FKD1 expression (A) and puncta FKD1-GFP expression (B) in wild type plants. Cytosolic FKD1 expression (C) and puncta FKD1-GFP expression (D) in *cvp2cvl1* mutant plants. E) Graphs representing % of cells with cytosolic and puncta FKD1-GFP expression in wild type, *cvp2cvl1* and *PI4Kβ1β2* mutants. Sample size for FKD1-GFP- n=16, for FKD1-GFP in *cvp2cvl1*-n=57 and FKD1-GFP with *PI4Kβ1β2*-n=16. (Scale bar:10μm). * represents significant difference from wild type ($p<0.05$), Fisher's test was done on raw data and % values are shown here.

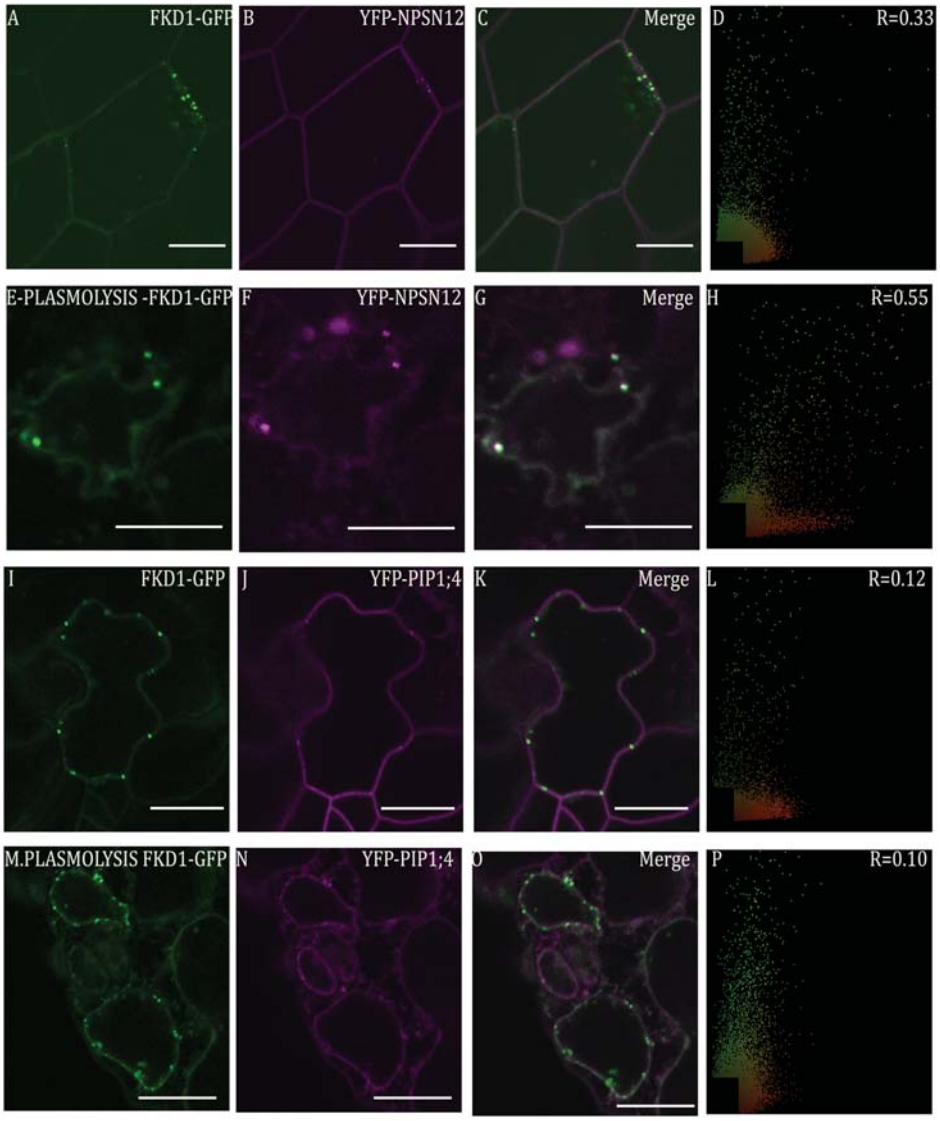

Figure 3.3: Subcellular localization of FKD1-GFP with PM markers.

Localization of FKD1-GFP with PM markers YFP-NPSN12 (A-G) and FKD1-GFP with YFP-PIP1;4, (I-O), both before (A-D; I-L) and after (E-G; M-O) plasmolysis treatment (5% NaCl, 20 min) of stably transformed Arabidopsis cotyledon pavement cells at 2.5 DAG. A, E, I & M are FKD1-GFP alone B, F, J & N are YFP-NPSN12 or YFP-PIP1;4, C, G, K and O are the merged images, D and L are scatter plots of the merged image with Pearson's coefficient of correlation (R) values (Scale bar:10μm).

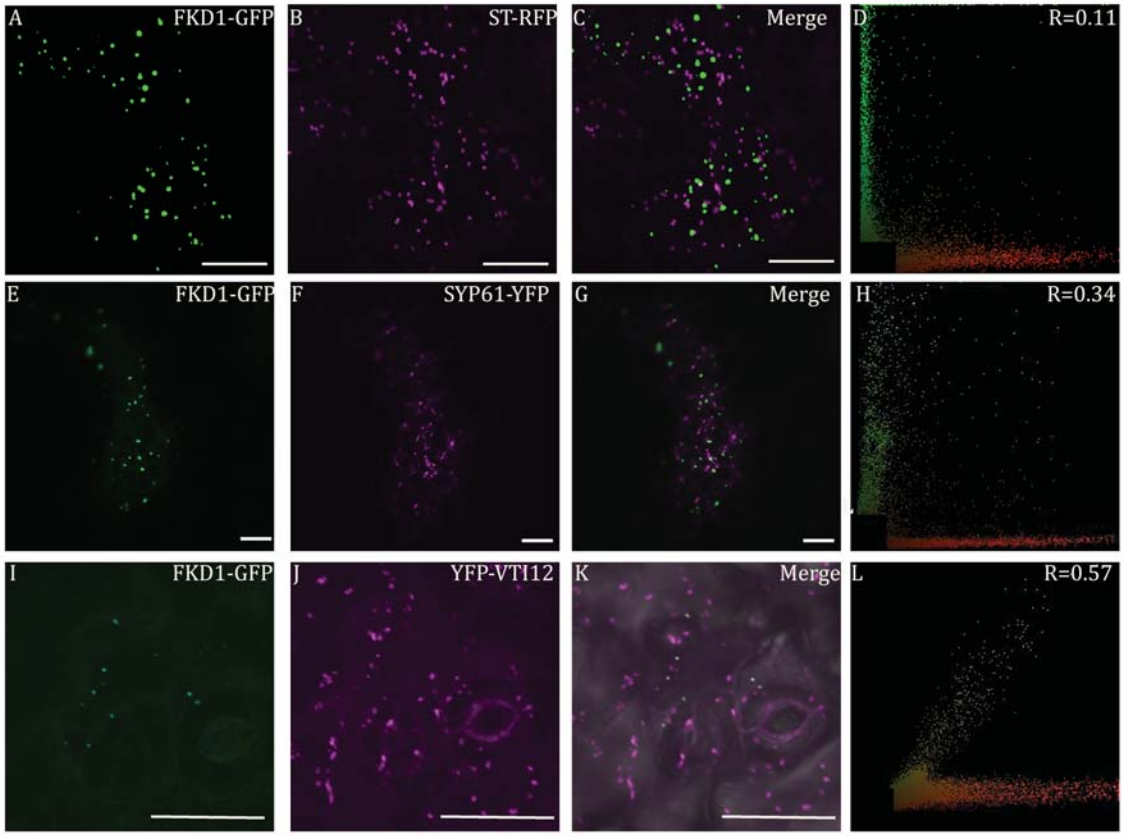

Figure 3.4: Subcellular localization of FKD1-GFP with Golgi and Trans-Golgi markers.

FKD1-GFP and Golgi marker, ST-RFP (A-D) or TGN markers SYP61-YFP (E-H) and YFP-VTI12 (I-L) were expressed transiently in Nicotiana (A-G) or stably in Arabidopsis (I-K). A, E and I are FKD1 alone; B, F and J are ST-RFP, SYP61-YFP and YFP-VTI12 respectively, C, G and K are the merged images, D, H and L are scatter plots of the merged image with Pearson's coefficient of correlation (R) values (Scale bar:10μm).

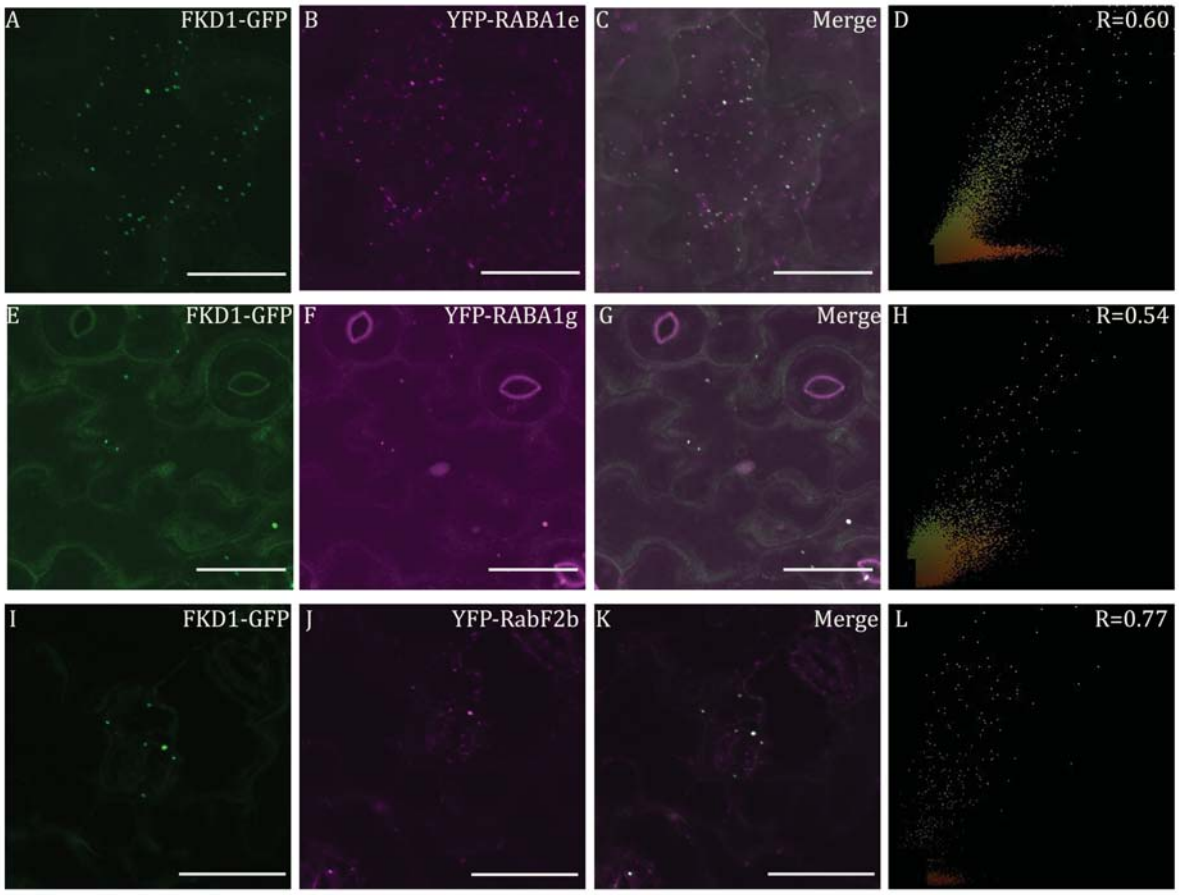

Figure 3.5: Subcellular localization of FKD1-GFP with endosome markers.

FKD1GFP with endosomal markers, YFP-RabA1e (A-D), YFP-RabA1g (E-H) and YFP-RabF2b (I-L) expressed in stably transformed Arabidopsis cotyledon pavement cells at 2.5 DAG. A, E and I are FKD1 alone; B, F and J are YFP-RabA1e, YFP-RabA1g are RabF2b respectively, C, G and K are the merged images, D, H and L are scatter plots of the merged image with Pearson's coefficient of Correlation (R) values (Scale bar:10μm).

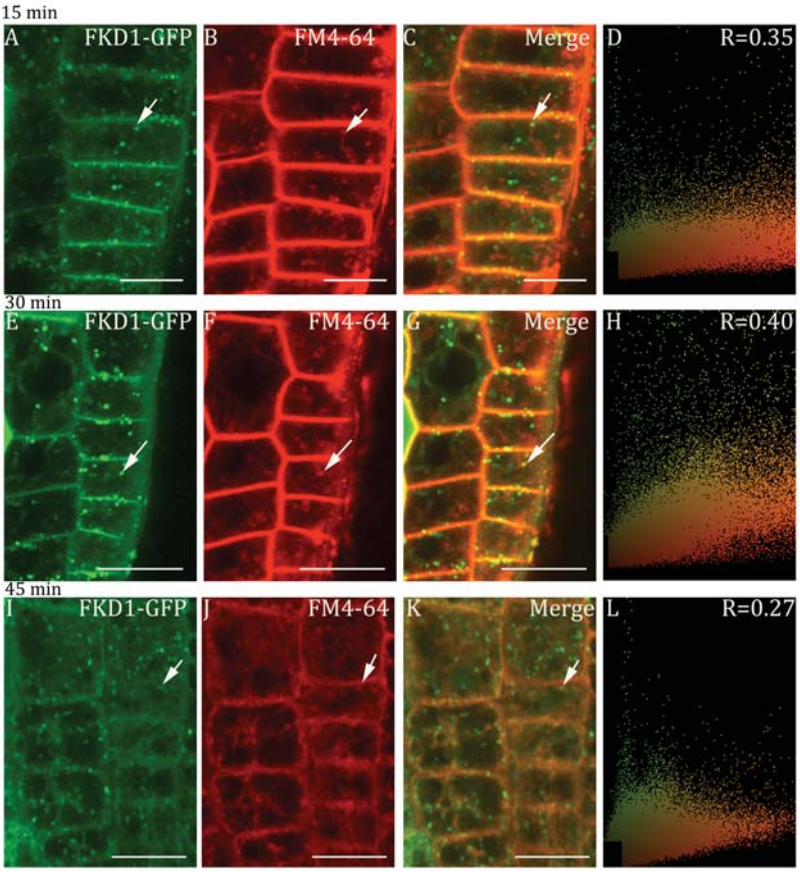

Figure 3.6: Colocalization of FKD1-GFP with FM4-64 at different time intervals.

Cells in the root elongation zone expressing FKD1-YFP stained with endocytic tracer FM4-64 after 15 min (A-D), 30 min (E-H) and 45 min (I-L). A, E and I are FKD1-GFP alone; B, F and J are FM4-64 alone; C, G and K are the merged images. D, H and L are scatter plots of the merged image with Pearson's coefficient of correlation (R) values. Arrows indicate punctae that are labeled by both FKD1-GFP and FM4-64 (Scale bar:10μm).

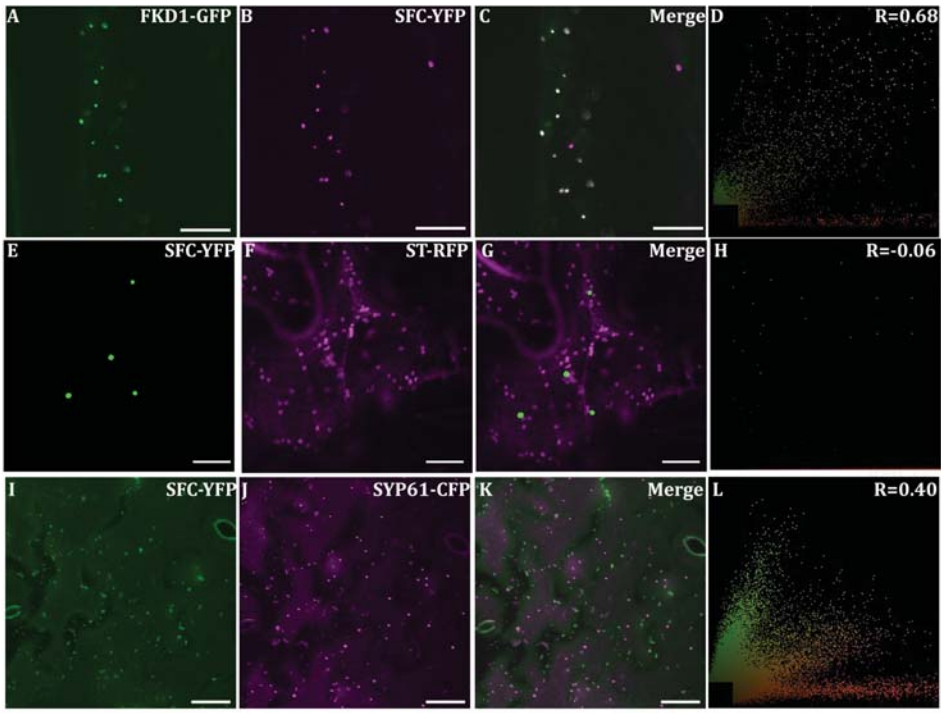

Figure 3.7: Subcellular localization of FKD1-GFP or SFC-YFP with either ST-RFP or SYP61-CFP.

FKD1GFP with SFC-YFP (A-D) and SFC-YFP with either Golgi marker ST-RFP (E-H) or SYP61-CFP (I-L) were expressed in stably transformed Arabidopsis (A-C; I-K) cotyledon pavement cells and in Nicotiana(E-G). A is FKD1 alone; B, E & I are SFC-YFP alone, F & J are ST-RFP and SYP61-YFP respectively. C, G and K are the merged images. D, H and L are scatter plots of the merged image with Pearson's coefficient of correlation (R) values (Scale bar:10μm).

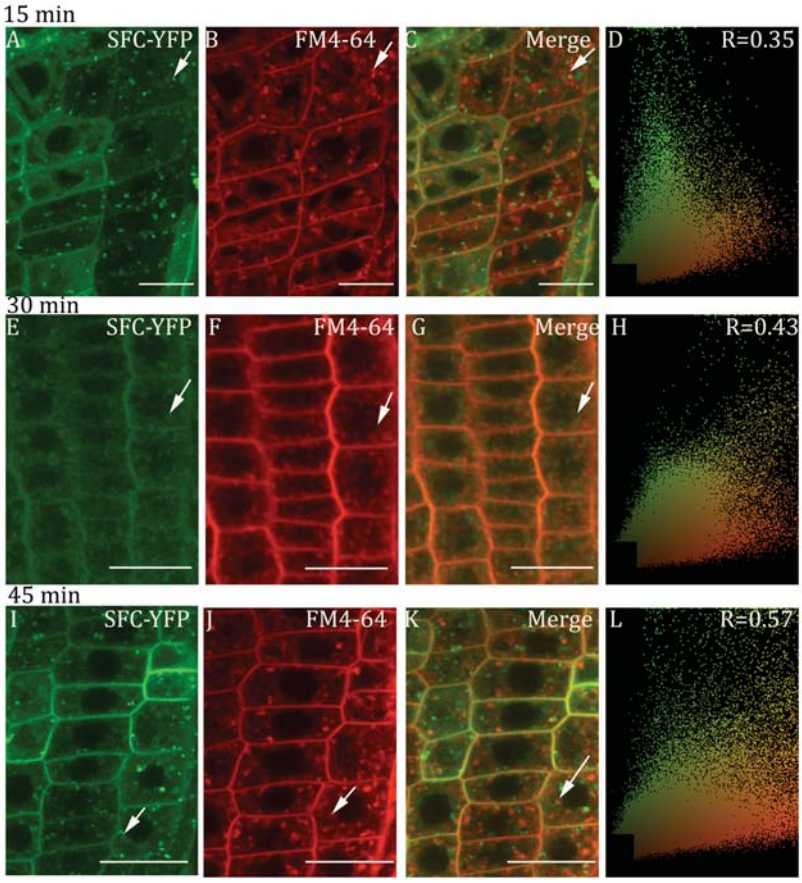

Figure 3.8: Colocalization of SFC-YFP with FM4-64 at different time intervals.

Cells in the root elongation zone expressing SFC-YFP stained with endocytic tracer FM4-64 after 15 min (A-D), 30 min (E-H) and 45 min (I-L). A, E and I are SFC-YFP alone; B, F and J are FM4-64 alone; C, G and K are the merged images. D, H and L are scatter plots of the merged image with Pearson's coefficient of correlation (R) values. Arrows indicate punctae that are labeled by both FKD1-GFP and FM4-64 (Scale bar:10μm).

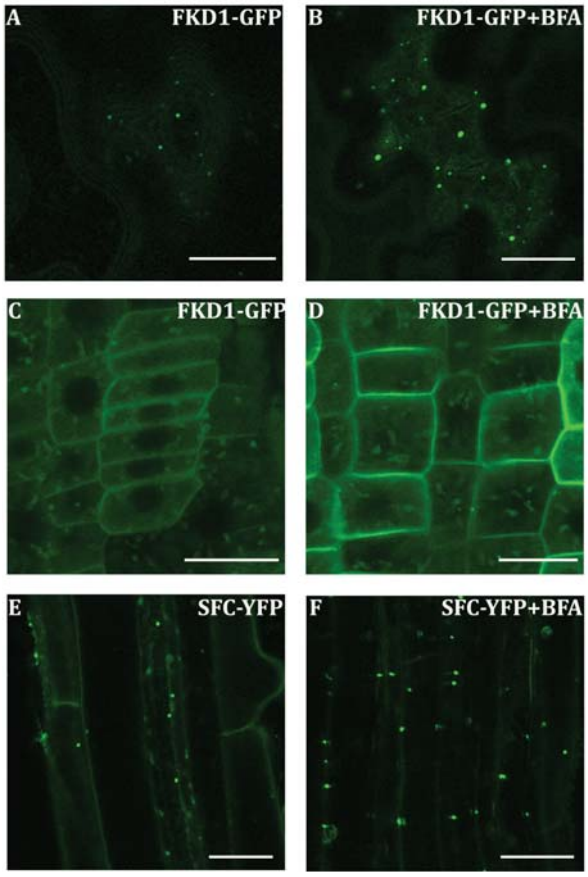

Figure 3.9: Subcellular localization of FKD1-GFP or SFC-YFP after BFA treatment.

FKD1-GFP (A-D) and SFC-YFP (E-F) were expressed in Arabidopsis cotyledon epidermis (A-B) or roots (C-F) and examined before (A, C, E) or after (B, D, F) BFA treatment (50 mm for 2h).

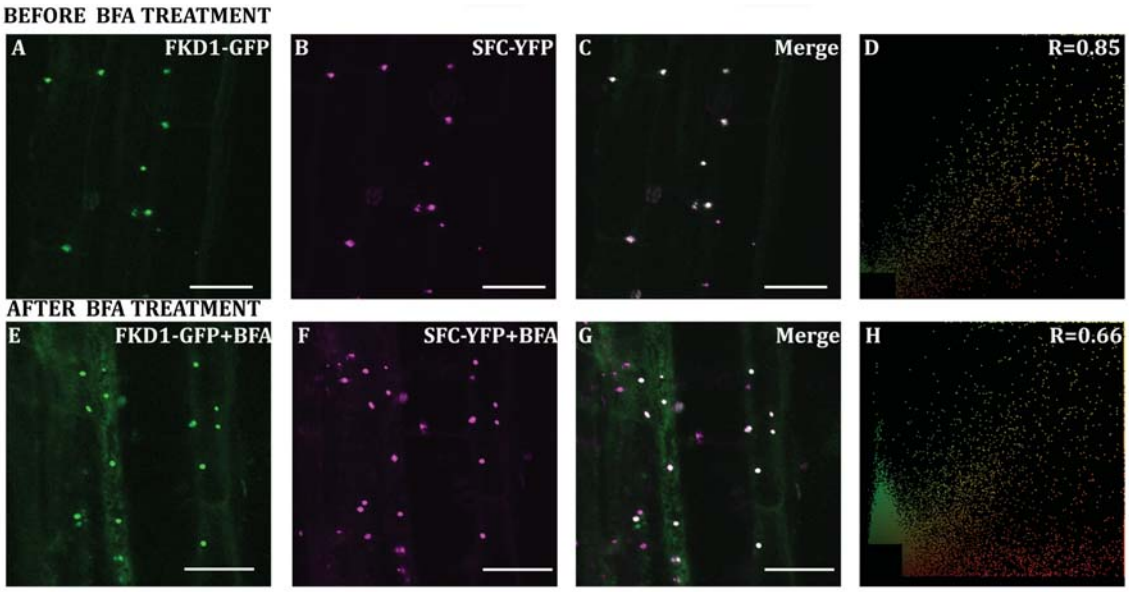

Figure 3.10: Subcellular localization of FKD1-GFP with SFC-YFP without and with BFA treatment.

Localization of FKD1-GFP with SFC-YFP without (A-C) and with (E-G) BFA treatment (50 mm for 2h) in root tissues of stably transformed Arabidopsis seedlings at 2.5DAG. A and E are FKD1GFP alone; B and F are SFC-YFP alone; C and G are the merged images; D and H are scatter plots of the merged image with Pearson's coefficient of correlation (R) values (Scale bar:10μm).

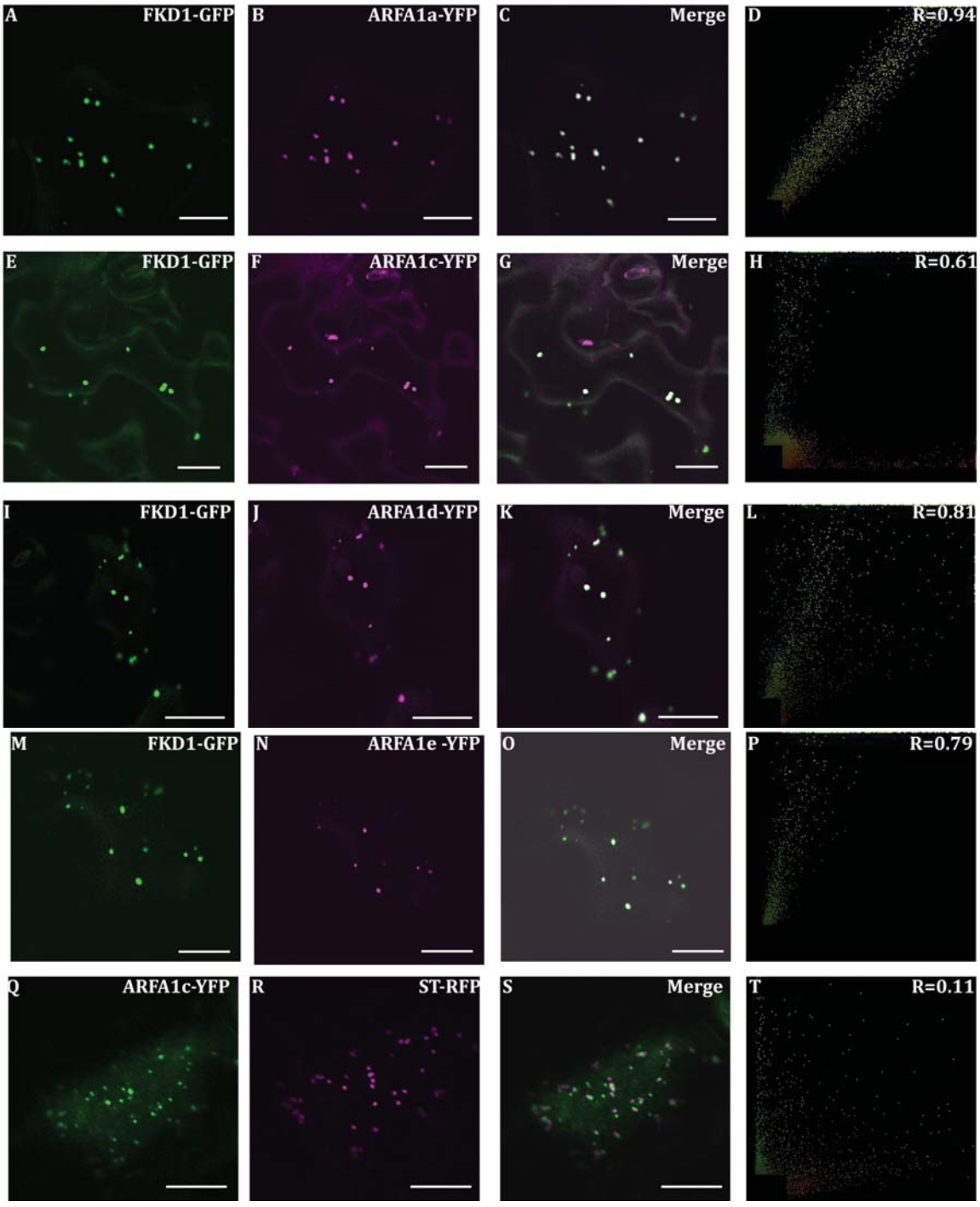
A FKD1-GFP
B ARFA1a-YFP
C Merge
D R=0.94
E FKD1-GFP
F ARFA1c-YFP
G Merge
H R=0.61
I FKD1-GFP
J ARFA1d-YFP
K Merge
L R=0.81
M FKD1-GFP
N ARFA1e -YFP
O Merge
P R=0.79
Q ARFA1c-YFP
R ST-RFP
S Merge
T R=0.11

Figure 3.11: Subcellular localization of FKD1-GFP with ARF1 proteins and ARF A1c with Golgi marker, ST-RFP.

FKD1-GFP with ARFA1a (A-D), ARFA1c (E-G), ARFA1d (I-K), ARFA1e (M-O) or ARFA1c with ST-RFP (Q-S) transiently expressed in Nicotiana. A, E, I and M are FKD1 alone; B, F, J and N are ARFA1a, ARFA1c, ARFA1d and ARFA1e fused to YFP. Q and R are ARFA1c-YFP and ST-RFP respectively. C, G, K, O and R are the merged images. D, H, L, P and T are scatter plots of the merged image with Pearson's coefficient of correlation (R) values (Scale bar:10μm).

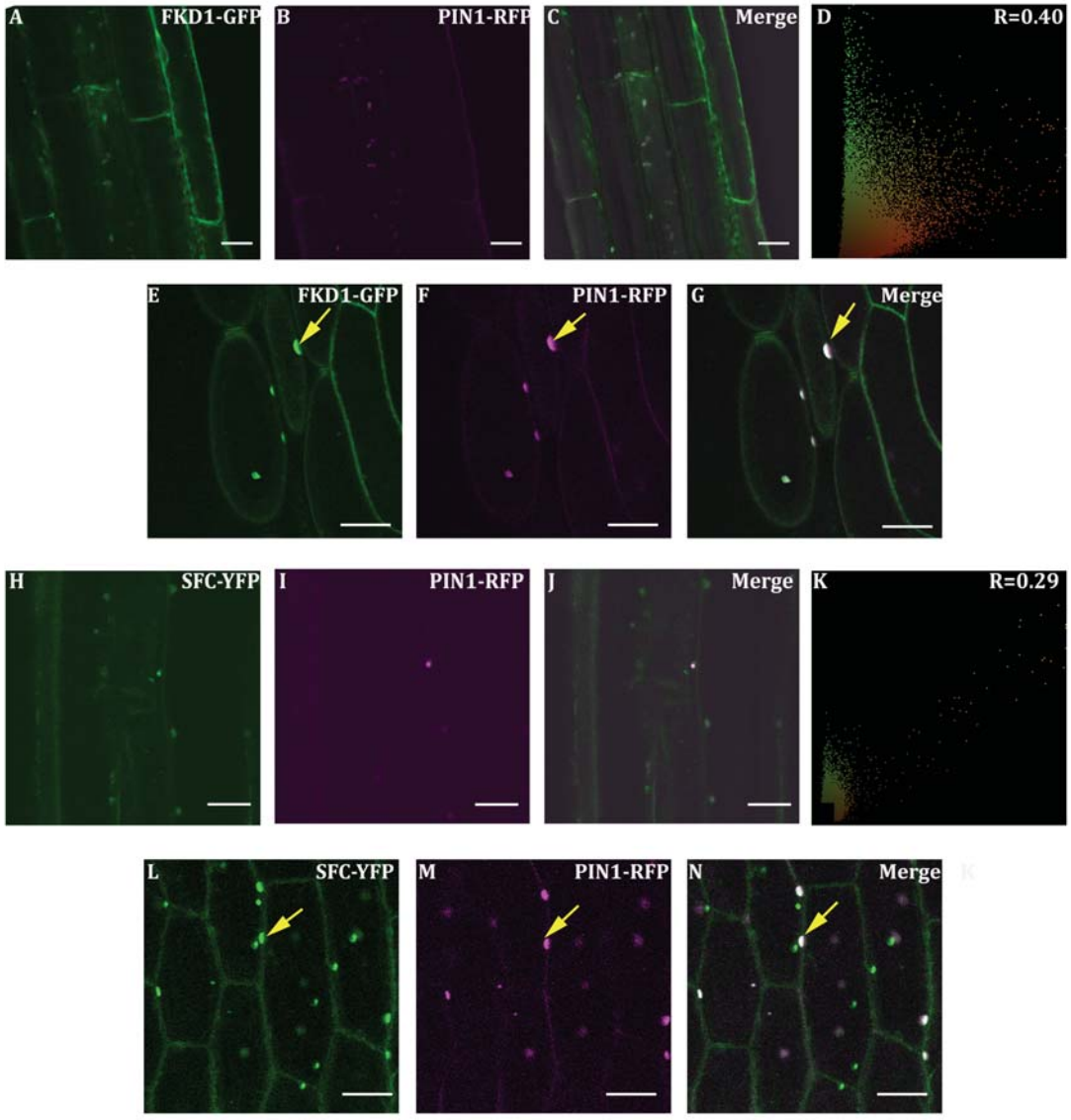

Figure 3.12: Subcellular localization of FKD1-GFP or SFC-YFP with PIN1-RFP.

FKD1-GFP and PIN1-RFP (A-G) or SFC-YFP and PIN1-RFP (H-N) stably expressed in Arabidopsis root tissues (A-C, H-J) or in hypocotyledons (E-G, L-N). A & E are FKD1-GFP alone; H & L are SFC-YFP alone; B, F, I and M are PIN1-RFP; C, G, J and N are merged images. D and K are scatter plots of the merged image with Pearson's coefficient of correlation (R) values. Arrow heads indicate chloroplast (Scale bar:10μm).

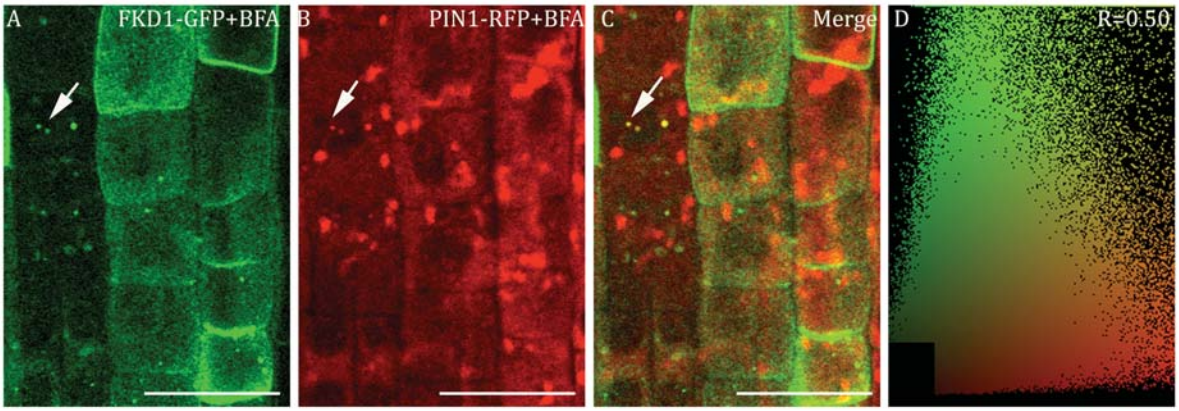

Figure 3.13: Subcellular localization of FKD1 with PIN1 after BFA treatment.

FKD1-GFP and PIN1-RFP stably expressed in Arabidopsis roots following a 3hr BFA treatment. A is FKD1-GFP, B is PIN1-RFP; C is the merged image and D is the scatter plot of merged image with Pearson's coefficient of correlation (R) values (Scale bar: 10μm).

CHAPTER 4: RESULTS

4.1 Evolution of Pleckstrin –Like/DUF 828 family in the plant kingdom

The *FKD1* gene encodes a protein with a plant specific 'Domain of Unknown function' (DUF828) and a Pleckstrin Like (PL) domain (Hou et al., 2010). DUF828 is a plant specific domain whose function has not been previously characterized and hence I sought to understand the significance of the DUF828 domain within the plant kingdom. GreenPhyl DB, a web resource for comparative and functional plant genomics (Conte et al., 2008) identifies 34 species with DUF828 encoding gene sequences available through out the plant kingdom (1 Bryophyte, 1 Lycophyte, 1 Gymnosperm and 31 Angiosperms). DUF828 appears first in the bryophyte *Physcomitrella patens* where it exists as a single copy; the lycophyte *Selaginella moellendorffii* and the gymnosperm *Picea abies* possess 4 copies of DUF 828 genes. In angiosperms, the basal angiosperm *Amborella trichopoda* possesses 4 DUF 828 genes, the monocot *Oryza sativa* possesses 8 DUF828 genes and eudicots, *Solanum lycopersicum* possesses 6 DUF 828 genes and both *Populus trichocarpa* and *Arabidopsis thaliana* possess 9 DUF 828 genes. The presence of DUF828 in the genome of *P. patens* suggests a bryophytic origin of this gene family and indicates that DUF828 has a function that predates vascular cells in plants. The conservation and expansion of the DUF 828 protein family over 400 million years of terrestrial plant evolution suggests that they must be involved in key biological functions.

GreenPhylV4 database identifies the Pleckstrin-like gene family (GP000860) as those proteins with InterPro (IPR) domain DUF 828 (IPR00856), which usually

occurs together with either or both the Pleckstrin Homology (PH) domain (IPR001849) and the Pleckstrin like (PL) domain (IPR013666). The vast majority of DUF 828 encoding proteins also contains either a PH or PL domain or both, including the ancestral sequence in *P. patens*. However, in some cases, the PH/PL domain has been lost.

To assess the relatedness amongst members of the protein family, I undertook a phylogenetic analysis using GreenPhylDB, which utilizes PHYML software (Guindon et al., 2005) a maximum-likelihood tree reconstruction method employing the Neighbor-Joining tree algorithm. A phylogenetic tree (Figure 4.1) was created using proteins from species representative of key groups including *P. patens*, *S. moellendorffii*, *P. abies*, *A. trichopoda, O. sativa, S. lycopersicum, P. trichocarpa* and *A. thaliana.* GreenPhylDB divides DUF 828 family proteins into three major groups (I–III), with Group III being further divided into three subgroups (A, B, C) (Figure 4.1.A). Group I is well supported (branch support 0.827), and consists of a single protein sequence from *P. abies*. Group II is poorly supported (branch support 0.172) and includes only sequences from *O. sativa* and *S. lycopersicum*. Group III is strongly supported (branch support 0.997) and includes sequences from all species included in my analysis. It is further divided into 3 subgroups: Group IIIA, Group IIIB and Group IIIC each of which is very strongly supported. Group IIIA forms a monophyletic angiosperm specific group with one protein (At5g57700) from Arabidopsis, along with one protein from each of *S. lycopersicum*, *P. trichocarpa* and the basal angiosperm *A. trichopoda.* Group IIIB is the largest and contains proteins from basal species (*P. patens* (1 protein)*, S. moellendorffii* (4 proteins) and *P. abies (3*

proteins) as well as from angiosperms (*A. trichopoda,* 1 protein; *P. trichocarpa*, 4 proteins; *S. lycopersicum*, 2 proteins; *O. sativa*, 3 proteins; *A. thaliana*, 4 proteins). Group IIIC forms a second angiosperm specific monophyletic group (branch support 0.947) including FKD1 (At3g63300) and three other proteins (At5g43870, At4g14740 and At3g22810) in *Arabidopsis thaliana* along with sequences from *A. trichopoda* (1 protein), *S. lycopersicum* (2 proteins), *P. trichocarpa* (4 proteins), and *O. sativa* (3 proteins).

4.2 Phylogenetic analysis of Arabidopsis DUF828 gene family

As described in section 4.1, a GreenPhylDB search retrieved nine proteins from Arabidopsis all of which possess DUF828, or DUF828 with PL or DUF 828 with PH and PL domains. To understand the evolutionary relationship between individual members, a phylogram was constructed using the full-length protein sequence of all Arabidopsis proteins within the Pleckstrin like family (Figure 4.1.B). On the basis of their relation with the *FKD1* gene (Hou et al., 2010), all the other members were named as *FKD-Like (FL) 1-8* and these eight genes, along with FKD1, were named the Arabidopsis DUF828 gene family. The Arabidopsis groups (Figure 4.1.B) correspond to the groups described in Figure 4.1.A. No members of Groups I and II are found in Arabidopsis, but all 3 Group III subgroups are represented. Group IIIA consists of only one protein At5g57770 (FL8), which is most divergent from the rest of the family. Group IIIB has four members; three of them (At4g17350/FL5, At4g47440/FL6 and At4g16670/FL7) possess DUF 828 and PH and PL domains and one member (At4g32780/FL4) is an outlier and possesses only a DUF 828 domain.

Group IIIC consists of FKD1 (At3g63300) and three proteins (At5g43870/FL1, At3g22810/FL2 and At4g14740/FL3). Within this group, FKD1 is the most divergent, and FL2 and FL3 the most similar.

Multiple sequence alignment of full-length amino acid sequence of FKD1 with members of the DUF828 family is shown in Figure 4.2 and domain organization in Table 4.1. Indicative of their similarity, the PH and PL domains overlap (Table 4.1) *FKD1* and the members of Group IIIC (FL1, FL2 and FL3) showed greater than 50% sequence identity over the entire sequence and higher identity in DUF828 and PL/PH domains (Table 4.1). The remaining five members (FL4-FL8) exhibited identity with FKD1 ranging from 17-35% in DUF828 and PL/PH domains (Table 4.1). One of the common features that is observed in many multigene families is redundancy in function (Overvoorde et al., 2005). Based on the sequence identity and the presence of conserved domains in members in DUF828 gene family, I speculated that they might be acting in a redundant manner. Hence, I focused on elucidating the biological and cellular function of these members of the DUF828 gene family. To begin with, I focused on understanding the cellular localization of members of FKD1 gene family.

4.3 DUF828 gene family members show variable localization to Golgi

To understand the cellular localization of the DUF828 gene family, I generated fusions of 5 members (FL1, FL3, FL5, FL6, and FL7) of the family to YFP and transformed them into Nicotiana or wild type Arabidopsis (FL3). All the members of the DUF828 gene family showed punctate expression similar to FKD1.

Based on the results of section 3.1, FKD1-GFP shows negative association with the Golgi marker (ST-RFP) (PCC= 0.11± 0.20, n=19). To establish if other members of the DUF 828 gene family localize to the Golgi, colocalization of the DUF 828 gene family members fused to YFP with ST-RFP was performed. Among Group IIIB members, FL6 and FL7 showed moderate colocalization with ST-RFP (PCC= 0.39 ± 0.17, n=19 and PCC= 0.11± 0.16, n=19 respectively) and FL5 was an outlier, showing strong co-localization with ST-RFP (PCC= 0.54± 0.22, n=19) (Table 4.2 and Figure 4.3.K). Group IIIC (FL1 and FL3) showed moderate colocalization with ST-RFP (PCC= 0.11± 0.20, n=19 and PCC= 0.25 ± 0.10, n=19) (Figures 4.2. C,G,O,S). I attempted to localize the members of FKD1 gene family with TGN marker (SYP61-RFP), however due to the weak expression of SYP61-RFP, I was not able to do colocalization experiments in *Nicotiana*. Because I was able to generate stable transformants of Arabidopsis with FL3, I was able to assess the colocalization with SYP61-CFP. FL3 (Group IIIC), like FKD1-GFP, showed moderate colocalization with SYP61(PCC= 0.33± 0.11, n=18). From these results it can be concluded that i) except for FL6, which showed strong Golgi association, the remaining members of the DUF828 gene family show a similar localization pattern relative to Golgi and ii) among members of Group IIIB, even though FL5 and FL6 are highly similar, they show divergent localization to Golgi, which suggests that sequence identity is not a good predictor of this localization.

4.4 DUF 828 gene family members colocalize with FKD1

To further delineate the cellular localization of the DUF 828 gene family members and to determine whether they might act redundantly with FKD1, I analyzed their co-localization with FKD1. Transient and stable expression systems were used to study co-localization patterns of the DUF 828 gene family members fused to YFP with FKD1-GFP. Among DUF 828 gene family members, FL1 (Group IIIC), showed very strong co-localization with FKD1-GFP (PCC= 0.95± 0.03, n= 28) (Table 4.3, Figure 4.4.C). The very strong colocalization of FL1 with FKD1 is not unexpected considering that FL1 has high sequence identity to FKD1. FL6 and FL7 (Group IIIB) showed strong co-localization with FKD1-GFP (PCC= PCC=0.75 ± 0.17, n= 24 and PCC=0.62 ± 0.25, n= 29 respectively) (Figures 4.4.S,W), even though their sequences are quite divergent from FKD1. FL3 (Group IIIC) showed moderate co-localization with FKD1-GFP in both transient (PCC=0.47± 0.30, n=24) and stable (PCC= 0.47 ± 0.24, n=21) expression systems (Table 4.3 and Figures 4.3.G,K) and FL5 (Group IIIB) showed moderate colocalization in transient expression (PCC=0.40± 0.20, n=34). The moderate to strong localization patterns of several DUF 828 gene family members with FKD1 supports the idea that they might be functionally redundant and acting in a similar pathway.

4.5 Mutations to DUF 828 gene family members enhance the *fkd1* leaf vein pattern phenotype

Mutation to the *FKD1* gene results in cotyledons and leaves with open venation due to lack of distal junctions between secondary and tertiary veins (Steynen and Schultz, 2003). Hence I focused on understanding the effect of knocking out multiple genes of the DUF 828 family on leaf vascular development in comparison with wild type *Arabidopsis thaliana.* Salk lines (T-DNA insertion mutants) were identified for five members of the DUF 828 family and the position (exon/intron or promoter region) of T-DNA insertions used in this study is given in Table 2.2. Based on the information obtained from the phylogenetic tree and co-localization with FKD1, I focused on analyzing leaf vascular patterning defects of two groups of DUF 828 gene family members: Group IIIC comprising of members FL1, FL2 and FL3 that are highly similar to FKD1 and Group IIIB made up of members FL6 and FL7 that are divergent from FKD1 but showed strong co-localization with FKD1. Homozygous T-DNA insertion mutants were identified by PCR using primers specific for T-DNA insertions (Table 2.1). Homozygous mutant lines were screened for defects in cotyledon and first leaf vascular patterning and development, but no obvious differences were seen. The general absence of a detectable phenotype could result from a large degree of functional redundancy amongst members of the DUF 828 gene family. To test for functional redundancies, crosses were made between plants that possess mutations in different members of the gene family. I created double, triple and quadruple mutants so that different mutant combinations are

involved. Cotyledons and first leaves of single, double, triple and quadruple mutant plants were analyzed for leaf area, leaf vein density and vein pattern defects. Veins that are disconnected at both ends (vascular islands) predominate in multiple mutant lines. Because definition of vein order depends on establishing vein connections, comparison of secondary, tertiary and quaternary vein number was not possible. Hence I analyzed vascular islands of various genotypes, as well as vein density and leaf area.

Introduction of mutations in Group IIIB (*fl6* and *fl7*) into the *fkd1* genotype had no effect on cotyledon (14DAG) area or vein pattern when compared to *fkd1* (Table 4. 4), whereas *fkd1* mutants have leaves larger than wild type, *fl6 and fl7* mutant leaves are smaller than wild type. Triple mutant leaves are smaller than *fkd1* and with a higher vein density than *fkd1*. No change in VI was seen (Table 4.5). These data suggest that Group IIIB genes do not act redundantly with FKD1 with respect to vein meeting and may act in opposition to FKD1 to regulate leaf size.

Mutations to Group IIIC genes both increase and decrease leaf and cotyledon area and vein density. A number of studies have shown that as leaf area increases, vein density tends to decrease (Sack et al., 2012), so the two characters are not independent. For example, both *fkd1* and *fl3* have larger leaves than wild type with a corresponding reduction in vein density. Surprisingly, while none of the single mutants result in leaves smaller than wild type, leaves of multiple mutant lines (except *fkd1/fl3* double mutant) are all smaller than wild type (Table 4.5). Further, although all the multiple mutant lines have smaller leaves than wild type, vein

density is only higher in two lines (*fkd1/fl1-1/fl2/fl3* and *fkd1/fl1-2/fl2/fl3*). Hence Group IIIC genes may also be important in coordinating leaf vein size and density.

The *fkd1* mutation results in reduced vein meeting particularly at the distal ends. Introduction of mutations within the Group IIIC (*fl1-1, fl1-2, fl2* and *fl3*) results in increased severity of non-meeting, as seen by the increased presence of VI in both cotyledons (Figure 4.5.N,R) and leaves (Figure 4.6.N,Q and R) of the multiple mutant plants. These results suggest that Group IIIC genes act redundantly to allow vein meeting. Hence, I focused on Group IIIC multiple mutant lines, which seem to act redundantly in vein meeting.

4.5.1 PIN1-GFP expression and localization is defective in triple (*fkd1/fl2/ fl3)* mutants

The directional transport of auxin is responsible for leaf vein formation and the paths of polar auxin transport (PAT) can be visualized through the subcellular localization of auxin exporters of the PIN family (Petrášek et al. 2006). PIN1 expression is the earliest known determinant for proper leaf vein formation in *Arabidopsis thaliana* (Scarpella et al., 2006, Wenzel et al 2007). Since the vein non-meeting in *fkd1* leaves has been correlated with defective PIN1 localization (Hou et al., 2010), I hypothesized that the more extreme non-meeting veins of the triple *(fkd1/fl2/fl3)* and quadruple mutants (*fkd1/fl1-2/fl2/fl3* and *fkd1/fl1-2/fl2/fl3*) might result from more extreme defects to PIN1 localization. Hence, PIN1-GFP was introduced into the triple mutant *(fkd1/fl2/fl3)* lines by crossing.

PIN1 expression and localization in developing veins is described in detail elsewhere (Scarpella et al., 2006, Wenzel et al., 2007), so I will focus only on aspects relevant to my comparison. PIN1 is first expressed in the epidermis of the emerging leaf primordia. Its apical localization results in an auxin "convergence point" at the leaf apex, from which auxin is proposed to spill into underlying cell layers (Benková et al., 2003). As expression spreads basally, PIN1-GFP localization becomes basal along the entire incipient midvein. Changes to PIN1 localization within the epidermis result in auxin convergence points arising at more proximal points along the leaf margin. PIN Expression Domains (PEDs) of second-order veins emerge in association with these epidermal convergence points, and finally connect each convergence point with the midvein PED (Scarpella et al., 2006) (Figure 4.7. a and b). These early second-order PEDs, referred to as the proximal lower loop (lower-loop domain, LLD), are composed of a transient, wide distal section near the marginal convergence point and a persistent, narrow proximal section near the midvein. PIN1 localization is lateral and basal in the distal section and basal in the proximal section. After the LLD is fully connected to midvein PED, initiation of the upper-loop domain occurs which gradually extends from the LLD toward the distal midvein to become a "connected" PED. Once the ULD connects to the midvein, the transient wide section of the LLD section near the marginal convergence point disappears. Connected ULDs are comprised of two segments, one at the midvein where PIN1 localization is apical and one at the LLD where PIN1 localization is basal. The two segments of opposite polarity are bridged by a single bipolar cell (Scarpella et al., 2006).

I focused on comparing PIN1-GFP expression and localization within the second and third set of secondary veins between wild type and triple (*fkd1/fl2/fl3)* mutants. While these veins always meet the midvein distally in all wild type leaves (n=68), only 18% of the second set of secondary veins and 31% of the third set of secondary veins meet distally in the triple mutant (n=95) (Table 4.6). Because leaf formation is slightly delayed in triple mutants, DAG was not a reliable measure for comparison. Instead, I compared leaves at the same stage of vein development. In this study, Stage I refers to the stage of secondary vein formation that includes the transient wide PED adjacent to the margin (Figures 4.7.A and 4.8.A). Stage II refers to the stage of development in which the transient wide PED is absent and the ULD of the secondary vein has formed (Figures 4.7.B and Figure 4.8.B).

Generally, PEDs in triple mutant secondary veins are wider, with less consistent PIN1 localization than in wild type. Comparing stage I of the second secondary vein, whereas 11% of wild type PEDs are 3 or more cells wide (Figure 4.7.B and Table 4.7), 30% of triple mutant PEDs are 3 or more cells wide (Figure 4.7.F). At stage II, wild type second secondary veins PEDs are mostly restricted to a single cell file with only 1% more than 3 cells wide (Figure 4.7.D), whereas in the triple mutant, restriction of PED into a single cell file occurs only in 4% of secondary veins and 16% of PEDs remain wider than 3 cells (Figure 4.7.H).

Regarding PIN1-GFP localization, triple mutant cells show differences in PIN-GFP localization in different stages of development. In wild type cells, during stage 1, LLD most cells have basal localization with some cells showing lateral PIN1 and

most cells near an epidermal convergence point have lateral PIN1-GFP localization. During stage II of wild type most of the cells in the ULD have apical localization and few cells have lateral PIN1-GFP localization. In triple mutants, in stage I and stage II of the 2nd set of secondary veins, basal localization was reduced compared to wild type. PEDs in both these stages had few cells with lateral localization as in wild type. However a larger number of cells had PIN1-GFP localized to all sides of the cells (Table 4.8) a situation never seen in wild type. Similarly, in triple mutants, during Stage II in the 3rd set of secondary veins, there was considerable reduction in apical and basal PIN1-GFP localization. A small proportion of cells in both stages had PIN1-GFP localized to the lateral sides of the cell. The most striking feature was that half the cells had PIN1-GFP localized to all sides of the cell (Table 4.8).

Occasionally in triple mutant leaves (2 of 63), a group of cells in the 3rd set of secondary veins were arranged in a peculiar fashion with PIN1 localized to all sides of a cell and the cells around it forming a circular arrangement rather than the normal linear arrangement (Figure 4.9.A,B). All these results taken together indicate that considerable variation exists in PIN1-GFP localization in developing veins at different developmental stages in triple mutants compared to wild type. In the triple mutants, there is more tendency towards symmetric PIN1-GFP localization with strong reduction in cells with only apical or only basal localization. The defects observed in PIN1-GFP localization and expression might result in impaired auxin transport, thereby resulting in the severe defects in leaf vascular patterning within triple mutants.

4.6 General defects in plant development

The results in section 4.5 and 4.6 suggest that PIN1 localization defects observed in multiple mutant lines might be contributing to defects in proper auxin canalization processes, thereby resulting in defective vein formation. In order to determine whether the mutations in the members of the DUF 828 gene family affect other auxin transport related developmental processes, phenotypes including flowering time, number and shape of rosette leaves and bracts, root length and gravitropic response were compared between wild type and *fkd1*, triple mutant I (*fkd1/fl2/fl3)* and two quadruple mutants (*fkd1/ fl1-1/fl2/fl-3* and *fkd1/fl1-2/ fl2/ fl3)* lines.

4.6.1 DUF 828 gene family alters leaf number and flowering time

The number of rosette leaves in wild type, *fkd1* and triple mutant (*fkd1/fl2/fl3*) is 6.4, whereas the number of rosette leaves in two quadruple mutants [(*fkd1/fl1-1/fl2/fl3)* and *(fkd1/fl1-2/fl/ fl3)*] are 7.6 and 8.9 respectively (Table 4.9). As well, leaves of the multiple mutant were smaller and purple in color. Rosette leaf number is often correlated with flowering time in plants. The increase in number of rosette leaves in quadruple mutants was accompanied by a slight, though not statistically significant delay in their flowering time (Figures 4.10.D,E). The average flowering time of wild type *Arabidopsis thaliana* and *fkd1* was about 19 DAG. The average flowering time for triple mutant (*fkd1/fl2/fl3*) and two quadruple mutants [(*fkd1/ fl1-1/fl2/fl3)* and *(fkd1/fl1-2/fl2/fl3)*] were 23 and 27 DAG respectively (Table 4.9). These results suggest that the growth rate of mutant lines is reduced

compared to wild type and *fkd1* (Figures 4.10.C, D, E), indicated by 2.2 days/leaf in triple mutant and 2.6 days/leaf in quadruple mutant. It is possible that the reduced growth grate results from the alterations to vein pattern seen in the multiple mutant lines.

4.6.2 DUF 828 gene family affects leaf and bract architecture

As I was analyzing leaf venation, I noticed that multiple mutant lines had defects in leaf shape including asymmetric leaf expansion as well as protrusions and depressions on the leaf surface (Figure 4.11). Auxin is a key regulator of cell division and expansion, which together determine cell shape and hence affect leaf development (Scarpella et al., 2006), and whose coordination determines the shape and size of the mature leaf. Hence I tried to investigate whether these processes are defective in multiple mutant lines.

Wild type and *fkd1* plants produced simple, unlobed, symmetric cotyledons and leaves with flat blades. In triple and quadruple mutants (*fkd1/fl1-1/fl2/fl3)* and *(fkd1/fl1-2/fl2/fl3)*, the leaves produced at later stages of development (leaf 3 onwards) showed defects in leaf shape and size, including asymmetric blades, bumps and depressions (Figures 4.11.C, D, E, L, M, N). Similarly, the bracts of wild type and *fkd1* plants are symmetric and flat (Figures 4.12.A, B, J, K), whereas bracts in triple ((*fkd1/fl2/fl3*) mutant and two quadruple mutants (*fkd1/fl1-1/fl2/fl3* and *fkd1/fl1-2/fl2/fl3)* were asymmetric with bumps and depression (Figures 4.12.C, D, E, L, M, N). These defects suggest that the DUF 828 gene family affect leaf shape and symmetry, possibly through influencing either cell division or cell expansion.

4.6.2.1 DUF 828 gene family affects epidermal cell morphogenesis

To investigate the cellular mechanisms associated with defective leaf shape, I focused on addressing cell expansion in rosette leaves and bracts. Cell polarity of pavement cells is multidirectional and during cell development, each cell co-ordinates expansion with polarized growth to determine the overall cell shape (Guimil and Dunand, 2007). Hence pavement cells of rosette leaves and bracts were chosen to address whether there are defects in cell expansion or elongation processes. Since the severe leaf shape defects were exhibited by the triple (*fkd1/fl2/fl3*) and the quadruple (*fkd/ fl1-2/fl2/fl-3)* mutant, I focused my analysis on these two mutant lines along with wild type and the *fkd1* mutant. To determine whether the defects observed in leaf and bract shape in mutants are due to defects in cell expansion, cellular phenotyping of epidermal pavement cells on adaxial and abaxial sides of 5th leaves and 2nd bracts was done.

4.6.2.1.1 Cell area and dimensions

Epidermal cell surface area of all genotypes was measured on adaxial and abaxial sides of fifth leaves and second bracts. First, cell area is highly variable on both abaxial and adaxial sides of fifth leaves and bracts of all genotypes (Figure 4.11 and 4.12). In fifth leaves of all genotypes except *fkd1*, adaxial cells are larger than the abaxial cells. In contrast, the adaxial cells of bracts are smaller than the abaxial cells, a difference seen in all genotypes (Figures 4.11 and 4.12). Cell area on the abaxial side of the *fkd1,* triple and quadruple mutant fifth leaves was larger than wild type (Figure 4.11.S). In the case of second bracts, the cells on the abaxial side of the triple

mutant and quadruple mutants had a smaller cell area than wild type and *fkd1* (Figure 4.12.S). While changes in cell size exist between the mutants and wild type, the lack of consistent correlation with defects seen in triple and quadruple mutant fifth leaves and bracts suggest that changes in cell area may not be the primary cause of the shape defects.

4.6.2.1.2 Cell shape and elongation

I next considered two aspects of cell shape, undulation index (UI) and cell elongation. Undulation Index is a measure of the formation of lobes and indentations independent of cell area. While differences in undulation existed among the genotypes, no consistent trend that could explain the leaf shape defects was seen. However, comparison of the UI on the adaxial and abaxial sides of pavement cells of fifth leaves and second bracts revealed that cells on the adaxial side had a smaller UI compared to cells on the abaxial side (Figure 4.11.T and 4.12.T). In the case of fifth leaves, no significant difference in the undulation index was observed between genotypes on each side. In the case of second bracts, on the adaxial side, the UI of the quadruple mutant was significantly lower ($p<0.05$) than that of the triple mutant. On the abaxial side, the UI of both triple and quadruple mutants were significantly lower ($p<0.05$) than wild type and *fkd1* (Figure 4.12.T).

To characterize the pattern of cell elongation in epidermal pavement cells, analysis of cell length of epidermal pavement cells on the abaxial and the adaxial sides of second bracts was performed. There is no significant difference in cell length of pavement cells on the adaxial side of second bracts, whereas on the abaxial side,

triple and quadruple mutants show significantly reduced ($p<0.05$) cell length compared to wild type and *fkd1* (Figure 4.13). Except in the quadruple mutant, cell length on the adaxial side of the second bracts is less than the cell length on the abaxial side (Figure 4.13). All these results suggest that cell elongation and undulation is lower on the abaxial side of the bracts in the multiple mutant lines. These results demonstrate that genetic defects in mutants might be affecting the process of cell elongation and cell expansion in leaves.

4.6.2.1.3 DUF 828 gene family influences polarity of epidermal pavement cells

Within wild type leaves and bracts, most cells are elongated parallel to the midvein. To assess whether the bumps and depressions in bracts of triple and quadruple mutants were due to altered direction of cell growth, orientation of cells relative to midvein was compared between the different genotypes. Images of the abaxial and adaxial surfaces were taken from nail varnish casts by SEM. From each image, cells (n=30) that had the most divergent orientation relative to midvein were chosen and their divergence in longitudinal axis relative to the midvein was assessed. In wild type plants, the most divergent abaxial epidermal pavement cells were oriented with a long axis of 43° relative to the midvein. *fkd1* mutants also exhibited more or less longitudinal orientation with cells oriented at an angle of 44°. However, the most divergent cells of triple (*fkd1/fl2/fl3*) and quadruple (*fkd1/fl1-2/fl2/fl3)* mutants exhibited wide divergences of 59° and 61° relative to the midvein (Figures 4.14.C, D), which is significantly different ($p< 0.05$) from wild type and *fkd1* mutants (Figures 4.14.A,B).

On the adaxial side of wild type and *fkd1* bracts the most divergent epidermal pavement cells were oriented with a long axis of 54° and 57°. In triple mutants, no wide divergence in cell angle was observed, while the quadruple mutants exhibited wide divergence of 69° relative to the midvein. The wide divergence in longitudinal axis suggests that multiple mutants fail to specify or maintain proper cell polarity. These results suggest that mutations in multiple members of Group IIIC DUF 828 gene family disrupt the polarity, arrangement and orientation of epidermal cells especially those on the abaxial side. Another possible explanation is that lack of cell coordination results in defects in establishing cell polarity.

4.7 DUF 828 gene family affects the growth rate of primary roots

Defects to auxin transport affect root growth and gravitropic response (Rashotte et al., 2000). To determine whether the DUF 828 gene family mutations affect auxin-regulated root developmental processes, root growth rate and gravitropic response were measured and compared among various genotypes. Plants of different genotypes were grown on vertical plates and primary root growth over 24h (growth from 4DAG to 5DAG) was assessed (Table 4.10, Figure 4.15). The average root growth of wild type and *fkd1* over 24 hours was not significantly different (3.90 mm and 3.1 mm, respectively). Triple mutants and quadruple mutant roots grow significantly less ($p<0.05$) over the same time (2.50 mm and 1.40 mm, respectively). To determine the gravitropic response in wild type and mutant genotypes, seedlings grown vertically on petri plates were rotated 90° at 5DAG. The

angle of root tip divergence was measured 2, 4 and 6 hours after rotation (Table 4.10, Figure 4.16). Over this time, wild type root tips reorient to gravity, turning to about 90° by 6h. The gravitropic response in the triple and quadruple mutants is reduced compared to both the wild type and *fkd1* (Table 4.10, Figure 4.16).

4.8 PIN1 localization is not defective in the root tissues of triple mutants

The reduced root growth and gravitropic response of the multiple mutants suggests that auxin transport may be defective in these lines. To investigate the role of the DUF 828 gene family in PIN1 trafficking in roots, BFA washout experiments were performed in wild type and triple mutants (*fkd1/fl2/fl3)* expressing PIN1-GFP. Both in wild type and triple mutants, PIN1 is localized to the basal side of root vascular cells (Figures 4.17.A,D). To investigate whether triple mutants are defective in PIN1 intracellular trafficking, seedlings were treated with BFA. BFA, a vesicle-trafficking inhibitor, blocks secretion and promotes vesicle aggregation to form BFA compartments (Nebenführ et al., 2002). In wild type root cells, PIN1–GFP accumulates in BFA compartments after treatment with BFA (50 mM, 2h; Figure 4.17.B). After BFA wash out, the intracellular aggregates rapidly decrease and the PM signals were recovered (Figure 4.17.C). Under the same conditions, the triple mutant expressing PIN1-GFP *(fkd1/fl2/fl3/*PIN1GFP*)* also showed intracellular aggregation into BFA compartments (Figure 4.17.E). BFA washout for 2h in the triple mutant resulted in PM recovery of PIN1-GFP (Figure 4.17.F). There was no obvious difference between wild type and triple mutants with PIN1-GFP, which

indicates that the mutations in the Group IIIC DUF828 gene family members do not affect PIN1 localization in root tissues.

Table 4.1: Domain organization [DUF 828 (IPR00856), Pleckstrin like domain (PL; IPR013666) and Pleckstrin Homology domain (PH; IPR001849) DUF828 gene family members.

DUF828 members	Position of Domains (aa)			aa sequence identity (%)		
	DUF828	PL	PH	FKD1	DUF828	PH/PL
At3g63300/FKD1	30-336	379-483	-			
At5g43870/FL1	22-307	341-446	-	53.90	57.70	64.20
At3g22810/FL2	18-312	358-462	353-463	56.10	59.40	59.70
At4g14740/FL3	19-178	224-328	-	56.10	57.60	68.60
At4g32780/FL4	54-263	-	-	27.10	34.20	-
At4g17350/FL5	44-86 111-258	283-386	278-386	28.80	26.00	39.80
At4g16670/FL6	58-93 126-174	307-411	302-411	27.30	17.60	28.80
At5g47440/FL7	43-108 133-257	283-385	278-386	27.1	25.20	34.10
At5g57770/FL8	21-268	289-390	-	26.20	20.80	20.60

(-) indicates that protein does not contain that domain. Amino acid identity of FKD1 full-length protein, DUF828 and PL or PH domain to the corresponding region in each member of the gene family.

Table 4.2: Correlation of expression between the intensities of members of the DUF 828 gene family fused to YFP with ST-RFP or SYP61-CFP in leaf epidermis of Nicotiana and in cotyledon epidermis of Arabidopsis seedling (*) at 2.5 DAG. Mean PCC was determined using the colocalization plugin in NIH image J from the intensity scatterplot of merged images.

Gene	Sample size	PCC
FL1-YFP	(n=19)	0.11± 0.20
FL3-YFP	(n=18)	0.25± 0.10
FL5-YFP	(n=19)	0.54± 0.22
FL7-YFP8	(n=17)	0.11± 0.16
FL6-YFP	(n=19)	0.39± 0.17
FL3-YFP -SYP61CFP*	(n=21)	0.33± 0.11

Table 4.3: Correlation of expression between the intensities of FKD1-GFP with members of FKD1 gene family fused to YFP in leaf epidermis of Nicotiana and in cotyledon epidermis of Arabidopsis seedling (*) at 2.5 DAG. Mean PCC was determined using colocalization plugin in NIH image J from intensity scatterplot of merged images.

Gene name	Sample size	Mean PCC
FL1-YFP	(n=28)	0.95± 0.03
FL3-YFP	(n=24)	0.47± 0.30
FL5-YFP	(n=34)	0.40± 0.20
FL6-YFP	(n=24)	0.75± 0.17
FL7-YFP	(n=29)	0.62± 0.25
FKD1GFP -FL3-YFP *	(n= 21)	0.47 ± 0.24

Table 4.4: Area and vein characteristics of 14 DAG cotyledons from various genotypes.

Genotype	Sample size	Area (mm^2)	Vein density mm/ mm^2	Vascular Islands
Wt	83	6.5 ± 1.5	1.6 ± 0.3	0
fkd1	84	4.6 ± 1.8[a]	1.9 ± 0.4[a]	0
fl1-1	23	7.3 ± 1.2[b]	1.6 ± 0.1[b]	0
fl1-2	15	5.6 ± 2.7[b]	1.9 ± 0.5[a]	0
fl2	54	6.6 ± 1.3[b]	1.7 ± 0.3[b]	0
fl3	45	6.9 ± 2.2[b]	1.7 ± 0.2[b]	0
fl6-1	38	6.7 ± 1.9[b]	1.8 ± 0.7[a,b]	0
fl6-2	29	5.8 ±1.0[a,b]	1.7 ± 0.1[b]	0
fl7	21	7.4 ± 1.5 [a,b]	1.6 ± 0.3 [b]	0
fkd/fl1-1	24	3.4 ±1.2 [a,b,c]	2.3 ± 0.4 [a,b,c]	0
fkd1/fl1-2	22	6.3 ± 0.9 [b]	1.5 ± 0.1 [b,c]	1.0 ± 0.0[a,b]
fkd1/fl2	41	5.3 ± 1.4[a,b,c]	2.0 ± 0.3[a,c]	1.0 ± 0.0[a,b]
fkd1/fl3	58	6.9 ±1.60 [b]	1.6 ± 0.26[b,c]	1.0 ± 0.0[a,b]
fkd1/fl2/fl3	71	6.8 ± 1.9 [b,d*]	1.4 ± 0.3[a,b,c,d]	1.5± 0.7[a,b]
fkd1/fl1-1/fl2/fl3	67	4.5 ± 1.9 [a,c,d,e]	1.8 ± 0.4[a,c*,d,e]	0
fkd1/fl1-2/fl2/fl3	19	6.8± 1.1 [b,d*]	1.4 ± 0.1 [a,b,c,d*]	1.2± 0.6[a,b]
fkd1/fl6-1/fl7	25	4.6 ± 1.0[a,c]	1.8 ± 0.2[a,c]	0
fkd1/fl6-2/fl7	29	5.2 ± 1.2[a,c*]	1.8 ± 0.2[a,c]	0

All values are means ± standard deviations. [a] is significantly different from wt, [b] is significantly different from *fkd1*, [c] is significantly different from single mutants, [d] is different from double mutants and [e] is different from triple mutant. * represents significant difference from one of tested double mutants, but not all.

Table 4.5: Area and vein characteristics of 21 DAG first leaves from various genotypes.

Genotype	Sample size	Leaf area mm^2	Leaf vein density mm/mm^2	Vascular Islands
Wt	134	34.3 ± 9.0	2.0 ± 0.2	0
fkd1	94	39.3 ± 14.1[a]	1.7 ± 0.2[a]	1.2 ± 1.0[a]
fl1-1	23	38.3 ± 6.7	2.0 ± 0.1	0
fl1-2	15	31.8 ± 10.3[b]	1.9 ± 0.2[b]	0
fl2	57	36.7 ± 11.6	1.9 ± 0.4[b]	0
fl3	97	42.5 ± 11.1[a,b]	1.7 ± 0.2[a]	0
fl6-1	32	29.5 ± 8.5[a,b]	1.7 ± 0.2[a]	0
fl6-2	28	34.0 ± 8.8[b]	1.9 ± 0.2[b]	0
fl7	30	27.6 ± 6.2[a,b]	1.96 ± 0.30[b]	0
fkd1/fl1-1	27	30.3 ± 7.8[a,b,c]	1.9 ± 0.1[b]	1.5 ± 1.3[a]
fkd1/fl1-2	24	20.1 ± 5.6[a,b,c]	2.5 ± 0.3[a,b,c]	2.5 ± 0.9[a,b]
fkd1/fl2	35	30.4 ± 6.2[a,b,c]	1.9 ± 0.1[b]	2.4 ± 1.4[a,b]
fkd1/fl3	46	36.2 ± 9.8[,c]	1.9 ± 0.1[b,c]	1.1 ± 0.4[a,]
fkd1/fl2/fl3	96	25.5 ± 9.4[a,b,c,d]	2.0 ± 0.3[b,c,d*]	4.9 ± 2.2[a,b,d]
fkd1/fl1-1/fl2/fl3	69	17.5± 5.7[a,b,c,d,e]	2.3 ± 0.30[a,b,c,d,e]	3.7 ± 1.3 [a,b,d]
fkd1/fl1-2/fl2/fl3	96	23.9 ± 6.05[a,b,c,d]	2.1± 0.2[b,c,d]	4.7± 2.1[b,d]
fkd1/fl6-1/fl7	31	30.7 ± 6.70[a,b]	2.0 ± 0.2[b,c*]	1.7 ± 1.3[a]
fkd1/fl6-2/fl7	32	30.1 ± 6.2[a,b,c*]	1.9 ± 0.1[b]	1.6 ± 0.7[a]

All values are means ± standard deviations. [a] is significantly different from wt, [b] is significantly different from *fkd1*, [c] is significantly different from single mutants, [d] is different from double mutant and [e] is different from triple mutant. * represents significant difference from one of tested double mutants, but not all.

Table 4.6: Frequency of non-meeting secondary veins (second and third set) in wild type and triple mutants.

Genotype	Leaves analyzed	Number of non-meeting secondary veins in ½ leaf ($2^{nd}$and 3^{rd}set)	% of non-meeting
Wild type	(n=68)	0	0
fkd1/ fl2/fl3	(n=95)	36* (second set of 2^0 veins)	18.94
		60 * (third set of 3^0 veins)	31.57

* represents significant difference from wild type (Fisher test $p<0.05$).

Table 4.7: Percentage of wide PIN1-GFP expression domains (PED) at different developmental stages of second and third 2° veins in wild type and triple mutant first leaves.

Genotype	2nd loop (% of PED 3 or more cells wide)		3rd loop (% of PED 3 or more cells wide)	
	Stage I	Stage II	Stage I	Stage II
WT (n=45)	10.67	1.06	26.42	10.02
fkd1/fl2/fl3 (n=63)	30.30*	15.95*	28.22	25.15

* represents significant difference from wild type ($p<0.05$), Fisher's test was done on raw data and % values are shown here.

Table 4.8: PIN1-GFP localization at developmental stages of second and third set of 2° veins in wild type and triple mutant first leaves.

Genotype	PIN1-GFP localization (%)			
	Apical	Basal	Lateral	All sides
WT -2^0 veins (2^{nd} set stage I)	7.760	40.77	53.33	0
WT -2^0 veins (2^{nd} set-stage II)	43.33	37.77	18.88	0
WT -3^0 veins (2^{nd} set-stage I)	3.03	56.66	40.00	0
WT -3^0 veins (2^{nd} set-stage II)	40.90	40.90	18.09	0
Triple mutant- 2^0 veins (2^{nd} set- stage I)	2.85	25.00	25.00	47.22*
Triple mutant-2^0 veins (2^{nd} set -stage II)	13.00*	19.33*	14*	53.33*
Triple -2^0 veins (3^{rd} set-stage I)	5.17	26.47*	15.44*	52.94*
Triple -2^0 veins- (3^{rd} set- stage II)	15.00*	18.33*	18.95	47.71*

Sample size, n=15 for both genotypes * represents significant difference from wild type, calculated from raw data using Fisher's test, % values shown here.

Table 4.9: Comparison of phenotypic characters between various genotypes

Genotype	Sample size	Rosette Leaves	Bracts	Days to Flowering	Growth rate (days/leaf)
WT	n=16	6.36 ± 1.02	2.21± 0.42	19	2.21
fkd1	n=15	6.40 ± 0.90	2.2 ± 0.44	19	2.20
fkd1/fl2/fl3	n=16	6.53 ± 1.07	2.65± 0.51	23	2.50
fkd1 /fl1-1)/fl2/fl3	n=15	7.60 ± 0.80*	2.82 ± 0.77	27	2.63
fkd1/ fl1-2/ fl2/fl3	n=16	8.90 ± 0.81*	2.94 ± 0.83	27	2.28

*represents significant difference from wild type, *fkd1* and triple mutant.

Table 4.10: Comparison of gravitropic response in different genotypes

		WT (n=19)	*fkd1* (n=21)	*fkd1/fl2/fl-3* (n=25)	*fkd1/fl1(2)/fl2/fl3* (n=18)
Gravitropism Horizontal angle of root after 90(°) rotation	2h	24.0 ± 13.3	25.2 ± 14.7	19.4 ± 10.8	15.1 ± 17.6
	4h	61.7 ± 17.3	63.2 ± 23.0	55.4 ± 22.5	42.4 ± 27.3[a]
	6h	81.0 ± 15.2	81.6 ± 17.8	76.6 ± 13.8[a]	60.6 ± 27.5[abc]

[a] represents significant difference from wild type, [b] represents significant difference from *fkd1* and [c] represents significant difference from triple mutant ($p<0.05$).

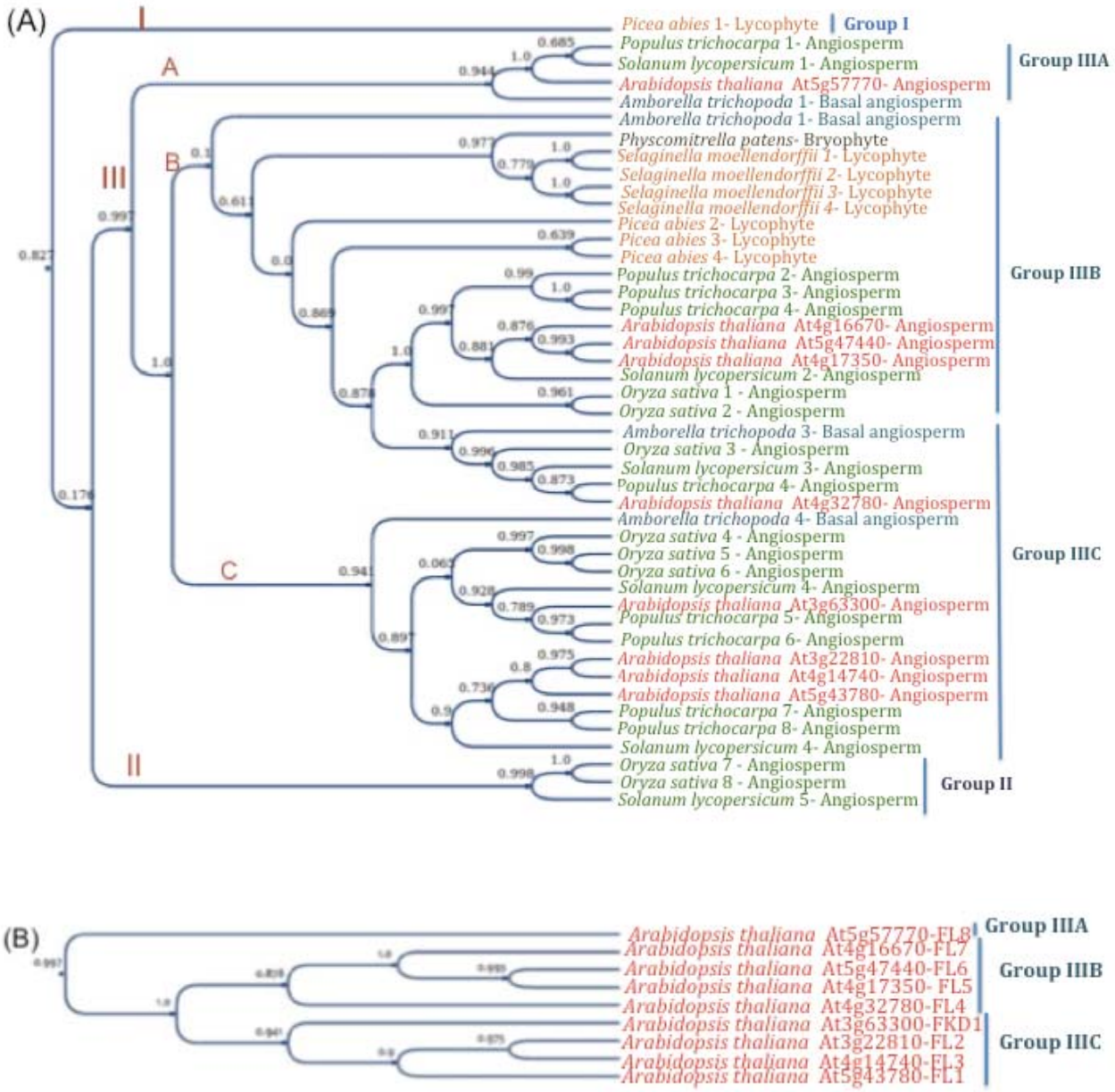
(A)
I
II
III
A
B
C
Picea abies 1- Lycophyte
Group I
Populus trichocarpa 1- Angiosperm
Solanum lycopersicum 1- Angiosperm
Arabidopsis thaliana At5g57770- Angiosperm
Amborella trichopoda 1- Basal angiosperm
Group IIIA
Amborella trichopoda 1- Basal angiosperm
Physcomitrella patens- Bryophyte
Selaginella moellendorffii 1- Lycophyte
Selaginella moellendorffii 2- Lycophyte
Selaginella moellendorffii 3- Lycophyte
Selaginella moellendorffii 4- Lycophyte
Picea abies 2- Lycophyte
Picea abies 3- Lycophyte
Picea abies 4- Lycophyte
Populus trichocarpa 2- Angiosperm
Populus trichocarpa 3- Angiosperm
Populus trichocarpa 4- Angiosperm
Arabidopsis thaliana At4g16670- Angiosperm
Arabidopsis thaliana At5g47440- Angiosperm
Arabidopsis thaliana At4g17350- Angiosperm
Solanum lycopersicum 2- Angiosperm
Oryza sativa 1 - Angiosperm
Oryza sativa 2 - Angiosperm
Group IIIB
Amborella trichopoda 3- Basal angiosperm
Oryza sativa 3 - Angiosperm
Solanum lycopersicum 3- Angiosperm
Populus trichocarpa 4- Angiosperm
Arabidopsis thaliana At4g32780- Angiosperm
Amborella trichopoda 4- Basal angiosperm
Oryza sativa 4 - Angiosperm
Oryza sativa 5 - Angiosperm
Oryza sativa 6 - Angiosperm
Solanum lycopersicum 4- Angiosperm
Arabidopsis thaliana At3g63300- Angiosperm
Populus trichocarpa 5- Angiosperm
Populus trichocarpa 6- Angiosperm
Arabidopsis thaliana At3g22810- Angiosperm
Arabidopsis thaliana At4g14740- Angiosperm
Arabidopsis thaliana At5g43780- Angiosperm
Populus trichocarpa 7- Angiosperm
Populus trichocarpa 8- Angiosperm
Solanum lycopersicum 4- Angiosperm
Group IIIC
Oryza sativa 7 - Angiosperm
Oryza sativa 8 - Angiosperm
Solanum lycopersicum 5- Angiosperm
Group II
(B)
Arabidopsis thaliana At5g57770-FL8
Group IIIA
Arabidopsis thaliana At4g16670-FL7
Arabidopsis thaliana At5g47440-FL6
Arabidopsis thaliana At4g17350- FL5
Group IIIB
Arabidopsis thaliana At4g32780-FL4
Arabidopsis thaliana At3g63300-FKD1
Arabidopsis thaliana At3g22810-FL2
Arabidopsis thaliana At4g14740-FL3
Arabidopsis thaliana At5g43780-FL1
Group IIIC

Figure 4.1: Phylogenetic tree of DUF 828-domain sequences from diverse species in plant kingdom and of DUF 828 encoding genes in *Arabidopsis thaliana.*

Representative species chosen are Bryophyte (*Physcomitrella patens*- PHYPA) lycophyte (*Selaginella moellendorffii*- SELMO), gymnosperm (*Picea abies*- PICAB), basal angiosperm (*Amborella trichopoda*- AMBTC), monocot (*Oryza sativa*- ORYSA), Dicots (*Solanum lycopersicum*- SOLLY), (*Populus trichocarpa*- POPTR) and (*Arabidopsis thaliana*- ARATH). The number for each branch represents bootstrap value. 3 major groups (I, II and III) are suggested with Group III further subdivided into Group IIIA, Group IIIB and Group IIIC. (B) Phylogenetic tree of DUF 828 encoding genes (At3g63300, FKD1; At5g43870, FL1; At3g22810, FL2; At4g14740, FL3; At4g32780, FL4; At4g17350, FL5; At5g474400, FL6; At4g16670, FL7 and At5g57770, FL8) in *Arabidopsis thaliana.* 3 groups (IIIA, IIIB, IIIC) corresponding to those in Figure A. The sequnce ID of genes used for the construction of phylogenetic tree are listed as follows:

Oryza sativa 1-Os02g44040.1_ORYSA, *Oryza sativa* 2-Os10g41060.1_ORYSA, *Oryza sativa* 3- Os01g13070.1_ORYSA, *Oryza sativa* 4-Os08g30350.1_ORYSA, *Oryza sativa* 5-Os12g41140.1_ORYSA ,*Oryza sativa* 6-Os03g43510.1_ORYSA, *Oryza sativa* 7-Os10g41860.1_ORYSA*, Oryza sativa* 8-Os10g41870.1_ORYSA.

Picea abies 1-MA_10432316g0010_ PICAB,*Picea abies* 2- MA_ 340269g0010_PICAB, *Picea abies* 3- MA_39658g0010_PICAB*,* ,*Picea abies* 4-MA_90368g0010_PICAB.

Amborella trichopoda 1-evm_27.model.AmTr_v1.0_scaffold00019.130_AMBTC, *Amborella trichopoda* 2-evm_27.model.AmTr_v1.0_scaffold00176.33_AMBTC,*Amborellatrichopoda*3evm_27.model.AmTr_v1.0_scaffold00109.149_AMBTC, *Amborella trichopoda* 4-evm_27.model.AmTr_v1.0_scaffold0002.606_AMBTC.

Populus trichocarpa 1-Potri.018G099000.1_POPTR, *Populus trichocarpa* 2-Potri.003G077900.1_POPTR, *Populus trichocarpa* 3-Potri.001G156700.1_POPTR, *Populus trichocarpa* 4-Potri.T151700.1_POPTR, *Populus trichocarpa* 5-Potri.018G042000.1_POPTR, *Populus trichocarpa* 6- Potri.005G213800.1, POPTR, *Populus trichocarpa* 7-Potri.002G049200.1_POPTR, *Populus trichocarpa* 8-Potri.010G082400.1_POPTR, *Populus trichocarpa* 9- Potri.008G157000.1_POPTR.

Solanum lycopersicum 1-Solyc07g006320.2.1_SOLLY, *Solanum lycopersicum* 2-Solycco8g078500.2.1. SOLLY*, Solanum lycopersicum* 3-Solyc08g066860.2.1_SOLLY, *Solanum lycopersicum* 4-09g065590.2.1_SOLLY, *Solanum lycopersicum* 5-Solyc09g082580.2.1_SOLLY, *Solanum lycopersicum* 6-Solyc06g072940.1.1_SOLLY.

Selaginella moellendorffii 1-selmo_269293_SELMO, *Selaginella moellendorffii* 2-selmo_268691_SELMO, *Selaginella moellendorffii* 3- selmo_267397,_SELMO, *Selagnella moellendorffii* 4- selmo_443866_SELMO.

Pyschometrilla patens 1-Pp1s155_109V6.1_PHYPA.

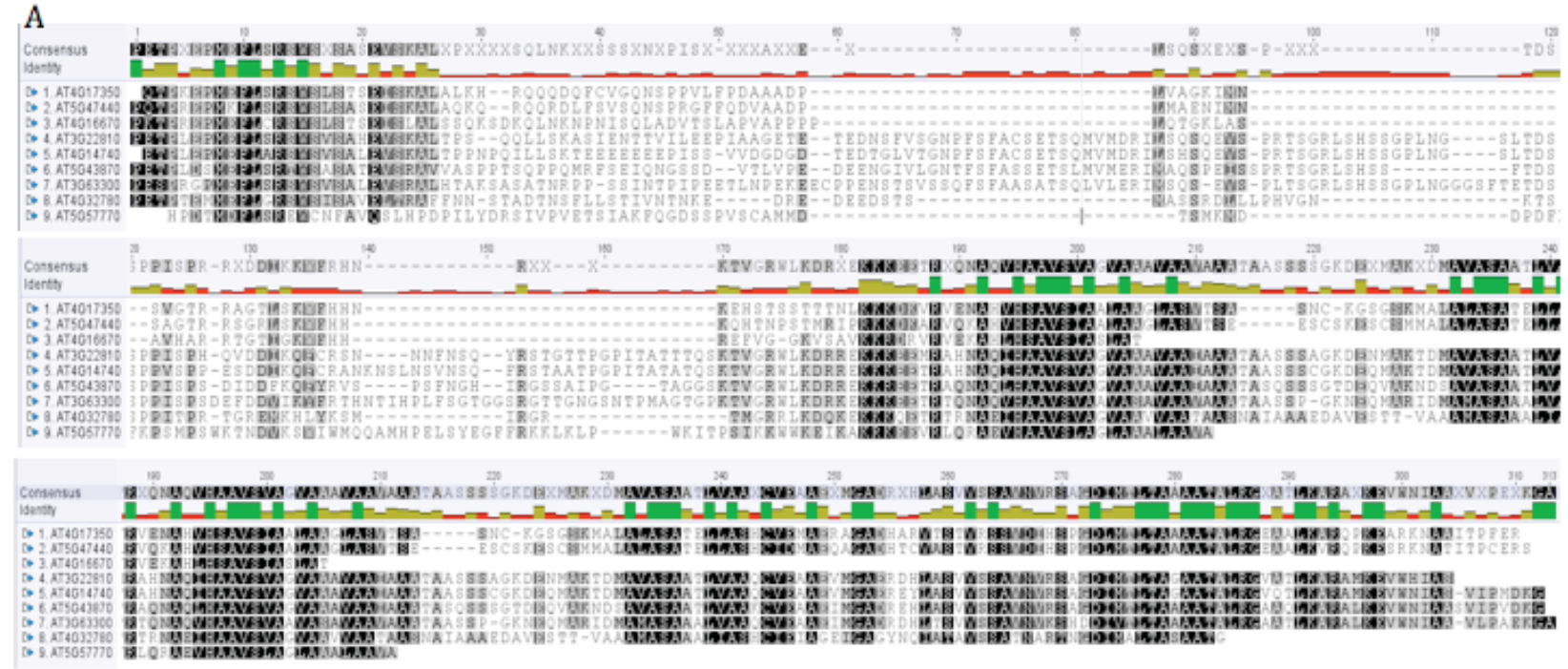
A
Consensus
Identity
1. AT4G17350
2. AT5G47440
3. AT4G16670
4. AT3G22810
5. AT4G14740
6. AT5G43870
7. AT3G63300
8. AT4G32780
9. AT5G57770

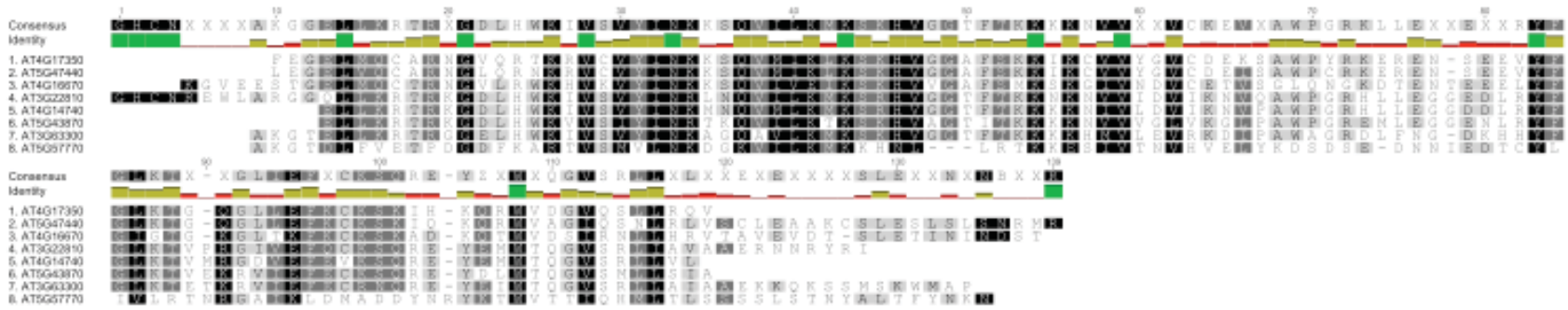
B
Consensus
Identity
1. AT4G17350
2. AT5G47440
3. AT4G16670
4. AT3G22810
5. AT4G14740
6. AT5G43870
7. AT3G63300
8. AT5G57770

Figure 4.2: Multiple sequence alignment of DUF 828 and PL/PH domain sequence of DUF 828 gene family.

Multiple sequence alignment of DUF 828 domains (A) and multiple sequence alignment of PL/PH domains (B) was done using Clustal W programme. Conserved sequences are represented by black and grey shades respectively. Numbers represents the start and end of amino acid sequence and an alignment of consensus sequence is shown at the top. Amino acid sequence was obtained from GreenPhyl DB databases and regions corresponding to DUF828, PL and PH domains were identified from InterPro.

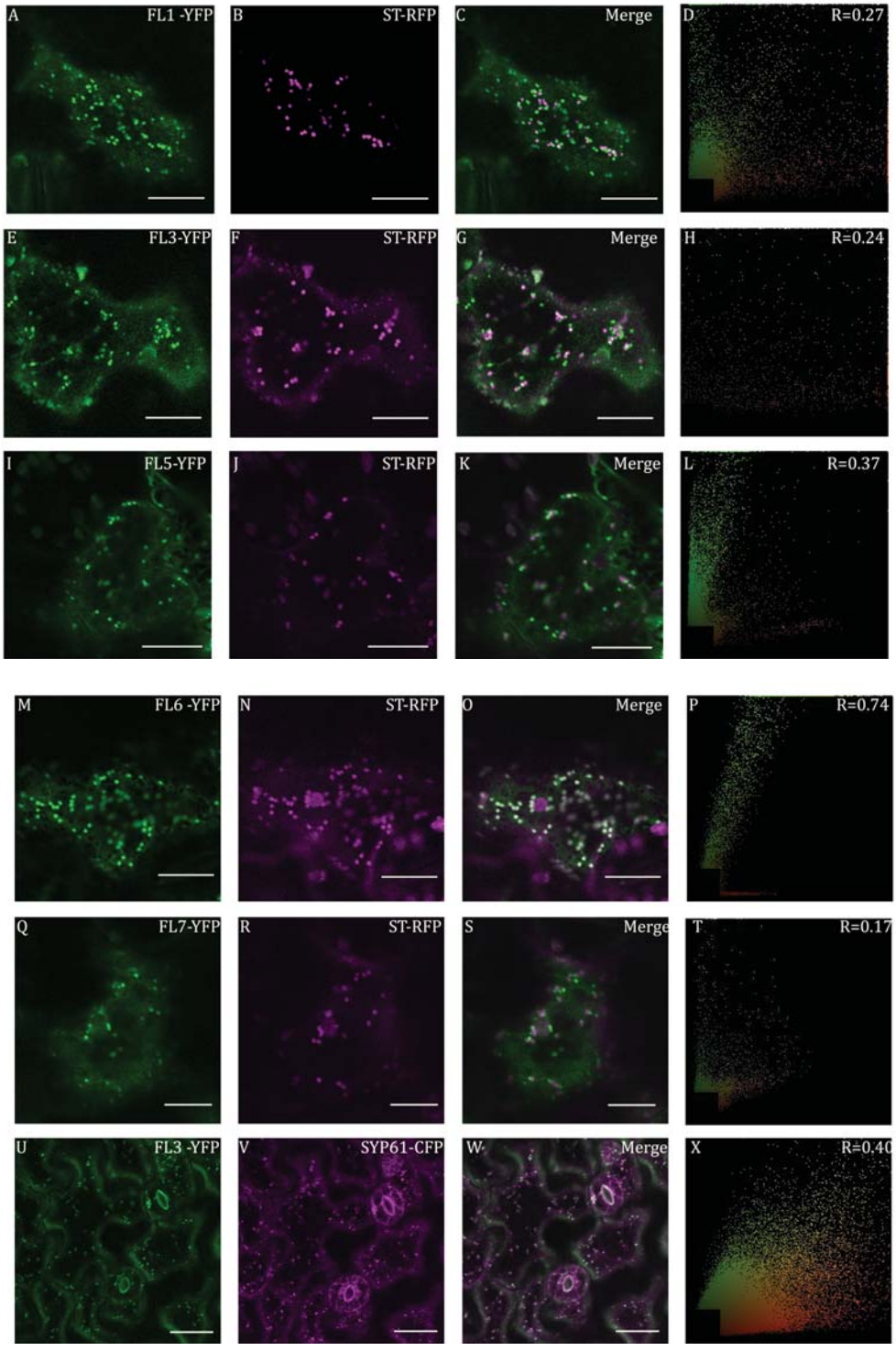
A FL1 -YFP
B ST-RFP
C Merge
D R=0.27
E FL3-YFP
F ST-RFP
G Merge
H R=0.24
I FL5-YFP
J ST-RFP
K Merge
L R=0.37
M FL6 -YFP
N ST-RFP
O Merge
P R=0.74
Q FL7-YFP
R ST-RFP
S Merge
T R=0.17
U FL3 -YFP
V SYP61-CFP
W Merge
X R=0.40

Figure 4.3: Subcellular localization of FKD1 with DUF828 gene family members with ST-RFP in Nicotiana and of FL3 with SYP61-CFP in stably transformed Arabidopsis.

Localization of DUF 828 family members fused to YFP with ST-RFP in Nicotiana (A-T) and FL3-YFP with TGN marker, SYP61-CFP in Arabidopsis (U-X). A, E, I, M and Q are FL1, FL3, F L5, FL6, FL7 fused to YFP. B, F, J, N and R are ST-RFP, U is FL3-YFP, V is SYP61-CFP, C, G, K, O, S and W are the merged images. D, H, L, P, T and X are scatter plots of the merged image with Pearson's coefficient of Correlation (R) values (Scale bar: 10μm).

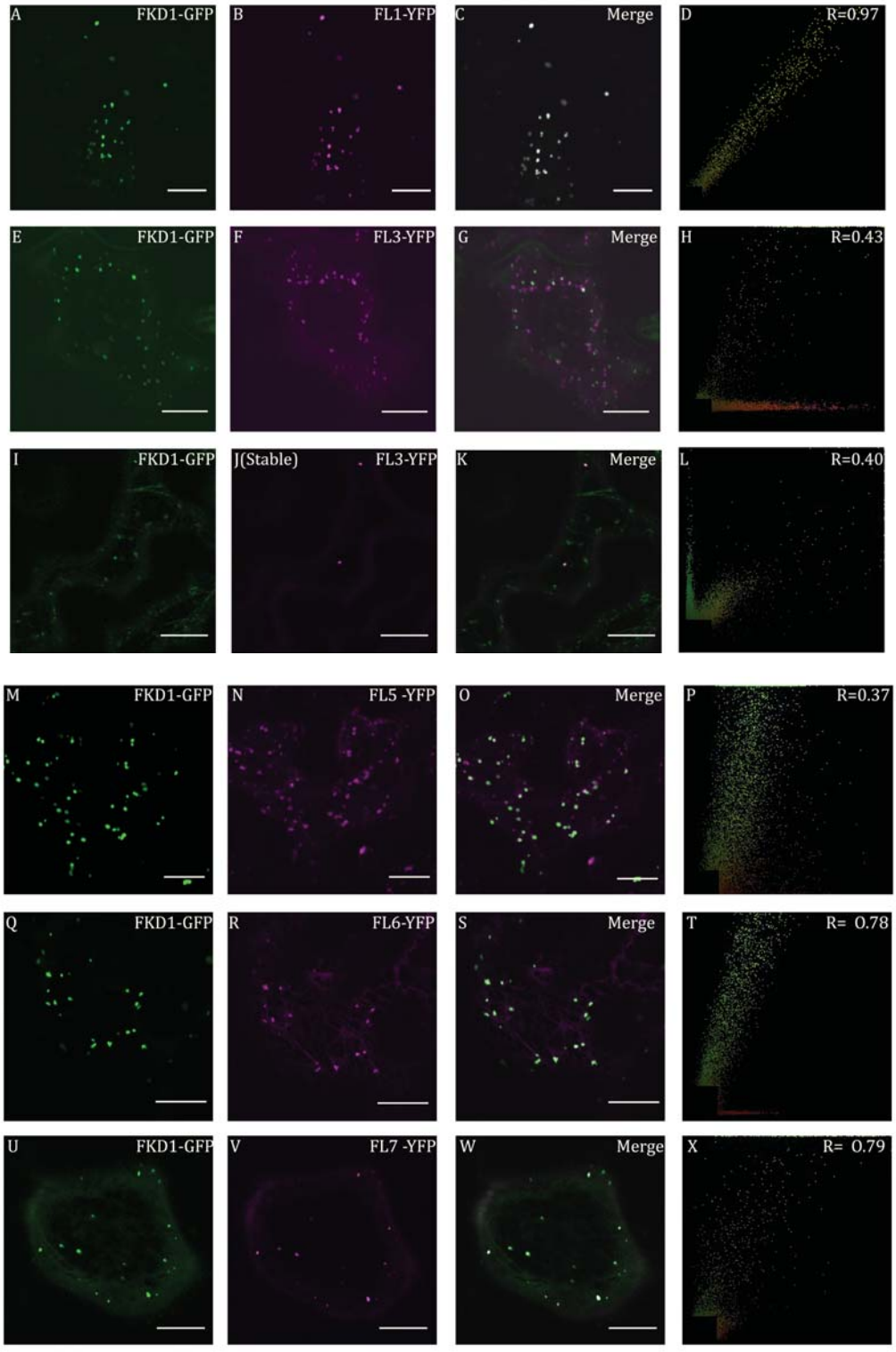
A FKD1-GFP
B FL1-YFP
C Merge
D R=0.97
E FKD1-GFP
F FL3-YFP
G Merge
H R=0.43
I FKD1-GFP
J(Stable) FL3-YFP
K Merge
L R=0.40
M FKD1-GFP
N FL5 -YFP
O Merge
P R=0.37
Q FKD1-GFP
R FL6-YFP
S Merge
T R= 0.78
U FKD1-GFP
V FL7 -YFP
W Merge
X R= 0.79

Figure 4.4: Subcellular localization of FKD1 with DUF 828 gene family members in Nicotiana and of FL3 with FKD1 in stably transformed Arabidopsis.

Localization of FKD1-GFP with DUF828 family members (A-H; M-X) in Nicotiana and FKD1-GFP with FL3-YFP (I-L) in Arabidopsis. A, E, I, M , Q and U are FKD1-GFP alone, E, F & J, N, R and V are FL1, FL3, FL5, FL6 and FL7 fused to YFP, C, G, K, O, S and W are the merged images. D, H, L, P, T and X are scatter plots of the merged image with Pearson's coefficient of Correlation (R) values (Scale bar:10μm).

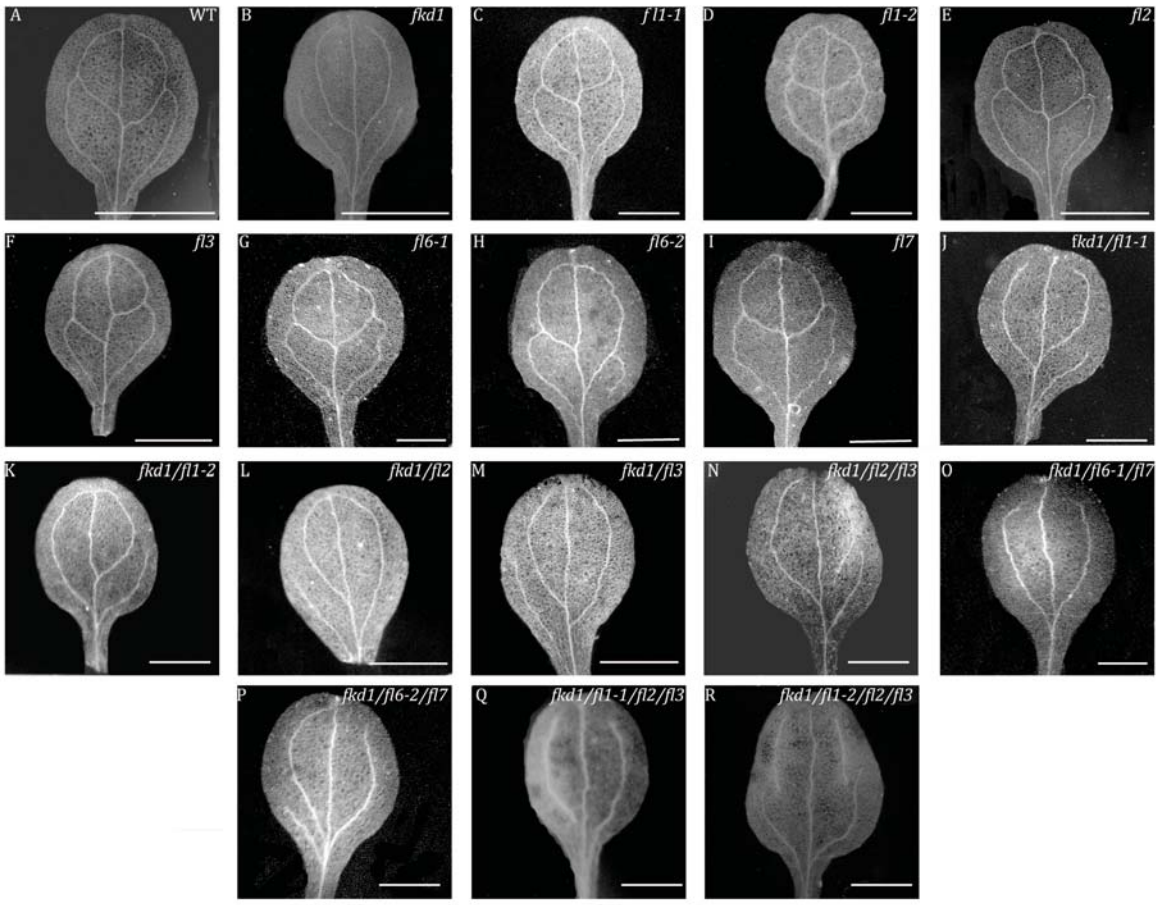

Figure 4.5: Vascular patterns of cotyledons of various genotypes at 14 DAG (Scale bar=2mm).

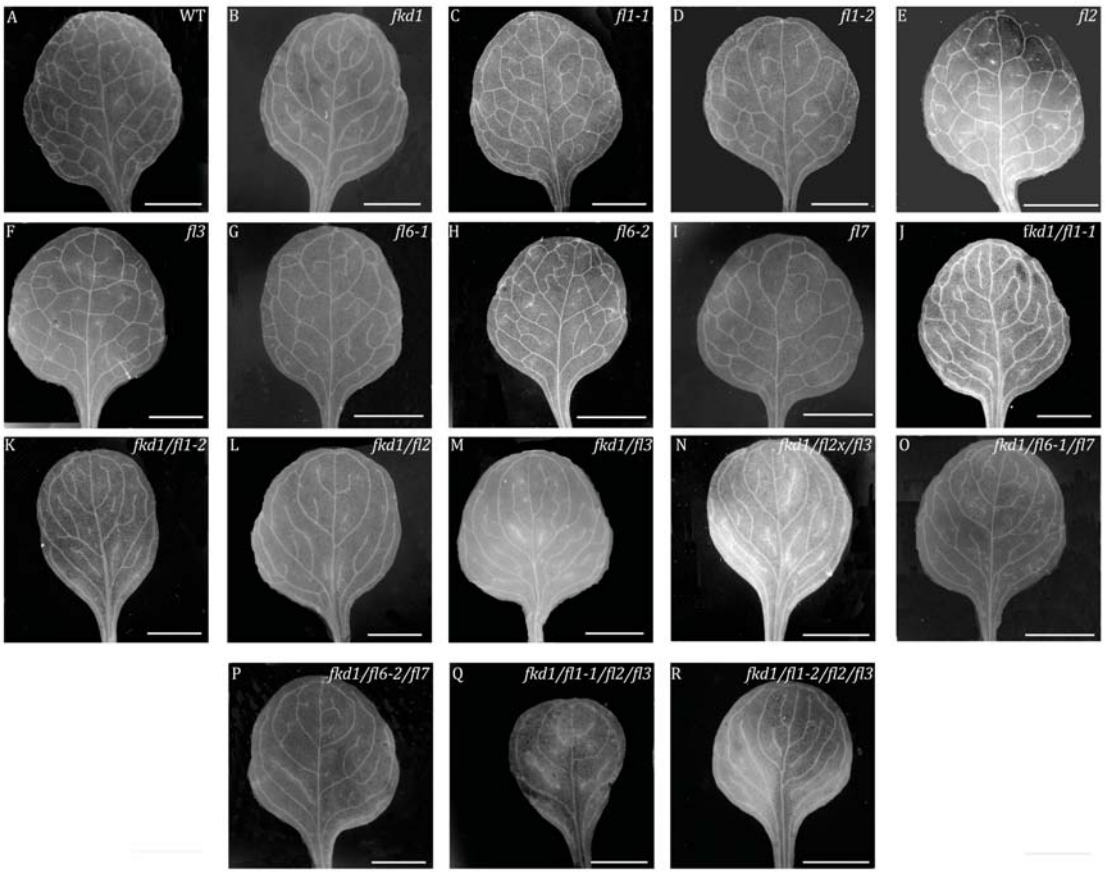

Figure 4.6: Vascular patterns of first leaves of various genotypes at 21 DAG (Scale bar=2mm.

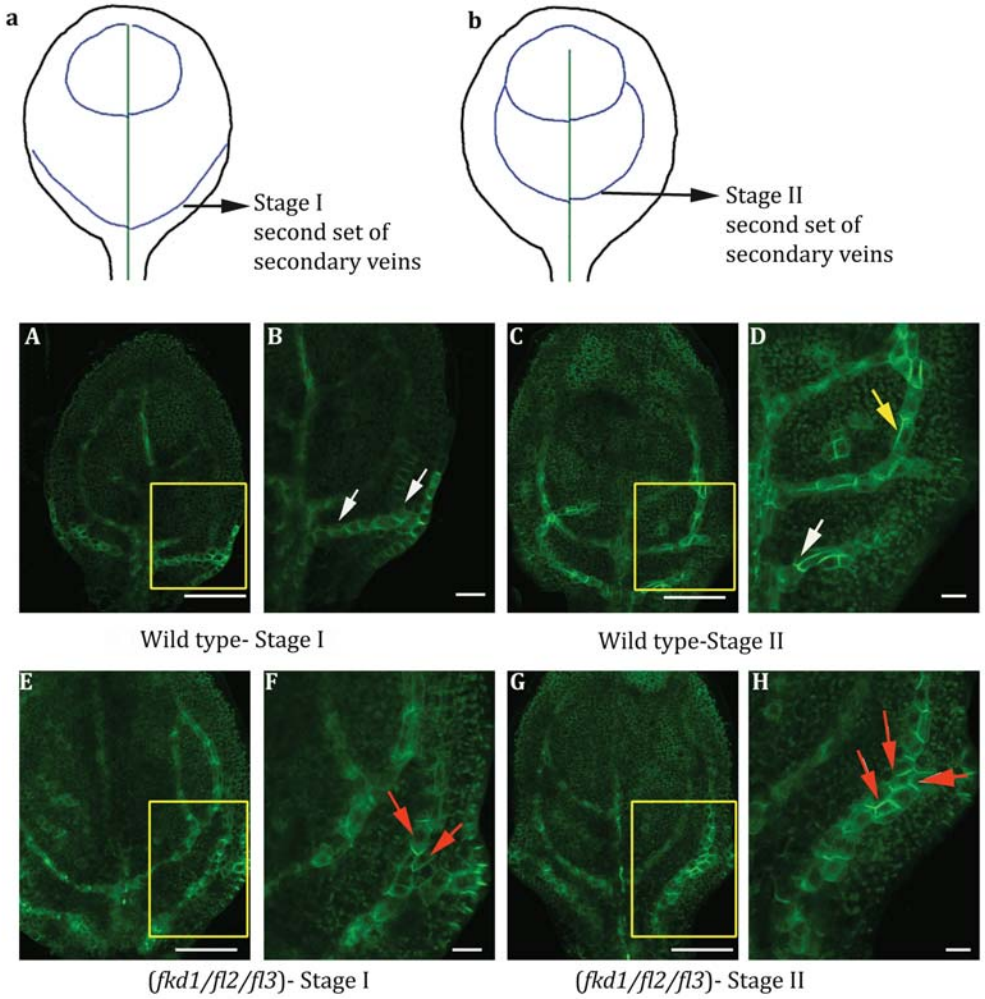

Figure 4.7: PIN1:GFP expression in the developing second set of secondary veins in wild type and triple mutant (*fkd1/ fl/2x fl/3*). (a and b) Diagram of successive stages of development of the second set of secondary veins, lines indicate PIN-GFP expression domains (PED). (A and C) PIN1:GFP expression in 2nd set of secondary veins of first leaf (Stage I and Stage II) respectively. (B and D) boxed area in A and C shown enlarged. (E and G) PIN1:GFP expression in 2nd set of secondary veins of triple mutant (Stage I and Stage II) respectively. (F and H) boxed area in E and G shown enlarged. White arrows indicate basal PIN1-GFP, yellow arrows indicate lateral PIN1-GFP and red arrows indicate PIN1 localization on all sides (Scale bar:10µm).

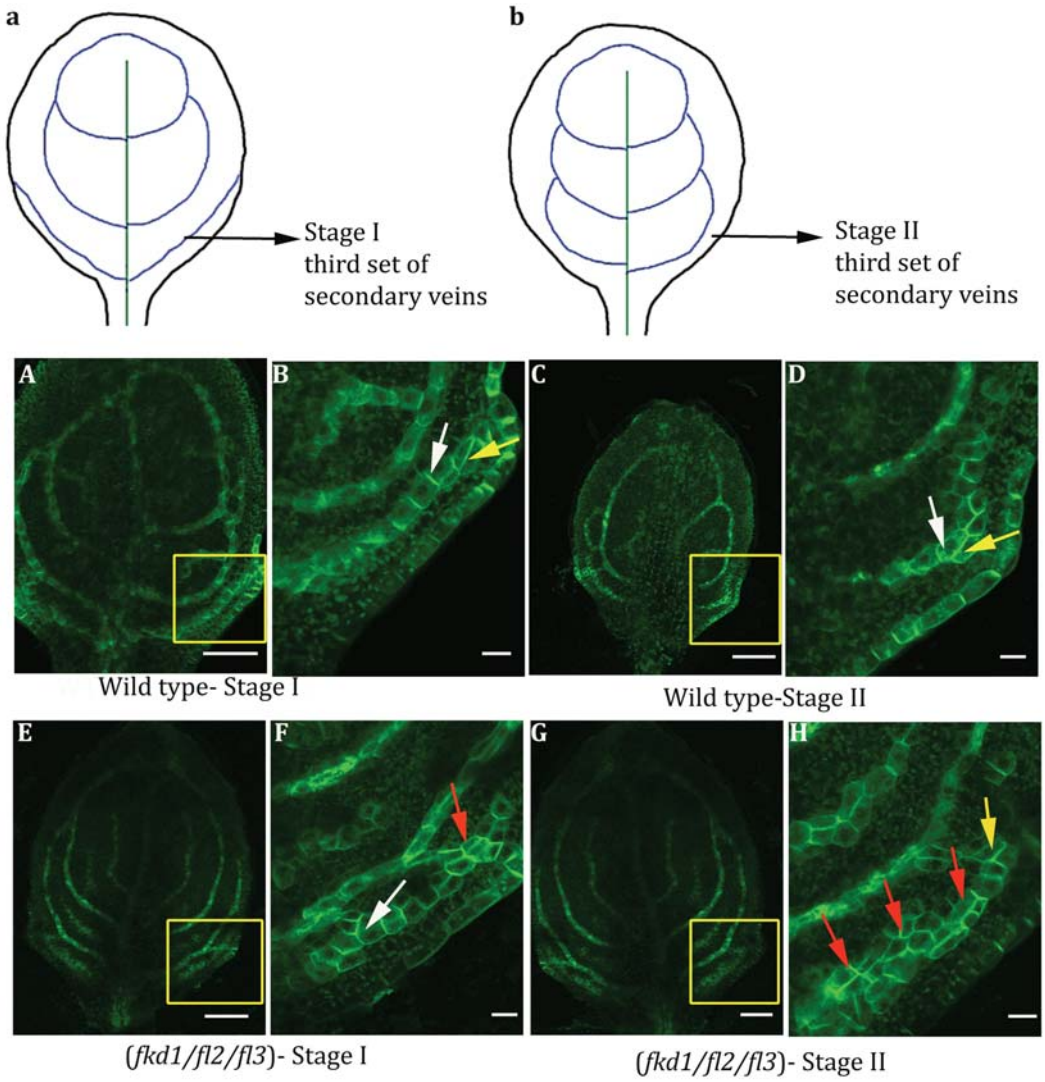

Figure 4.8: PIN1:GFP expression in the developing third set of secondary veins in wild type and triple mutant (*fkd1/ fl-2/ fl-3*). (a and b) Diagram of successive stages of development of the second set of secondary veins, lines indicate PIN-GFP expression domains (PED) (A and C) PIN1:GFP expression in 3rd set of secondary veins of first leaf (Stage I and Stage II) respectively. (B and D) boxed area in A and C shown enlarged. (E and G) PIN1:GFP expression in 2nd set of secondary veins of triple mutant (Stage I and Stage II) respectively. (F and H) boxed area in E and G shown enlarged. White arrows indicate basal PIN1-GFP, yellow arrows indicate lateral PIN1-GFP and red arrows indicate PIN1 localization on all sides (Scale bar: 10μm).

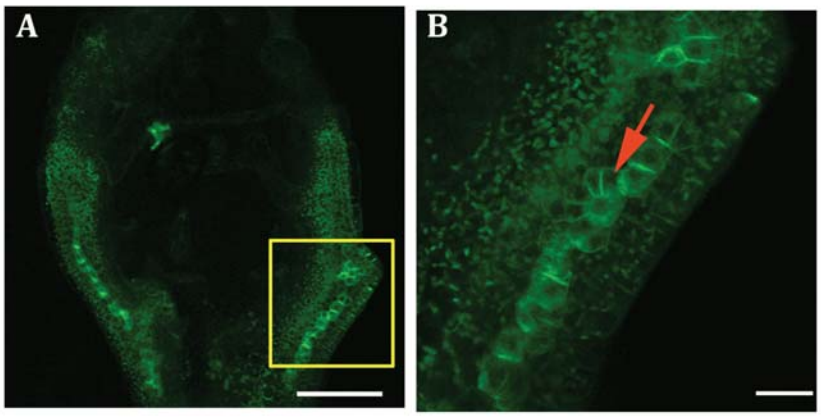

Figure 4.9: PIN1 expression in LLD of 3rd secondary veins showing PIN1-GFP localization.

PIN1-GFP expression in particularly arranged group of cells in developing veins (Stage I) of first leaves in triple mutant (*fkd1/fl2/fl3*) (A). Boxed area in A shown enlarged in B. (Scale bar:10µm). Red arrows indicate PIN1 localization on all sides (Scale bar:10µm). Note that PIN1-GFP is localized to all sides of the cell marked by the arrow head and cells surrounding that cell.

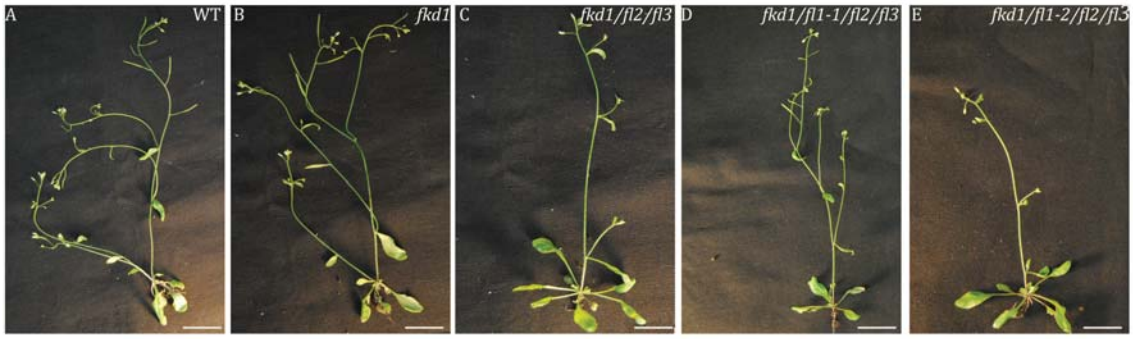

Figure 4.10: Adult plant phenotype of various genotypes

(A) Wild type at 19DAG (B) *fkd1* at 19 DAG (C) triple mutant (*fkd1/fl2/fl3*) at 23 DAG (D and E) two quadruple mutants (*fkd1/fl1-1/fl2/fl3 and fkd1xfl1-2/fl2/fl3*) at 27 DAG (Scale bar:5mm).

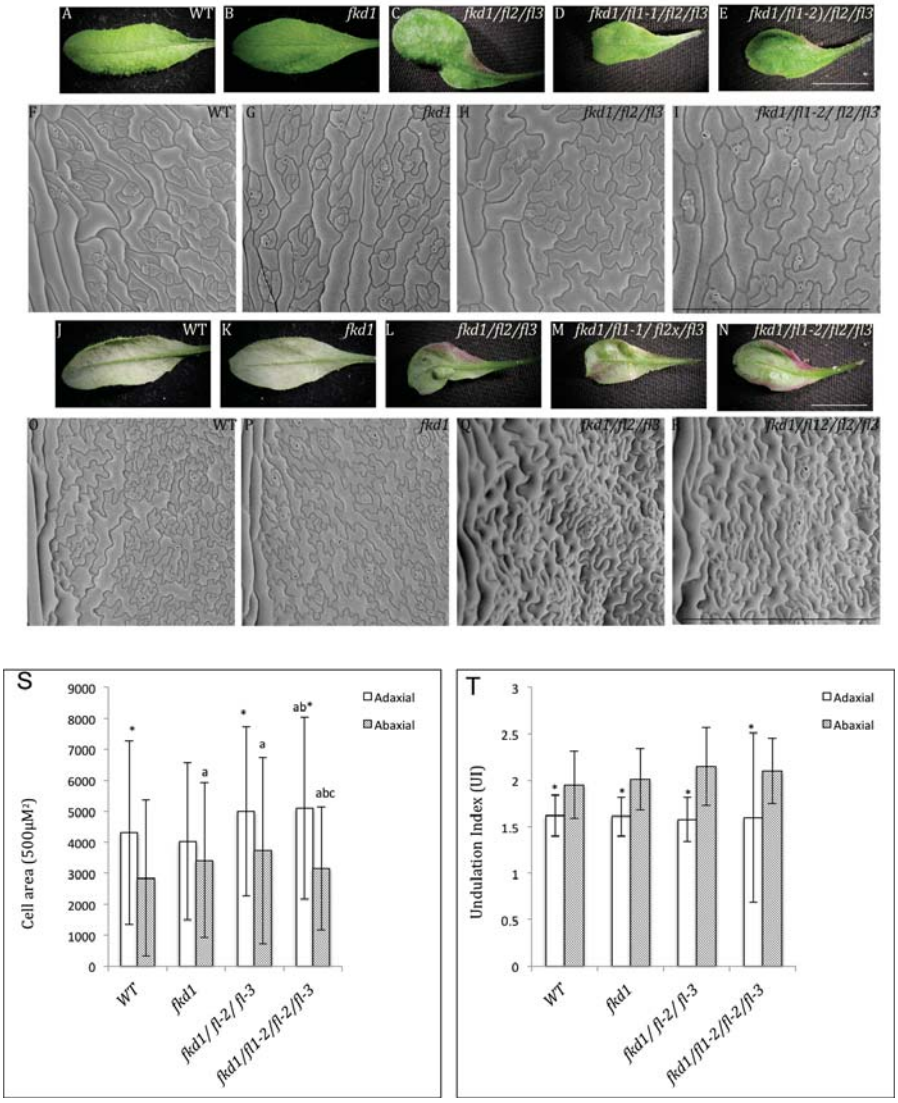

Fig 4.11: Adaxial (A-E; F-I) and abaxial (J-N;O-R) view of entire fifth leaves and SEM micrographs of fifth leaf epidermal pavement cells of various genotypes. (A, F, J and O) are wild type, (B,G, K and P) are *fkd1,* (C, H, L and Q) are triple mutant, (D, I, N and R) are quadruple mutant. (A-E, J-N; Scale bar:5mm). (A-E, J-N) are photographs and (F-I, O-R) are scanning electron micrographs with midvein along the left side of the image. (F-I, O-R; Scale bar:500μm). S and T are graphs of the cell area and UI of epidermal pavement cells on adaxial & abaxial side of fifth leaves. Error bars represent SD. [a] represents significant difference from wild type, [b] represents significant difference from *fkd1*, [c] represents significant difference from triple mutant ($p<0.05$, means were then compared using the least squares mean linear hypothesis test LSMEANS/PDIFF in ANOVA). * represents significant difference in cell area or UI of adaxial pavement cells compared to abaxial side of fifth leaves ($p<0.05$, means were then compared using the least squares mean linear hypothesis test LSMEANS/PDIFF in ANOVA). Sample size (n=150) for all genotypes.

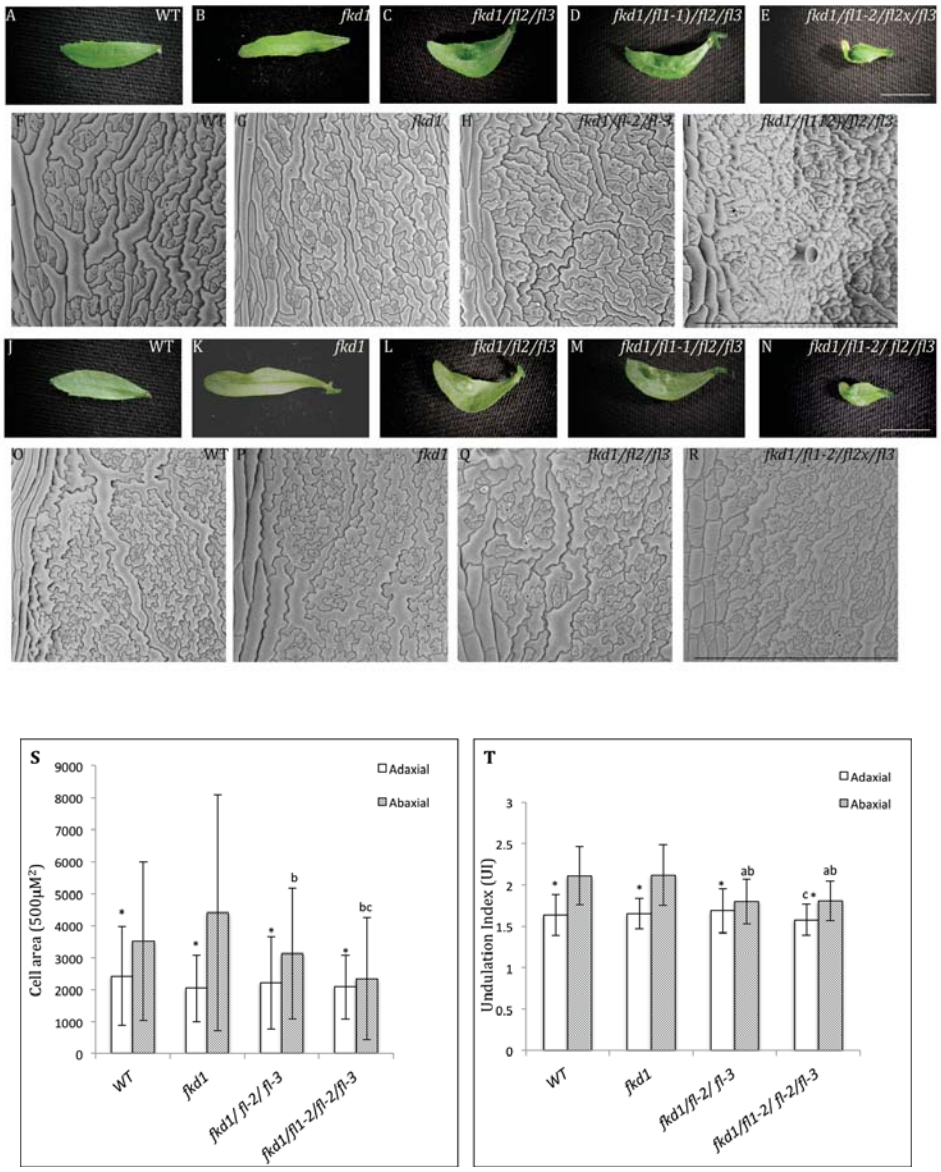

Fig 4.12: Adaxial (A-E; F-I) and abaxial (J-N;O-R) view of entire second bracts and SEM micrographs of second bract epidermal pavement cells of various genotypes.(A, F, J and O) are Wild type, (B,G, K and P) are *fkd1,* (C, H, L and Q) are triple mutant, (D, I, N and R) are quadruple mutants. (A-E, J-N; Scale bar:5mm). (A-E, J-N) are photographs and (F-I, O-R) are scanning electron micrographs with midvein along the left side of the image.(F-I, O-R; Scale bar:500µm). S and T are graphs of the cell area and UI of epidermal pavement cells on adaxial & abaxial side of second bracts. Error bars represent SD.[a] represent significant difference from wild type, [b] represents significant difference from *fkd1*, [c] represents significant difference from triple mutant ($p<0.05$, means were then compared using the least squares mean linear hypothesis test LSMEANS/PDIFF in ANOVA). * represents significant difference in cell area or UI of adaxial pavement cells compared to abaxial side of second bracts ($p<0.05$) (ANOVA). Sample size (n=100) for all genotypes.

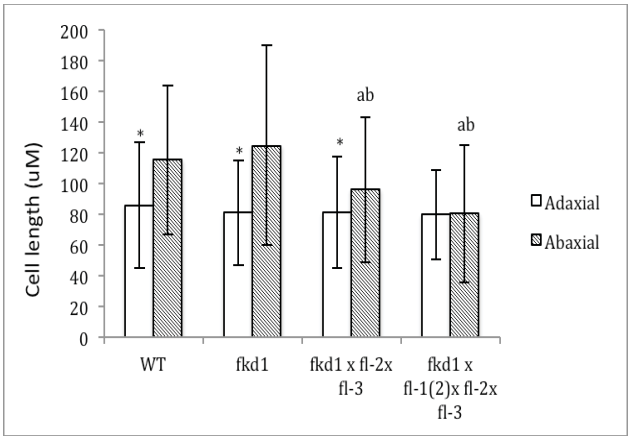

Figure 4.13: Graphs representing the cell length of epidermal pavement cells on adaxial and abaxial sides of second bracts. Error bars represent SD. a represents a significant difference from wild type, b represents a significant difference from *fkd1.* * represents a significant difference in cell length on the adaxial side compared to abaxial side of second bracts ($p<0.05$, Sample size ($n=100$) for all genotypes.

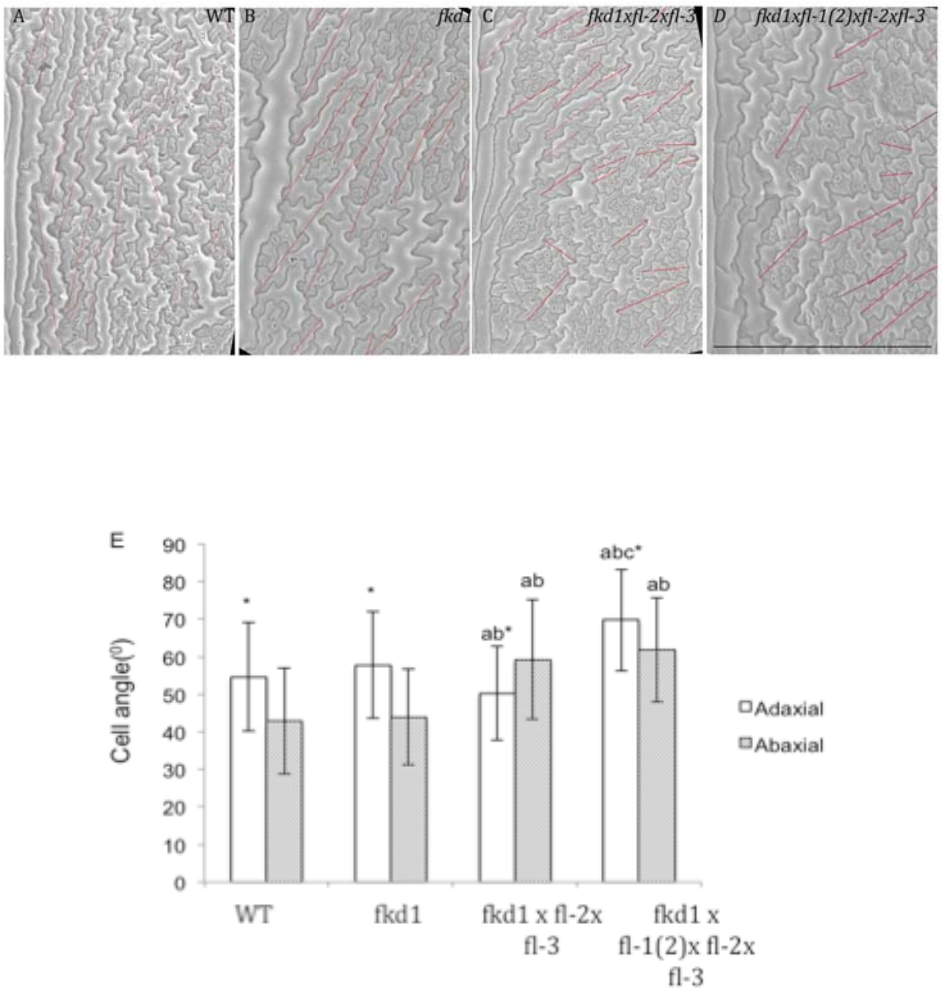

Figure 4.14: Cell polarity of epidermal pavement cells on abaxial and adaxial sides of second bracts. SEM micrographs of abaxial epidermal pavement cells (A-D). Wild type (A), *fkd1* (B), triple mutant (C) and quadruple mutant (D). Lines on figures indicate the longitudinal axis of the 30 cells most divergent from the midvein. Scale bar: 250µm. (E) Graph comparing the cell angle of epidermal pavement cells of adaxial side of second bracts. Error bars represent SD. a represent significant difference from wild type, b represents significant difference from *fkd1* ($p<0.05$, T-Test).

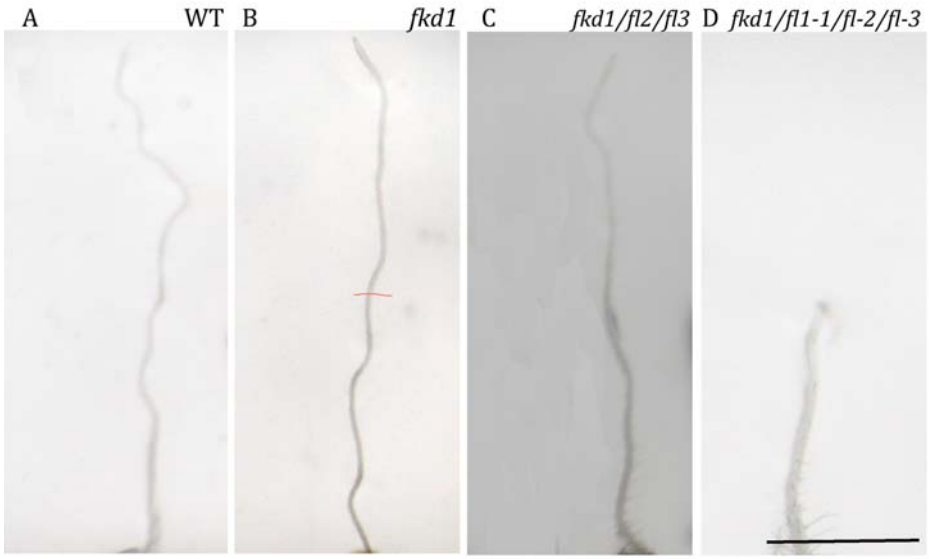

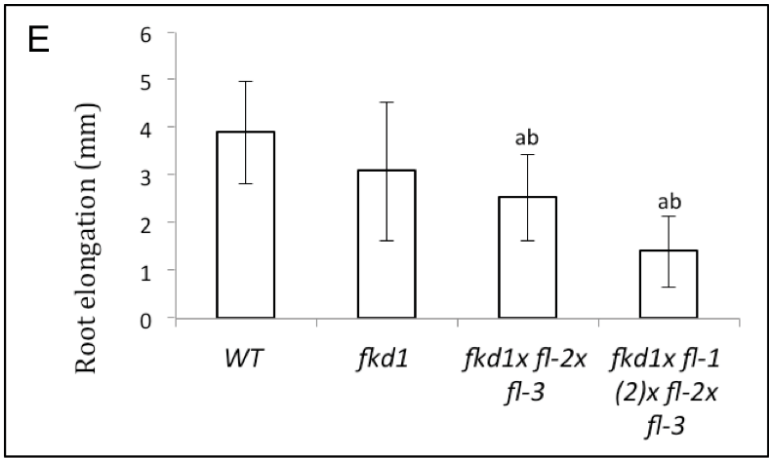

Figure 4.15: Primary root growth of Arabidopsis seedlings assessed over 24h (4DAG-5 DAG) (A-D). Wild type (A), *fkd1* (B), triple mutant(C) and quadruple mutant (D). (Scale bar: 2mm). (E) Graph comparing the root length among different genotypes. Error bars represent SD. a is significantly different from wild type and b is significantly different from *fkd1* genotypes ($p < 0.05$. T- test).

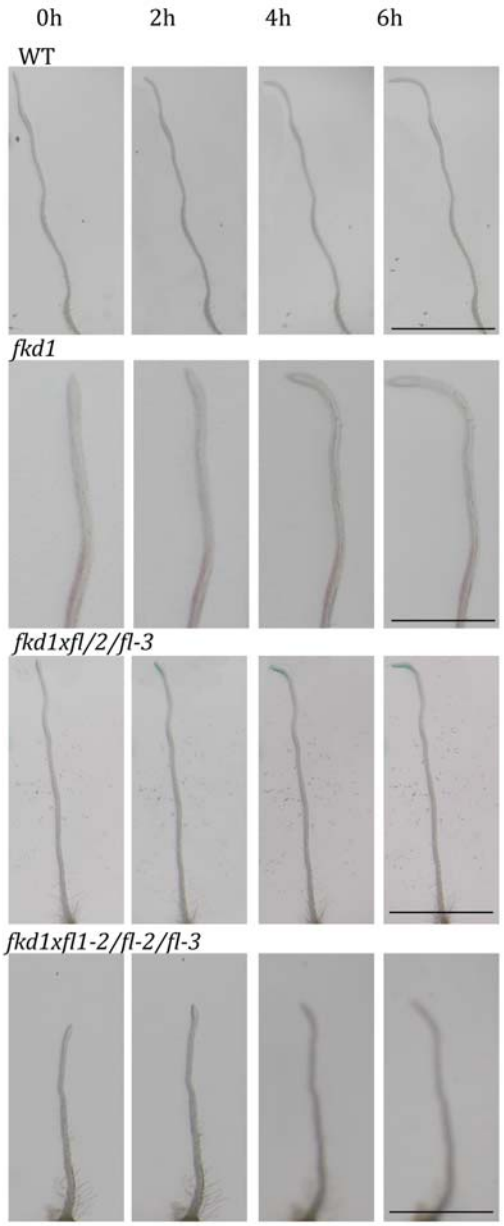

Figure 4.16: Gravitropic response showing the angle of root tip divergence from 0-6h of seedlings of various genotypes at 5DAG (Scale bar = 2mm).

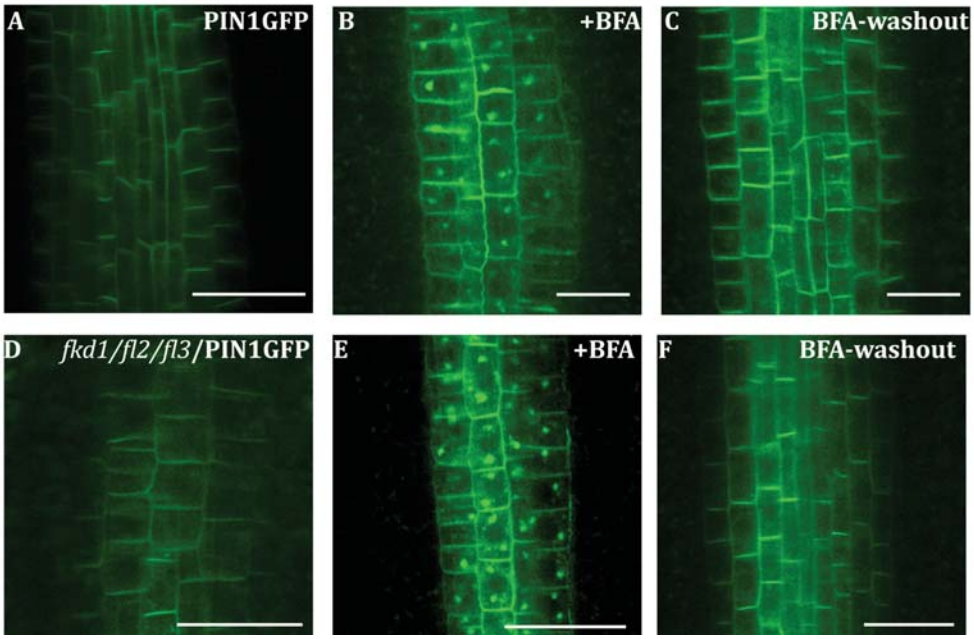

Figure 4.17: PIN1 trafficking is not altered in wild type and triple mutant roots. Confocal laser scanning microscopy of roots of wild type and triple mutants expressing PIN1-GFP at 2.5 DAG, before and after BFA washout (A-F). Polar PM localization of PIN in root vascular cells of wild type (A) and in triple mutant (D). (B) Accumulation of PIN1 in BFA compartments in wild type (B) and in triple mutant (E). After BFA washout, PIN1 is observed on PM in wild type (C) and in triple mutant (F). Scale bars = 10 µm.

CHAPTER 5: DISCUSSION

5.1 FKD1 localizes to the PM and throughout the post-Golgi endosome

My data suggest that FKD1 is localized to the plasma membrane, as well as to motile, punctate structures that are labeled by markers of the post-Golgi endosome. The moderate association of FKD1 with PM markers, YFP-NPSN12 and YFP-PIP1;4, and retention of that association after plasmolysis confirms that a proportion of FKD1 is acting at the PM. As well, when root tissue was labeled with FM4-64, initial uptake of FM4-64 into the plasma membrane (PM) strongly overlapped with membrane associated FKD1-GFP.

FKD1-GFP showed negative associaton to Golgi marker ST-RFP and moderate co-localization to markers of the TGN/EE (VTI12-YFP and SYP61-YFP). FM4-64 is quickly endocytosed into endocytic vesicles (Geldner et al., 2003; Grebe et al., 2003; Samaj et al., 2005; Geldner et al., 2009) and thus provides a marker of the early endosome. However, FKD1 vesicles colocalized only weakly with FM4-64 labeled vesicles at different time intervals, suggesting that only a small proportion of FKD1 is likely localized to the Early Endosome. FKD1 was shown to colocalize most strongly with RabA1e, RabA1g and RabF2b (ARA7)-YFP markers that have been delineated to various compartments (EE, RE and LE) within the endosome (Geldner et al., 2003; Grebe et al., 2003; Samaj et al., 2005; Geldner et al., 2009). Surprisingly, whereas RabF2b, RabA1e, RabA1g and VTI12 all become incorporated into BFA compartments following BFA treatment (Geldner et al., 2009), FKD1-GFP punctate structures do not become part of the BFA compartment in either cotyledon or root

cells. Together, these results suggest that FKD1 is localized to a BFA resistant compartment of the endosome, and is likely not involved in the early events of endocytosis.

The strong colocalization of FKD1 with RabF2b and RabA1e and very strong localization with RabA1g suggests that FKD1 may reside in a subcompartment of the endosome defined by these Rab GTPases. RabF2b (Ara7) has been described as localizing to both the LE (Ebine et al, 2011; Lee et al., 2004b) and the Early Endosome (Ueda et al., 2004; Geldner, 2004; Ebine et al., 2004). ARA7 was suggested to be involved in recycling the auxin efflux PIN1 to the PM and was found to be present in EE (Ueda et al., 2004, Geldner, 2004; Ebine et al., 2004). In *gnom* mutant cells, ARA7 positive endosomes appeared as large patches/clustered ring like structures (Geldner et al., 2003). RabF2b/ARA7 was assigned a LE/PVC localization based on its low BFA sensitivity, partial localization with FM4-64 (Geldner et al., 2009) and localization in multi vesicular bodies (Nielsen et al., 2008) and to LE (Kotzer et al., 2004).

RabA1e and Rab1g are members of the Rab-A clade that is most similar to the animal Rab11 which functions within the recycling endosome (Rutherford and Moore, 2002). RabA1e and RabA1g were suggested to mark endosomal compartments because of their partial association with FM4-64, and to the RE because of their strong sensitivity to BFA (Geldner et al., 2009). However, of the Rab-A clade that have been well characterized (RabA4b, RabA2, RabA3, RabA1b, RabA1c) most seem to be localized to the TGN and lie on the secretory pathway to

the PM (Chow et al., 2008; Preuss et al., 2004; Asaoka et al., 2013; Feraru et al., 2012; Qi and Zheng, 2013).

The largest subgroup within the Rab-A clade is RabA1, consisting of 9 members including RabA1e and RabA1g. The high amino acid sequence identity among the members of RABA1p proteins (70-80%) suggests that they may act redundantly, a suggestion supported by the colocalization of RabA1a, RabA1b and RabA1c (Asaoka et al., 2013) and analysis of multiple mutants for RabA1a, RabA1b, RabA1c and RabA1d (Asaoka et al., 2013; Qi and Zheng, 2013). While careful localization of RabA1e and RabA1g has not been done, we suggest that recent characterization of their close homologs RabA1a, RabA1b and RabA1c suggests that, like other members of the RabA1 group, they may be acting within the post-Golgi secretory pathway.

Like FKD1, RabA1b and RabA1c show weak to moderate colocalization with TGN, EE and LE markers including VTI12, and RabF2b (Ara7) (Asaoka et al., 2013). As well, while RabA1b compartments are described in one study as BFA sensitive (Feraru et al., 2012), in a second study, the authors point out that a large proportion of RabA1b punctae do not become incorporated into BFA compartments (Asaoka et al., 2013). The endocytic and secretory pathways merge within the TGN (Dettmer et al., 2006) and populations of endosomes are not completely stable compartments, but can gradually change their components and properties (Ueda et al., 2004). My analysis suggests that FKD1 localizes to a subcompartment within the TGN/ endosomal compartments. Furthermore, the BFA insensitive nature of FKD1

punctae and the weak association with FM4-64 suggests that FKD1 is more likely involved to be in the secretory pathway than in the endocytic pathway.

5.2 FKD1 localizes to SFC/VAN3 (ARF-GAP) and ARF proteins

I have shown that, in stably transformed Arabidopsis root and cotyledon cells, FKD1 colocalizes strongly with SFC/VAN3. While SFC and FKD1 localize strongly, a proportion of each is not colocalized. Previously, SFC together with GNOM, was found to have a role in clathrin mediated endocytosis (Naramoto et al., 2010), a suggestion supported by my finding that SFC shows higher colocalization with SYP61 and FM4-64 than FKD1 does. Thus, it seems likely that SFC acts independently of FKD1 in some compartments of the TGN/EE. Like punctae marked by FKD1-GFP, those labeled by SFC-YFP were insensitive to BFA treatment in root tissues, suggesting that both FKD1 and SFC are part of a BFA insensitive vesicle trafficking pathway.

SFC is an ARF-GAP of the ACAP class, and is predicted to act upon members of the ARF1 group, represented by ARFa1a-ARFa1f in Arabidopsis. FKD1 colocalized moderately or strongly with all members of the ARF1 group tested (ARFA1a, ARFA1c, ARFA1d, ARFA1e). Together with previous evidence that FKD1 forms a complex with SFC/VAN3, this suggests that the FKD1/SFC complex might in some way affect ARF1 activity.

ARF1 single mutants have no visible phenotype, suggesting that the high sequence similarity (>95%) reflects cellular redundancy (Xu and Scheres, 2005). However, a dominant negative allele of ARF1A1c (*bex-1*) affects the exocytosis or

recycling of PIN1 to the PM (Tanaka et al., 2014). At levels of BFA that did not affect wild type, PIN1 was depleted from the PM and formed intracellular agglomerations in the *bex-1* mutant, suggesting that trafficking from the BFA sensitive endosomes to the PM was defective (Tanaka et al., 2014). Overexpression of a GTP-locked version of ARFA1c resulted in PIN1 mislocalization in embryos (Tanaka et al., 2014), as well as defects to root growth and root hair formation (Xu and Scheres, 2005). The colocalization of FKD1, SFC and ARF1 proteins, and the fact that mutation to any of the three genes results in PIN1 PM mislocalization (Hou et al., 2010; Scarpella et al., 2006; Tanaka et al. 2014) suggests that they may be working together to properly establish PIN1 at the plasma membrane.

All these results lead to the idea that FKD1 might be associating with SFC in some way to modify the activity of ARF proteins. The association of FKD1, SFC (ARF-GAP) and ARF1 proteins suggests that ARF-GEFs could also be a part of this complex, however the identity of ARF-GEFs is not clear. Plants contain two ARF- GEF subfamilies i) the GBF subfamily that comprises of GNOM, GNOM LIKE1 (GNL1) and GNL2 and ii) the BIG subfamily, which comprises of five members (BIG1-5) (Richter et al., 2007). ARF1A1c colocalizes with a number of ARF-GEFs including GNOM, GNL1, BEN1/MIN7/BIG5 (Tanaka et al., 2014), BIG3 and BIG4 (Richter et al., 2014), suggesting it may be regulated by multiple ARF-GEFs in different compartments. As well, BIG3 has shown to interact *in vitro* with ARF1-A1c protein by catalyzing the nucleotide exchange of ARF1 in a BFA-insensitive manner (Nielsen et al., 2008). Thus, it seems that the ARF1 group might be quite promiscuous in its use of ARF-GEFs.

While SFC/VAN3 has been proposed to interact with GNOM at the PM and be required for clathrin mediated endocytosis (Naramoto et al. 2010), it seems unlikely that FKD1, which shows weak colocalization with FM4-64 labelled vesicles, would be part of this complex. ARF-GEF proteins are localized in overlapping compartments within the endomembrane system, and although recent studies have clarified their localization, considerable debate remains. Based on the localization of the ARF-GEFs, it seems that the BIG subfamily, which, like FKD1 and SFC localize to the TGN/EE, are more likely candidates than the GBF subfamily, which primarily localizes to the Golgi. Because *gnom* mutants exhibit defects in endocytic recycling of PIN1 proteins, and because analysis of GNOM localization was primarily done in BFA treated cells, GNOM was originally thought to reside in the recycling endosome (Steinmann et al., 1999: Geldner et al, 2003). However, recent studies have shown that GNOM is mostly localized at the Golgi apparatus and its affects on recycling PIN and other proteins to the PM are indirect (Naramoto et al., 2014). GNL1 localizes to Golgi and is involved in regulating COP1-coated vesicle formation (Geldner et al., 2003). *gnl1* mutants show defects in secretion but not in general endocytic recycling (Teh and Moore, 2007) and GNOM and GNL1 have recently been found to both work in an early secretory pathway which is important for localization of newly synthesized PIN to the basal PM (Doyle et al., 2015). BIG family (BIG1-4) proteins have been suggested to have a role in trafficking of proteins, including newly synthesized PIN1 proteins, from the TGN to the PM and to the vacuole (Richter et al., 2014). BIG 3 and BIG4 have been shown to colocalize with the TGN marker VHA-a1 and colocalize with FM4-64 after a brief uptake, suggesting that these ARF-GEFs

localize to the TGN/EE (Richter et al., 2014). BIG5/BEN1 (BFA *visualized endocytic trafficking defective*) /MIN7 localizes to TGN/ EE and has been suggested to be involved in early endosomal trafficking events through the TGN, which is essential for polar localization of PIN1 and PIN2 proteins, a pathway distinct from other pathways involving known ARF-GEF proteins. The cotyledons of *ben1* mutants displayed disconnected vasculature and aberrant PIN1 localization (lateral PIN1 localization) in the primary roots (Tanaka et al., 2009; Tanaka et al., 2013).

Since both FKD1 and SFC labeled compartments are BFA insensitive, it seems likely that the ARF-GEF partner might be BFA resistant. In Arabidopsis, out of the eight ARF-GEFs, only three (GNL1, BIG3 and BEN1/MIN7/BIG5) are resistant to Bredfeldin A (BFA) (Geldner et al., 2003, Richter et al., 2014). Given the cellular localization of GNL1 (Golgi) and BIG3/BIG5 (TGN), BIG3 and BIG5 seem to be the most likely candidates.

5.3 FKD1 and SFC play a role in vesicle trafficking of PIN1 proteins

As evident from the results mentioned in previous sections, FKD1 associates with PM, TGN/endosomal compartments, and association of FKD1 with VAN3/SFC and ARF1 proteins suggests that they might have a role in intracellular vesicle trafficking processes. Since both *fkd1* and *sfc* mutants have defective PIN1 localization in veins of first leaves, colocalization experiments with PIN1-RFP were performed. The moderate colocalization of FKD1 with PIN1 and association of FKD1 with SFC suggest a possible role for FKD1 in PIN1 protein trafficking pathway, through its association with SFC. Colocalization of FKD1 with PIN1 vesicles outside

the BFA compartments suggests that FKD1 is involved in PIN1 trafficking through a BFA insensitive pathway.

PIN protein trafficking to apical and basal sides of the cell are regulated by ARF-GEF mediated BFA sensitive and BFA insensitive pathways and also by the phosphorylation status of proteins. Recycling of PIN1 to the basal side of the membrane is mediated by GNOM, a BFA sensitive ARF-GEF. Phosphorylation of PIN proteins by AGC-3 kinases (PID/WAG1/WAG2) results in apical targeting of PIN proteins. It has been proposed that ACG-3 kinases phosphorylate PIN1 proteins predominantly at the PM for eventual PIN1 internalization and PIN sorting to ARF-GEF, GNOM independent polar recycling pathways (Dhonukshe et al., 2011). In an opposing reaction, dephosphorylation by PP2A results in basal targeting of PIN proteins (Kania et al., 2014). A loss-of-function PID mutant resulted in the shift of PIN1 from apical to the basal side of shoot epidermal cells and PID overexpression leads to a shift of PINs from the basal to the apical side in stele and ground tissues of the roots (Friml et al., 2004). Similarly, mutants deficient in PP2A activity displayed a basal-to-apical shift in PIN localization (Michniewicz et al., 2007)

Two different endocytic trafficking pathways have been suggested for the PM receptor FLAGELLIN SENSING 2 (FLS2) depending on its activation status (with or without fls22). The non-activated FLS2 enters a recycling and BFA sensitive pathway whereas activated FLS2 is trafficked through a BFA insensitive pathway (Beck et al., 2012). Interestingly, the compartment through which the activated FLS2 travels is labeled by SYP61 (early) and Ara7 (early and late) but not VHA-a1 (Choi et al.,

2013). Colocalization of SYP61 and Ara7 only occurred in the presence of FLS2, suggesting that the compartment is highly dynamic and induced by endocytosis. Finally, the results indicate the importance of the RabA family in FLS2 trafficking, since dominant negative mutations in either RabA4c or RabA6a affected the endocytic entry of FLS2, while a similar mutation in Raba1b affected the secretion of newly synthesized FLS2 to the plasma membrane. Apical and basal localization of PIN1 is known to depend on the phosphorylation status of PIN1. It would be interesting if, like activation status of FLS2, the phosphorylation status of PIN1 directed it to either BFA sensitive or insensitive pathways.

5.4 FKD1 localization is influenced by PI(4)P

My results suggest that PI4P, the product of 5PTases CVP2 and CVL1, is at least in part required for the punctate localization of FKD1. The FKD1 PL domain was found to act redundantly with the SFC/VAN3 PH domain so that either is required for proper cellular localization (Naramoto et al., 2009). Fat western blotting revealed that SFC/VAN3 binds to PtdIns(4)P with higher affinity than to PtdIns and to PtdIns(4,5)P2 (Koizumi et al.,2005). Mislocalization of VAN3 from the TGN to the cytosol in a double knockout of *CVP2* and *CVL1* supports the idea that SFC/VAN binds to PtdIns(4)P (Naramoto et al., 2009), a product generated from PI(4,5)P_2 by CVP2 and CVL1 (Carland et al., 2009). Consistent with the localization of FKD1 to the TGN and endosomes, PI(4)P has been shown to occur within the Golgi and Plasma membrane (Vermeer et al., 2008) and within post-golgi endosomes (Simon et al., 2014). I found that, although punctate localization was not eliminated, FKD1GFP localization was more frequently cytosolic in cotyledons of lines

homozygous for *cvp2cvl*, suggesting that, like SFC/VAN3, FKD1 also interacts with PtdIns(4)P. *Arabidopsis thaliana* encodes 15 5PTase genes capable of hydrolyzing 5-phosphates from a variety of inositol phosphate and phosphoinositide substrates (Ercetin and Gillapsy, 2002; Berdey et al., 2001). It is likely that these redundant functions allow production of some PI4P in the *cvp2cvl1* mutant, allowing for localization of FKD1-GFP. Alternatively, it may be that the FKD1 PL domain is more promiscuous than the PH domain of SFC/VAN3, and binding of FKD1 to endomembrane structures labeled by other PIs occurs even in the absence of PI(4)P. I also tested localization of FKD1-GFP in a PI4Kβ1β2 double mutant, but found no change in FKD1-GFP localization. This can be attributed to the presence of 12 PI4K isoforms in Arabidopsis genome and their possible redundant function, so that there will still be some PI(4)P generated from those members for the PL domain to bind to.

PI(4)P and PtdIns(4,5)P_2 are enriched in the apical and basal plasma membranes of root cells (Tejos et al., 2014). Mutants in PIP5 kinases result in a range of auxin related phenotypes including root agravitropism, reduced root growth, embryonic defects, and vascular islands in cotyleons, all of which may be explained by the observed alteration to PIN1 and PIN2 localization (Tejos et al., 2014; Ischebeck et al., 2013). In the *PIP5K1PIP5K2* double mutant, PIN1 localization to the basal membrane of the stele is more diffuse, suggesting a reduction in protein secretion. In contrast, PIN2, rather than being exclusively localized to the apical membrane of cortex cells, is frequently localized to the lateral side. In the double mutant, both PIN1 and PIN2 show reduced accumulation in BFA compartments,

which has been attributed to defects in clathrin-mediated endocytosis (Ischebeck et al., 2013). It also seems possible that the reduced accumulation in BFA compartments could be due to reduced protein secretion, as described by Doyle et al., (2015) for *gn* and *gnl1* mutants. Interestingly, developing veins in the *PIP5K1PIP5K2* double mutant fail to establish clear basal localization of PIN1 and instead localize PIN1 to all sides of the cell (Tejos et al., 2014). While it is not clear if the defect in veins is due to changes in secretion or endocytosis, the observation clearly demonstrates that the distribution of PtdIns4P and PtdIns(4,5)P_2 is important to proper vein formation.

5.5 DUF828 gene family acts redundantly to control leaf vein patterning

Analysis of lines multiple mutant for members of the DUF828 gene family suggests that they act redundantly to control vein connectivity and vein density in cotyledons and leaves. The number of VI is higher in lines doubly, triply and quadruply mutant for Group IIIC genes (FKD1, FL1, FL2, FL3), and this was correlated with more defective PIN1 localization in *fkd1/fl2/fl3* triple mutants compared to that previously described in *fkd1* single mutants (Hou et al., 2010). In wild type secondary veins at later stages of development, most of the cells have basal localization (LLD and ULD) or apical localization (upper portion of ULD). The proportion of cells with lateral PIN1 localization at later stages was almost same in wild type and triple mutant (15-18%). Interestingly, triple mutant had 50% of cells with PIN1 localized to all sides of the membrane. The very strong colocalization of FKD1 with FL1 and partial localization with FL3 suggests that the Group IIIC

proteins may be acting in the same compartment to properly position PIN1 on the membrane, and that they may be particularly important in directing PIN1 to the apical membrane.

Proper polar PIN1 localization and expression is required for auxin canalization, which allows narrowing of the PIN1 expression domain and results in formation of continuous vascular strands (Sauer et al., 2006; Scarpella et al., 2006; Wenzel et al., 2007) and defects to PIN1 localization in *fkd1* single mutant are correlated with wider PIN expression domains (Hou et al., 2010). In triple mutant leaves, PEDs remained wider in comparison to wild type plants and PIN1 restriction to a single cell file occurred only in 4% and 7% of veins in second and third set of secondary veins respectively.

Introduction of members of group IIIB into the *fkd1* background do not increase the severity of non-meeting veins, suggesting that this group is not required for vein meeting despite the fairly strong colocalization of FKD1 with FL6 and FL7. However, lines mutant for two members of this group (*FL6* and *FL7*) together with *fkd1* result in leaves that are smaller than wild type, but maintain the same vein density as wild type. The formation of smaller leaves with similar vein density to wild type is also seen in several double, triple and quadruple mutants within Group IIIC. The trend towards smaller leaves having higher vein density is well conserved throughout angiosperms (Sack et al., 2012), but the mechanism controlling the relationship is not known. My data suggests that Group IIIA and Group IIIC genes may have a role in this process.

5.6 FKD1 gene family affects root elongation processes

The severe defects exhibited in the leaf vascular patterns by the loss of function mutations in the triple and quadruple mutants suggest that these genes participate in auxin related developmental processes in plants. Analysis of root gravitropic response and primary root length suggests that mutations in three or four members of the Group IIIC FKD1 gene family result in reduced primary root elongation and reduced response to gravity. Despite these differences, I could detect no differences to PIN1 localization in triple mutants, nor was relocalization of PIN1 following BFA altered, suggesting that in roots, the growth defects are not due to PIN1 trafficking defects. As mentioned earlier (Section 1.3.3.3) several PIN proteins with distinct localization are responsible for the continuous flow of auxin that controls root elongation. AUX1, PIN2 and PIN3 proteins have been suggested to have a role in transport of auxin to the elongation zone (Friml et al., 2002; Swarup and Péret, 2005; Marchant et al., 2002; Eshel and Beeckman, 2013). *pin1pin2* double mutants display a more than additive reduction in root length (Blilou et al., 2005). Single mutants of *pin*2, *pin3 and aux1* mutants are agravitropic (Rashotte et al., 2000; Swarup and Péret, 2005; Baluska et al., 2010). PIN1 has basal localization in vascular cells, whereas PIN2 localizes apically in epidermal and lateral root cap (Blilou et al., 2005) and PIN3 localizes laterally in the columella. We have seen that in leaves, the lack of FKD1 Group IIIC genes affects apical more than basal PIN1 localization. It is possible that in roots, the influence of these genes influence apical localization of PIN2 more than basal localization of PIN1.

5.7 DUF 828 gene family controls leaf morphology through polarity specific elongation of cells

One of the characteristic phenotypic traits exhibited by triple and quadruple mutant in Class IIIC genes is the formation of asymmetric rosette leaves and depressions and bumps on bracts. The first visible effect of DUF 828 gene family mutation on leaf development is in third leaves, which suggests that the gene family does not affect morphology during the initiation and early development of leaves. Later on, the phenotypic defects with respect to leaf morphology become more prominent resulting in the formation of bracts with depressions and bumps. It is possible that redundantly acting genes are expressed during early vegetative growth, but not during later vegetative growth and reproductive development, resulting in the expression of the phenotype only in later growth stages.

My analysis revealed a number of changes to cell shape and cell orientation that might account for the distorted leaf shape. For example, in fifth leaves, cells were consistently larger than mutants compared to the wild type. In bracts, abaxial cells of the mutants were smaller, less elongated and less undulated, while adaxial cells were no different from wild type. It is possible that lack of growth coordination between abaxial and adaxial surfaces accounts for the distorted leaf shape. I also found some evidence for lack of coordination within the abaxial epidermal cells of the triple and quadruple mutant bracts. In wild type bracts, most pavement cells are oriented with their longitudinal axis parallel to the midvein, although some cells diverge from parallel. I compared the most divergent cells in wild type, *fkd1* and

triple and quadruple Class IIIC mutants and found that the divergence was significantly greater ($p<0.05$) in the multiple mutant lines than in wild type or *fkd1*. Together with the reduced cell elongation, this suggests that the cells are improperly polarized within the epidermis, and that Class IIIC genes of the FKD1 gene family may be involved in establishing planar cell polarity within the leaf and hence regulation of polarity-specific elongation in pavement cells.

A critical factor that controls the organ architecture in plants is the direction of cell expansion, which determines final cell shape (Abe et al., 2004). During the development of a cell, cell-expansion is coordinated with polarized cell growth, which determines cell shape. The jigsaw puzzle shape of pavement cells is established at the cell proliferation-to-cell expansion transition, where precise cell expansion and elongation results in formation of indentations and lobes. Thus, the appearance of the puzzle shape fits with the moment at which differential relative cell expansion rates in adjacent cells would first appear.

It is also possible that the reduced undulation of pavement cells on the abaxial side of bracts is not the indirect affect of polarity but rather due to direct effects on lobe and indentation formation. Undulation index is a measure of lobe and indentation formation in pavement cells. Auxin is involved in modulating the shape of PC. Auxin accumulation in cell wall between lobes and indentation is facilitated by the polar localization of PIN proteins in PM at the lobes mediated by ROP2 and ROP6 proteins (Fu et al., 2005). If auxin transport is restricted, limited expansion of lobes with less prominent indentations and therefore less undulation occurs. Group IIIC

members might be involved in PIN1 protein localization that leads to proper accumulation of auxin in pavement cell lobes.

The epidermal pavement cells on abaxial and adaxial side of second bracts display defects like reduced cell elongation and defects in alignment of the cells to the longitudinal axis of the midvein. These might be due to planar polarity defects in which cells have lost their ability to coordinate the polarity within the tissue. Planar polarity is important for morphogenesis of pavement cells and the formation of lobes and indentations require dynamic polarity formation (Fu et al., 2005). Auxin plays role in establishing cell polarity, through PIN mediated auxin efflux which in turn is related to ROP signaling that regulates polarity of pavement cells. Hence it suggests that this signaling pathway might be impaired in triple mutants rendering them with polarity defects.

5.8 Evolution of DUF domain containing proteins

The DUF828 gene family encodes proteins with DUF828 and PH/Pleckstrin-Like (P-Iike) domains. A search for species containing DUF828 domain family proteins revealed that it exists only in the plant kingdom, and that its expansion can be correlated with key events in plant kingdom evolution (Fig.4.2.B). The presence of a single DUF828 containing gene within the genome of *Physcomitrella patens* suggests a bryophytic origin of this gene family, indicating that the origin of the family coincided with the emergence of terrestrial plants approximately 443-490 million years ago (Douzery et al., 2004). Moreover, since *Physcomitrella patens* is a non-vascular plant, the family's original role was not associated with vascular tissue.

However recent studies have shown that polar targeting of PIN proteins and PIN protein mediated auxin transport is responsible for gravitropic responses, gametophyte, sphorophyte, and leaf development in *P. patens* (Bennett et a., 2014), which implies the function role of PIN proteins in evolution of plant forms. Interestingly, the emergence of vascular tissue is correlated with an amplification of the gene number to four in *Selaginella moellendorffii*. A four member gene family is retained in gymnopsperms (*Picea abies*) and *Amborella trichopoda,* a sister species to all other extant angiosperms (Chamala et al., 2013). Interestingly, in the basal angiosperm *Amborella trichopoda*, the emergence of a reticulate vein pattern (Takhtajan, 2009) is correlated with the emergence of two angiosperm specific groups, Group IIIA and Group IIIC. While only single gene members of group IIIA exist in more derived Angiosperms (*Arabidopsis thaliana, Populus trichocarpa, Solanum lycopersicum*), Group IIIC is expanded to 4 members in *Arabidopsis thaliana,* 3 members in *Oryza sativa,* 4 members in *Populus trichocarpa* and 2 members in *Solanum lycopersicum*. It is tempting to speculate that the presence of monophyletic angiosperm specific groups indicates the functional importance of DUF 828 family during the evolution of vein pattern within the angiosperms.

Strong variation in the leaf venation systems exists across major plant lineages. It has been suggested that during the early Devonian period (400 Ma), leaf-like organs evolved independently in two lineages (Lycophytes), from microphylls, evolving through enation and later becoming vascularized (Sack and Scoffoni, 2013; Floyd and Bowman, 2006). Almost all plants with fern-like leaves (ferns, progymnosperms and gymnosperms) in the Devonian and Carboniferous era had an

open venation pattern. The open venation pattern represents primitive vein architecture and the modern network/reticulation patterns evolved from open venation patterns (Roth-Nebelsick, 2000). While the oldest angiosperm fossils date from 130 to 136 million years ago (Ma), it has been estimated that angisoperms emerged at least 160 Ma (Magallón et al., 2013; Doyle et al., 2012; Zhang et al., 2012 and Jiao et al., 2011). Vein traits contribute to greater performance of plants, and angiosperms evolved distinctive vein traits compared to their earlier evolved lineages. Earlier angiosperms possessed lower-order veins with less organization, whereas more derived angiosperms had increasing number of vein orders (Brodribb and Field, 2010; Sack and Scoffoni, 2013) with the hierarchy of vein orders forming the reticulate mesh typical of angiosperms (McKown et al., 2010). Later on during evolution, large leaves with large major veins for mechanical support and a high leaf vein length per unit area (VLA) enabled better transpirational cooling and higher photosynthetic rates (Sack et al., 2012). Multiple mutants in the Class IIIC group result in leaves that lack the reticulate mesh, and which have a low vein density despite having small leaves. It is possible that the emergence and expansion of the Class IIIC group within angiosperms has enabled the formation of high vein density and improved vein connections, two characteristics upon which the success of angiosperms is proposed to be based. The expansion of DUF 828 genes and the presence of angiosperm specific groups might highlight the biological and functional role of these domains in evolution of angiosperms, of which the reticulate vein pattern is of potential significance. The members of FKD1 gene family show variable localization to FKD1 and ST-RFP (Golgi marker), which indicates likely localization

of the family through the GA and post-Golgi endosomes, suggesting function at multiple points in vesicle trafficking.

CHAPTER 6: CONCLUSIONS AND FUTURE DIRECTIONS

In the research work presented here, I have characterized members of the *Arabidopsis* DUF 828 gene family, which encodes proteins with DUF828 and Pleckstrin Homology or Pleckstrin Like domains. DUF828 is a plant specific domain whose function has never been characterized before, and my data suggests that the family may act in the trafficking of PIN1.

I have shown that FKD1 associates with SFC, confirming the prior colocolization of FKD1 with VAN3/SFC (ARF-GAP) (Naramoto et al., 2009). I also observed colocalization of FKD1 with members of the ARF1 family, suggesting that FKD1 might be associating with ARF1 proteins through their interaction with VAN3/SFC (ARF-GAP). Using different molecular markers of endosomal compartments and the plasma membrane, I have shown that FKD1 localizes to the PM and to motile, punctae post-Golgi compartments. The lack of colocalization of the FKD1-GFP labeled punctae with the endoctyic tracer dye FM4-64 suggests that FKD1 is not involved in endocytosis. I found that FKD1 and SFC/VAN3 labeled compartments do not aggregate in BFA compartments, suggesting that they may act in a BFA-insensitive pathway. FKD1-GFP strongly associates with RabA1e and RabA1g, whose closest homologues act in either post-Golgi secretion to the PM or in endocytosis. Together, these results suggest that FKD1 may be involved in secretion of PIN1 to the PM, a process that has previously been shown to involve the ARF-GEFs GN and GNL1 (Doyle et al., 2015) as well as the BIG family (Richter et al., 2014). GNOM, which is BFA sensitive, has been suggested to act in recycling of PIN to

the basal side of the PM (Geldner et al., 2003). In contrast, BFA-insensitive ARF-GEFs regulate PIN localization at apical side of the cell (Kleine-Vehn et al., 2008). Of the eight ARF-GEFs available, GNL1 and BIG3 are BFA insensitive. Hence, further investigation can be carried out to identify whether FKD1 colocalizes with BFA-sensitive ARF-GEFs (GNL1, BIG3 and BIG5), which would give an idea whether FKD1 is involved in apical PIN localization. As well, assessing colocalization of FKD1 with RabA1a, RabA1b or RabA1c, all of which are involved in post-Golgi secretion (Qi and Huang, 2013; Asaoka et al., 2013) would provide further evidence that FKD1 is involved in post-Golgi secretion.

I have observed that both FKD1 and SFC colocalize with PIN, suggesting a role for FKD1 in PIN1 trafficking, possibly through the interaction with SFC (ARF-GAP) and ARF proteins. PIN protein trafficking is regulated by the phosphorylation status of PIN proteins, in which phosphorylation of PIN proteins (mediated via PID/WAG kinases) results in apical PIN protein targeting and dephosphorylation of PIN proteins (mediated by PP2A) results in basal targeting (Dhonukshe, 2011). In order to further confirm that FKD1 gene mediates PIN1 apical targeting, PIN1-RFP and FKD1-GFP can be introduced into a *pid* mutant background. Since PIN proteins can not be phosphorylated in pid mutants, might result in more basa localization of PIN1 with FKD1 can be observed at the basal side of the cell. Similarly introducing PIN1-RFP and FKD-GFP in a *pp2a* mutant, might result in more apical localization of PIN1 and FKD1.

Introduction of mutations belonging to two members (Group IIIC) of the DUF 828 gene family into *fkd1* resulted in an extreme non-meeting vascular phenotype, suggesting these genes might be acting redundantly to regulate leaf vascular formation. PIN1 localization was found to be more symmetric in the developing veins, with a very high reduction in apical PIN1 localization, which suggests a possible role of this gene family in PIN1 trafficking. PIN1-GFP could be introduced into the quadruple mutant line and PIN1 localization can be assessed. The multiple mutants showed general defects in auxin transport related processes such as primary root length and root gravitropic response. However, no change in PIN1 localization was seen in roots, suggesting that other PIN family member localization might be affected. Of particular interest is PIN2, which is apically localized in the root epidermis and is important for root elongation. To determine if FKD1 gene family members are involved in localization of other PIN proteins, labeled PIN2 and PIN3 could be introduced into the quadruple mutant background and their localization determined.

Characterization of the *Arabidopsis thaliana* DUF 828 gene family provides insights into the role of these genes in regulating auxin transport during developmental processes in plants. The appearance of a DUF 828 domain in bryophytes suggests that this domain is not related to vascular tissue. However, the presence of angiosperm specific clades of DUF 828 domains in the plant kingdom suggests their possible role in reticulate vein formation and increased vein density typical of angiosperms. Further experiments need to be done to elucidate the PIN1 trafficking pathway that is mediated by FKD1 and closely related members of the

family, which in turn will give more information into the precise mechanisms by which they regulate leaf vein patterning process.

REFERENCES

Abe, T., Thitamadee, S., & Hashimoto, T. (2004). Microtubule defects and cell morphogenesis in the lefty1lefty2 tubulin mutant of Arabidopsis thaliana. *Plant and cell physiology*, *45*(2), 211-220.

Abel, S. (2007). Auxin is surfacing. *ACS chemical biology*, *2*(6), 380-384.

Alassimone, J., Naseer, S., & Geldner, N. (2010). A developmental framework for endodermal differentiation and polarity. *Proceedings of the National Academy of Sciences of the United States of America*, *107*(11), 5214–5219.

Asaoka, R., Uemura, T., Ito, J., Fujimoto, M., Ito, E., Ueda, T., & Nakano, A. (2013). Arabidopsis RABA1 GTPases are involved in transport between the trans-Golgi network and the plasma membrane, and are required for salinity stress tolerance. *The Plant Journal*, *73*(2), 240-249.

Badescu, G. O., & Napier, R. M. (2006). Receptors for auxin: will it all end in TIRs? *Trends in plant science*, *11*(5), 217-223.

Bajguz, A., & Piotrowska, A. (2009). Conjugates of auxin and cytokinin. *Phytochemistry*, *70*(8), 957-969.

Baluška, F., Mancuso, S., Volkmann, D., & Barlow, P. W. (2010). Root apex transition zone: a signalling–response nexus in the root. *Trends in plant science*, *15*(7), 402-408.

Bassham, D. C., Brandizzi, F., Otegui, M. and Sanderfoot, A. A. (2008). The secretory system of Arabidopsis. The Arabidopsis Book, Somerville C.R., Meyerowitz E.M., eds (Rockville, MD: American Society of Plant Biologists), 25039–25046.

Bassham, D. C., Sanderfoot, A. A., Kovaleva, V., Zheng, H., & Raikhel, N. V. (2000). AtVPS45 complex formation at the trans-Golgi network. *Molecular Biology of the Cell*, *11*(7), 2251-2265.

Batoko, H., Zheng, H. Q., Hawes, C., & Moore, I. (2000). A Rab1 GTPase is required for transport between the endoplasmic reticulum and Golgi apparatus and for normal Golgi movement in plants. *The Plant Cell*, *12*(11), 2201-2217.

Bayer, E. M., Smith, R. S., Mandel, T., Nakayama, N., Sauer, M., Prusinkiewicz, P., & Kuhlemeier, C. (2009). Integration of transport-based models for phyllotaxis and midvein formation. *Genes & development*, *23*(3), 373-384.

Beck, M., Zhou, J., Faulkner, C., MacLean, D., & Robatzek, S. (2012). Spatio-temporal cellular dynamics of the Arabidopsis flagellin receptor reveal activation status-dependent endosomal sorting. *The Plant Cell*, *24*(10), 4205-4219.

Benjamins, R., & Scheres, B. (2008). Auxin: the looping star in plant development. *Annu. Rev. Plant Biol.*, *59*, 443-465.

Benjamins, R., Quint, A. B., Weijers, D., Hooykaas, P., & Offringa, R. (2001). The PINOID protein kinase regulates organ development in Arabidopsis by enhancing polar auxin transport. *Development*, *128*(20), 4057-4067.

Benková, E., Michniewicz, M., Sauer, M., Teichmann, T., Seifertová, D., Jürgens, G., & Friml, J. (2003). Local, efflux-dependent auxin gradients as a common module for plant organ formation. *Cell*, *115*(5), 591-602.

Bennett, T. A., Liu, M. M., Aoyama, T., Bierfreund, N. M., Braun, M., Coudert, Y., ... & Harrison, C. J. (2014). Plasma membrane-targeted PIN proteins drive shoot development in a moss. *Current Biology*, *24*(23), 2776-2785.

Berdy S. E., Kudla J., Gruissem W., Gillaspy G. E. Molecular characterization of At5PTase1, an inositol phosphatase capable of terminating inositol trisphosphate signaling. Plant Physiol. 2001;126:801–810.

Blakeslee, J. J., Bandyopadhyay, A., Lee, O. R., Mravec, J., Titapiwatanakun, B., Sauer, M., ... & Murphy, A. S. (2007). Interactions among PIN-FORMED and P-glycoprotein auxin transporters in Arabidopsis. *The Plant Cell Online*, *19*(1), 131-147.

Blilou, I., Xu, J., Wildwater, M., Willemsen, V., Paponov, I., Friml, J., Heidstra,R., Aida,M., Klaus Palme,K., and Scheres, B. (2005). The PIN auxin efflux facilitator network controls growth and patterning in Arabidopsiroots. *Nature*, *433*(7021), 39-44.

Bolte, S., Talbot, C., Boutte, Y., Catrice, O., Read, N. D., & Satiat□Jeunemaitre, B. (2004). FM-dyes as experimental probes for dissecting vesicle trafficking in living plant cells. *Journal of microscopy*, *214*(2), 159-173.

Bonifacino, J. S., & Glick, B. S. (2004). The mechanisms of vesicle budding and fusion. *Cell*, *116*(2), 153-166.

Brandizzi, F., Snapp, E. L., Roberts, A. G., Lippincott-Schwartz, J., & Hawes, C. (2002). Membrane Protein Transport between the Endoplasmic Reticulum and the Golgi in Tobacco Leaves Is Energy Dependent but Cytoskeleton Independent Evidence from Selective Photobleaching. *The Plant Cell Online*, *14*(6), 1293-1309.

Brodribb, T. J., & Feild, T. S. (2010). Leaf hydraulic evolution led a surge in leaf photosynthetic capacity during early angiosperm diversification. *Ecology Letters*, *13*(2), 175-183.

Carland, F. M., Berg, B. L., FitzGerald, J. N., Jinamornphongs, S., Nelson, T., & Keith, B. (1999). Genetic regulation of vascular tissue patterning in Arabidopsis. *The Plant Cell Online*, *11*(11), 2123-2137.

Carland, F., & Nelson, T. (2009). CVP2-and CVL1-mediated phosphoinositide signaling as a regulator of the ARF GAP SFC/VAN3 in establishment of foliar vein patterns. *The Plant Journal*, *59*(6), 895-907.

Chamala, S., Chanderbali, A. S., Der, J. P., Lan, T., Walts, B., Albert, V. A., ... & Barbazuk, W. B. (2013). Assembly and validation of the genome of the nonmodel basal angiosperm Amborella. *Science*, *342*(6165), 1516-1517.

Chandler, J. W. (2009). Auxin as compère in plant hormone crosstalk. *Planta*, *231*(1), 1-12.

Chapman, E. J., & Estelle, M. (2009). Mechanism of auxin-regulated gene expression in plants. *Annual review of genetics*, *43*, 265-285.

Choi, S. W., Tamaki, T., Ebine, K., Uemura, T., Ueda, T., & Nakano, A. (2013). RABA members act in distinct steps of subcellular trafficking of the FLAGELLIN SENSING2 receptor. *The Plant Cell*, *25*(3), 1174-1187.

Chow, C. M., Neto, H., Foucart, C., Moore, I. (2008). Rab-A2 and Rab-A3 GTPases define a trans-golgi endosomal membrane domain in Arabidopsis that contributes substantially to the cell plate. Plant Cell 20: 101–123

Conte, M. G., Gaillard, S., Lanau, N., Rouard, M., & Périn, C. (2008). GreenPhylDB: a database for plant comparative genomics. *Nucleic acids research*, *36*(suppl 1), D991-D998.

Contento, A. L., & Bassham, D. C. (2012). Structure and function of endosomes in plant cells. *Journal of cell science*, *125*(15), 3511-3518.

Davis, A. J., Im, Y. J., Dubin, J. S., Tomer, K. B., & Boss, W. F. (2007). Arabidopsis phosphatidylinositol phosphate kinase 1 binds F-actin and recruits phosphatidylinositol 4-kinase β1 to the actin cytoskeleton. *Journal of Biological Chemistry*, *282*(19), 14121-14131.

de Matteis, M. A., Godi, A., & Corda, D. (2002). Phosphoinositides and the Golgi complex. *Current opinion in cell biology*, *14*(4), 434-447.

Dengler, N., & Kang, J. (2001). Vascular patterning and leaf shape. *Current opinion in plant biology*, *4*(1), 50-56.

Dettmer, J., Hong-Hermesdorf, A., Stierhof, Y. D., & Schumacher, K. (2006). Vacuolar H+-ATPase activity is required for endocytic and secretory trafficking in Arabidopsis. *The Plant Cell*, *18*(3), 715-730.

Deyholos, M. K., Cordner, G., Beebe, D., & Sieburth, L. E. (2000). The SCARFACE gene is required for cotyledon and leaf vein patterning. *Development*, *127*(15), 3205-3213.

Dhonukshe, P. (2011). PIN polarity regulation by AGC-3 kinases and ARF-GEF: a recurrent theme with context dependent modifications for plant development and response. *Plant signaling & behavior*, *6*(9), 1333-1337.

Dhonukshe, P., Aniento, F., Hwang, I., Robinson, D. G., Mravec, J., Stierhof, Y. D., & Friml, J. (2007). Clathrin-mediated constitutive endocytosis of PIN auxin efflux carriers in Arabidopsis. *Current Biology*, *17*(6), 520-527.

Dhonukshe, P., Huang, F., Galvan-Ampudia, C. S., Mähönen, A. P., Kleine-Vehn, J., Xu, J., ... & Offringa, R. (2010). Plasma membrane-bound AGC3 kinases phosphorylate PIN auxin carriers at TPRXS (N/S) motifs to direct apical PIN recycling. *Development*, *137*(19), 3245-3255.

Donaldson, J. G., & Jackson, C. L. (2000). Regulators and effectors of the ARF GTPases. *Current opinion in cell biology*, *12*(4), 475-482.

Douzery, E. J., Snell, E. A., Bapteste, E., Delsuc, F., & Philippe, H. (2004). The timing of eukaryotic evolution: does a relaxed molecular clock reconcile proteins and fossils? *Proceedings of the National Academy of Sciences of the United States of America*, *101*(43), 15386-15391.

Doyle, J. A. (2012). Molecular and fossil evidence on the origin of angiosperms.*Annual Review of Earth and Planetary Sciences*, *40*, 301-326.

Doyle, S. M., Haeger, A., Vain, T., Rigal, A., Viotti, C., Łangowska, M., ... & Robert, S. (2015). An early secretory pathway mediated by GNOM-LIKE 1 and GNOM is essential for basal polarity establishment in Arabidopsis thaliana. *Proceedings of the National Academy of Sciences*, *112*(7), E806-E815.

Drakakaki, G., van de Ven, W., Pan, S., Miao, Y., Wang, J., Keinath, N. F., ... & Raikhel, N. (2012). Isolation and proteomic analysis of the SYP61 compartment reveal its role in exocytic trafficking in Arabidopsis. *Cell research*, *22*(2), 413-424.

Du W., Tamura K., Stefano G., Brandizzi, F. (2013). The integrity of the plant golgi apparatus depends on cell growth-controlled activity of GNL1. Mol. Plant 6, 905–915

Ebine, K., Fujimoto, M., Okatani, Y., Nishiyama, T., Goh, T., Ito, E., ... & Ueda, T. (2011). A membrane trafficking pathway regulated by the plant-specific RAB GTPase ARA6. *Nature Cell Biology*, *13*(7), 853-859.

Eitzen, G. (2003). Actin remodeling to facilitate membrane fusion. *Biochimica et Biophysica Acta (BBA)-Molecular Cell Research*, *1641*(2), 175-181.

Ercetin, M. E., & Gillaspy, G. E. (2004). Molecular characterization of an Arabidopsis gene encoding a phospholipid-specific inositol polyphosphate 5-phosphatase. *Plant physiology*, *135*(2), 938-946.

Eshel, A., & Beeckman, T. (Eds.). (2013). *Plant roots: the hidden half*. CRC Press.

Feraru, E., Feraru, M. I., Asaoka, R., Paciorek, T., De Rycke, R., Tanaka, H., ... & Friml, J. (2012). BEX5/RabA1b regulates trans-Golgi network-to-plasma membrane protein trafficking in Arabidopsis. *The Plant Cell*, *24*(7), 3074-3086.

Feugier, F. G., & Iwasa, Y. (2006). How canalization can make loops: a new model of reticulated leaf vascular pattern formation. *Journal of theoretical biology*, *243*(2), 235-244.

Floyd, S. K., & Bowman, J. L. (2006). Distinct developmental mechanisms reflect the independent origins of leaves in vascular plants. *Current Biology*,*16*(19), 1911-1917.

French, A. P., Mills, S., Swarup, R., Bennett, M. J., & Pridmore, T. P. (2008). Colocalization of fluorescent markers in confocal microscope images of plant cells. *Nature protocols*, *3*(4), 619-628.

Friml, J. (2010). Subcellular trafficking of PIN auxin efflux carriers in auxin transport. *European journal of cell biology*, *89*(2), 231-235.

Friml, J., Vieten, A., Sauer, M., Weijers, D., Schwarz, H., Hamann, T., ... & Jürgens, G. (2003). Efflux-dependent auxin gradients establish the apical–basal axis of Arabidopsis. *Nature*, *426*(6963), 147-153.

Friml, J., Wiśniewska, J., Benková, E., Mendgen, K., & Palme, K. (2002). Lateral relocation of auxin efflux regulator PIN3 mediates tropism in Arabidopsis. *Nature*, *415*(6873), 806-809.

Friml, J., Yang, X., Michniewicz, M., Weijers, D., Quint, A., Tietz, O., ... & Offringa, R. (2004). A PINOID-dependent binary switch in apical-basal PIN polar targeting directs auxin efflux. *Science*, *306*(5697), 862-865.

Fu, Y., Gu, Y., Zheng, Z., Wasteneys, G., & Yang, Z. (2005). Arabidopsis interdigitating cell growth requires two antagonistic pathways with opposing action on cell morphogenesis. *Cell*, *120*(5), 687-700.

Fukuda, H. (2004). Signals that control plant vascular cell differentiation. *Nature Reviews Molecular Cell Biology*, *5*(5), 379-391.

Gälweiler, L., Guan, C., Müller, A., Wisman, E., Mendgen, K., Yephremov, A., & Palme, K. (1998). Regulation of polar auxin transport by AtPIN1 in Arabidopsis vascular tissue. *Science*, *282*(5397), 2226-2230.

Ganguly, A., Park, M., Kesawat, M. S., & Cho, H. T. (2014). Functional analysis of the hydrophilic loop in intracellular trafficking of Arabidopsis PIN-FORMED proteins. *The Plant Cell*, *26*(4), 1570-1585.

Ganguly, A., Sasayama, D., & Cho, H. T. (2012). Regulation of the polarity of protein trafficking by phosphorylation. *Molecules and cells*, *33*(5), 423-430.

Gao, X., Nagawa, S., Wang, G., & Yang, Z. (2008). Cell polarity signaling: focus on polar auxin transport. *Molecular plant*, *1*(6), 899-909.

Geldner, N. (2004). The plant endosomal system—its structure and role in signal transduction and plant development. *Planta*, *219*(4), 547-560.

Geldner, N., Anders, N., Wolters, H., Keicher, J., Kornberger, W., Muller, P., ... & Jürgens, G. (2003). The Arabidopsis GNOM ARF-GEF mediates endosomal recycling, auxin transport, and auxin-dependent plant growth. *Cell*, *112*(2), 219-230.

Geldner, N., Dénervaud Tendon, V., Hyman, D. L., Mayer, U., Stierhof, Y. D., & Chory, J. (2009). Rapid, combinatorial analysis of membrane compartments in intact plants with a multicolor marker set. *The Plant Journal*, *59*(1), 169-178.

Geldner, N., Friml, J., Stierhof, Y. D., Jürgens, G., & Palme, K. (2001). Auxin transport inhibitors block PIN1 cycling and vesicle trafficking. *Nature*,*413*(6854), 425-428.

Geldner, N., Richter, S., Vieten, A., Marquardt, S., Torres-Ruiz, R. A., Mayer, U., & Jürgens, G. (2004). Partial loss-of-function alleles reveal a role for GNOM in auxin transport-relatedpost-embryonicdevelopment of Arabidopsis. *Development*, *131*(2), 389-400.

Gillingham, A. K., & Munro, S. (2007). The small G proteins of the Arf family and their regulators. *Annu. Rev. Cell Dev. Biol.*, *23*, 579-611.

Grebe, M., Xu, J., Möbius, W., Ueda, T., Nakano, A., Geuze, H. J., ... & Scheres, B. (2003). Arabidopsis sterol endocytosis involves actin-mediated trafficking via ARA6-positive early endosomes. *Current Biology*, *13*(16), 1378-1387.

Guimil, S., & Dunand, C. (2007). Cell growth and differentiation in Arabidopsis epidermal cells. *Journal of experimental botany*, *58*(14), 3829-3840.

Habets, M. E., & Offringa, R. (2014). PIN-driven polar auxin transport in plant developmental plasticity: a key target for environmental and endogenous signals. *New Phytologist*, *203*(2), 362-377.

Hanton, S. L., Bortolotti, L. E., Renna, L., Stefano, G. and Brandizzi, F. (2005). Crossing the divide – transport between the endoplasmic reticulum and Golgi apparatus in plants. Traffic, 6, 267–277.

Hawes, C., Schoberer, J., Hummel, E., & Osterrieder, A. (2010). Biogenesis of the plant Golgi apparatus. *Biochemical Society Transactions*, *38*(3), 761.

Hayashi, K. I. (2012). The interaction and integration of auxin signaling components. *Plant and Cell Physiology*, *53*(6), 965-975.

Hou, H., Erickson, J., Meservy, J., & Schultz, E. A. (2010). FORKED1 encodes a PH domain protein that is required for PIN1 localization in developing leaf veins. *The Plant Journal*, *63*(6), 960-973.

Hwang, I. (2008). Sorting and anterograde trafficking at the Golgi apparatus. *Plant physiology*, *148*(2), 673-683.

Ischebeck, T., Stenzel, I., & Heilmann, I. (2008). Type B phosphatidylinositol-4-phosphate 5-kinases mediate Arabidopsis and Nicotiana tabacum pollen tube growth by regulating apical pectin secretion. *The Plant Cell Online*, *20*(12), 3312-3330.

Ischebeck, T., Werner, S., Krishnamoorthy, P., Lerche, J., Meijón, M., Stenzel, I., ... & Heilmann, I. (2013). Phosphatidylinositol 4, 5-bisphosphate influences PIN polarization by controlling clathrin-mediated membrane trafficking in Arabidopsis. *The Plant Cell*, *25*(12), 4894-4911.

Jackson, C. L., & Casanova, J. E. (2000). Turning on ARF: the Sec7 family of guanine-nucleotide-exchange factors. *Trends in cell biology*, *10*(2), 60-67.

Jahn, R., & Scheller, R. H. (2006). SNAREs—engines for membrane fusion.*Nature reviews Molecular cell biology*, *7*(9), 631-643.

Jia D. J., Cao X., Wang W., Tan X. Y., Zhang X. Q., Chen L. Q., et al. (2009). GNOM-LIKE 2, encoding an adenosine diphosphate-ribosylation factor-guanine nucleotide exchange factor protein homologous to GNOM and GNL1, is essential for pollen germination in Arabidopsis. J. Integr. Plant Biol. 51, 762–773.

Jiao, Y., Wickett, N. J., Ayyampalayam, S., Chanderbali, A. S., Landherr, L., Ralph, P. E., ... & Leebens-Mack, J. (2011). Ancestral polyploidy in seed plants and angiosperms. *Nature*, *473*(7345), 97-100.

Jochum, A., Jackson, D., Schwarz, H., Pipkorn, R., and Singer-Kruger, B. (2002). Yeast Ysl2p, homologous to Sec7 domain guanine nucleotide exchange factors, functions in endocytosis and maintenance of vacuole integrity and interacts with the Arf-Like small GTPase Arl1p. *Mol. Cell. Biol.* 22, 4914-4928.

Jürgens, G. (2004). Membrane trafficking in plants. *Annu. Rev. Cell Dev. Biol.*, *20*, 481-504.

Jürgens, G., & Geldner, N. (2002). Protein secretion in plants: from the trans-Golgi network to the outer space. *Traffic*, *3*(9), 605-613.

Kang, B. H. (2011). Shrinkage and fragmentation of the trans-Golgi network in non-meristematic plant cells. *Plant signaling & behavior*, *6*(6), 884-886.

Kania, U., Fendrych, M., & Friml, J. (2014). Polar delivery in plants; commonalities and differences to animal epithelial cells. *Open biology*, *4*(4), 140017.

Keuskamp, D. H., Pollmann, S., Voesenek, L. A., Peeters, A. J., & Pierik, R. (2010). Auxin transport through PIN-FORMED 3 (PIN3) controls shade avoidance and fitness during competition. *Proceedings of the National Academy of Sciences*, *107*(52), 22740-22744.

Kim, D.H., Eu, Y.-J., Yoo, C.M., Kim, Y.W., Pih, K.T., Jin, J.B., Kim, S.J., Stenmark, H., and Hwang, I. (2001). Trafficking of phosphatidylinositol 3-phosphate from the *trans*-Golgi network to the lumen of the central vacuole in plant cells. *Plant Cell* 13, 287–301.

Kleine-Vehn, J., & Friml, J. (2008). Polar targeting and endocytic recycling in auxin-dependent plant development. *Annual review of cell and developmental biology*, *24*, 447-473.

Kleine-Vehn, J., Huang, F., Naramoto, S., Zhang, J., Michniewicz, M., Offringa, R., & Friml, J. (2009). PIN auxin efflux carrier polarity is regulated by PINOID kinase-mediated recruitment into GNOM-independent trafficking in Arabidopsis. *The Plant Cell Online*, *21*(12), 3839-3849.

Koizumi, K., Naramoto, S., Sawa, S., Yahara, N., Ueda, T., Nakano, A., ... & Fukuda, H. (2005). VAN3 ARF–GAP-mediated vesicle transport is involved in leaf vascular network formation. *Development*, *132*(7), 1699-1711.

Korasick, D. A., Enders, T. A., & Strader, L. C. (2013). Auxin biosynthesis and storage forms. *Journal of experimental botany*, *64*(9), 2541-2555.

Kotzer, A. M., Brandizzi, F., Neumann, U., Paris, N., Moore, I., & Hawes, C. (2004). AtRabF2b (Ara7) acts on the vacuolar trafficking pathway in tobacco leaf epidermal cells. *Journal of Cell Science*, *117*(26), 6377-6389.

Křeček, P., Skůpa, P., Libus, J., Naramoto, S., Tejos, R., Friml, J., & Zažímalová, E. (2009). The PIN-FORMED (PIN) protein family of auxin transporters. *Genome Biol*, *10*(12), 249.

Lam, S. K., Tse, Y. C., Robinson, D. G., & Jiang, L. (2007). Tracking down the elusive early endosome. *Trends in plant science*, *12*(11), 497-505.

Laxmi, A., Pan, J., Morsy, M., & Chen, R. (2008). Light plays an essential role in intracellular distribution of auxin efflux carrier PIN2 in Arabidopsis thaliana.*PLoS one*, *3*(1), e1510.

Lee, G. J., Sohn, E. J., Lee, M. H., & Hwang, I. (2004b). The Arabidopsis rab5 homologs rha1 and ara7 localize to the prevacuolar compartment. *Plant and Cell Physiology*, *45*(9), 1211-1220.

Lee, M. C., Miller, E. A., Goldberg, J., Orci, L., & Schekman, R. (2004a). Bi-directional protein transport between the ER and Golgi. *Annu. Rev. Cell Dev. Biol.*, *20*, 87-123.

Lemmon, M. A. (2003). Phosphoinositide recognition domains. *Traffic*, *4*(4), 201-213.

Liljegren, S. J., Leslie, M. E., Darnielle, L., Lewis, M. W., Taylor, S. M., Luo, R., ... Ecker, J. R. (2009). Regulation of membrane trafficking and organ separation by the NEVERSHED ARF-GAP protein. *Development (Cambridge, England)*, *136*(11), 1909–1918.

Ljung, K., Bhalerao, R. P., & Sandberg, G. (2001). Sites and homeostatic control of auxin biosynthesis in Arabidopsis during vegetative growth. *The Plant Journal*, *28*(4), 465-474.

Ljung, K., Hull, A. K., Celenza, J., Yamada, M., Estelle, M., Normanly, J., & Sandberg, G. (2005). Sites and regulation of auxin biosynthesis in Arabidopsis roots. *The Plant Cell Online*, *17*(4), 1090-1104.

Lofke, C., Ischebeck, T., Konig, S., Freitag, S., & Heilmann, I. (2008). Alternative metabolic fates of phosphatidylinositol produced by phosphatidylinositol synthase isoforms in Arabidopsis thaliana. *Biochem. J*,*413*, 115-124.

Luschnig, C., & Vert, G. (2014). The dynamics of plant plasma membrane proteins: PINs and beyond. *Development*, *141*(15), 2924-2938.

Magallón, Susana, Khidir W. Hilu, and Dietmar Quandt. "Land plant evolutionary timeline: gene effects are secondary to fossil constraints in relaxed clock estimation of age and substitution rates." *American Journal of Botany*100.3 (2013): 556-573.

Malinowski, R. (2013). Understanding of Leaf Development—the Science of Complexity. *Plants*, *2*(3), 396-415.

Marchant, A., Bhalerao, R., Casimiro, I., Eklöf, J., Casero, P. J., Bennett, M., & Sandberg, G. (2002). AUX1 promotes lateral root formation by facilitating indole-3-acetic acid distribution between sink and source tissues in the Arabidopsis seedling. *The Plant Cell*, *14*(3), 589-597.

Matheson, L. A., Hanton, S. L., Rossi, M., Latijnhouwers, M., Stefano, G., Renna, L., & Brandizzi, F. (2007). Multiple roles of ADP-ribosylation factor 1 in plant cells include spatially regulated recruitment of coatomer and elements of the Golgi matrix. *Plant physiology*, *143*(4), 1615-1627.

Mayer, U., Buttner, G., & Jurgens, G. (1993). Apical-basal pattern formation in the Arabidopsis embryo: studies on the role of the gnom gene. *Development*, *117*(1), 149-162.

McKown, A. D., Cochard, H., & Sack, L. (2010). Decoding leaf hydraulics with a spatially explicit model: principles of venation architecture and implications for its evolution. *The American Naturalist*, *175*(4), 447-460.

McMahon, H. T., & Boucrot, E. (2011). Molecular mechanism and physiological functions of clathrin-mediated endocytosis. *Nature reviews Molecular cell biology*, *12*(8), 517-533.

McMahon, H. T., & Mills, I. G. (2004). COP and clathrin-coated vesicle budding: different pathways, common approaches. *Current opinion in cell biology*, *16*(4), 379-391.

Meijer, H. J., & Munnik, T. (2003). Phospholipid-based signaling in plants.*Annual review of plant biology*, *54*(1), 265-306.

Michniewicz, M., Zago, M. K., Abas, L., Weijers, D., Schweighofer, A., Meskiene, I., ... & Friml, J. (2007). Antagonistic regulation of PIN phosphorylation by PP2A and PINOID directs auxin flux. *Cell*, *130*(6), 1044-1056.

Minamisawa, N., Sato, M., Cho, K. H., Ueno, H., Takechi, K., Kajikawa, M., ... & Tsukaya, H. (2011). ANGUSTIFOLIA, a plant homolog of CtBP/BARS, functions outside the nucleus. *The Plant Journal*, *68*(5), 788-799.

Möller, B., & Weijers, D. (2009). Auxin control of embryo patterning. *Cold Spring Harbor perspectives in biology*, *1*(5), a001545.

Morris, D. A., Friml, J., & Zažímalová, E. (2010). The transport of auxins. *Plant Hormones*, 451-484.

Mravec, J., Skůpa, P., Bailly, A., Hoyerová, K., Křeček, P., Bielach, A., ... & Friml, J. (2009). Subcellular homeostasis of phytohormone auxin is mediated by the ER-localized PIN5 transporter. *Nature*, *459*(7250), 1136-1140.

Mueller-Roeber, B., & Pical, C. (2002). Inositol phospholipid metabolism in Arabidopsis. Characterized and putative isoforms of inositol phospholipid kinase and phosphoinositide-specific phospholipase C. *Plant Physiology*, *130*(1), 22-46.

Nakamura, M., Yagi, N., Kato, T., Fujita, S., Kawashima, N., Ehrhardt, D. W., & Hashimoto, T. (2012). Arabidopsis GCP3-interacting protein 1/MOZART 1 is an integral component of the γ-tubulin-containing microtubule nucleating complex. *The Plant Journal*, *71*(2), 216-225.

Naramoto S., Kleine-Vehn J., Robert S., Fujimoto M., Dainobu T., Paciorek T., et al. (2010). ADP-ribosylation factor machinery mediates endocytosis in plant cells. Proc. Natl. Acad. Sci. U.S.A. 107, 21890–21895

Naramoto, S., Otegui, M. S., Kutsuna, N., De Rycke, R., Dainobu, T., Karampelias, M., ... & Friml, J. (2014). Insights into the localization and function of the membrane trafficking regulator GNOM ARF-GEF at the Golgi apparatus in Arabidopsis. *The Plant Cell Online*, *26*(7), 3062-3076.

Naramoto, S., Sawa, S., Koizumi, K., Uemura, T., Ueda, T., Friml, J., ... & Fukuda, H. (2009). Phosphoinositide-dependent regulation of VAN3 ARF-GAP localization and activity essential for vascular tissue continuity in plants. *Development*, *136*(9), 1529-1538.

Nebenführ, A. (2002). Vesicle traffic in the endomembrane system: a tale of COPs, Rabs and SNAREs. *Current opinion in plant biology*, *5*(6), 507-512.

Nebenführ, A., Ritzenthaler, C., & Robinson, D. G. (2002). Brefeldin A: deciphering an enigmatic inhibitor of secretion. *Plant physiology*, *130*(3), 1102-1108

Neumann, U., Brandizzi F., Hawes, C. (2003). Protein transport in plant cells: in and out of the Golgi. Ann. Bot. 92, 167–180.

Nielsen, M., Albrethsen, J., Larsen, F. H., & Skriver, K. (2006). The Arabidopsis ADP-ribosylation factor (ARF) and ARF-like (ARL) system and its regulation by BIG2, a large ARF–GEF. *Plant science*, *171*(6), 707-717.

Nielsen, E., Cheung, A. Y., & Ueda, T. (2008). The regulatory RAB and ARF GTPases for vesicular trafficking. *Plant Physiology*, *147*(4), 1516-1526.

Otegui, M. S., & Spitzer, C. (2008). Endosomal functions in plants. *Traffic*, *9*(10), 1589-1598.

Overvoorde, P. J., Okushima, Y., Alonso, J. M., Chan, A., Chang, C., Ecker, J. R., ... & Theologis, A. (2005). Functional genomic analysis of the AUXIN/INDOLE-3-ACETIC ACID gene family members in Arabidopsis thaliana. *The Plant Cell*, *17*(12), 3282-3300.

Paciorek, T., Zažímalová, E., Ruthardt, N., Petrášek, J., Stierhof, Y. D., Kleine-Vehn, J., ... & Geldner, N. (2005). Auxin inhibits endocytosis and promotes its own efflux from cells. *Nature*, *435*(7046), 1251-1256.

Papanov, I. A., Teale, W.D., Trebar, M., Blilou, I., & Palme, K. 2005. The PIN auxin efflux facilitators: evolutionary and functional perspectives. Trends in Plant Science. 10(4): 170-177.

Petrášek, J., & Friml, J. (2009). Auxin transport routes in plant development. *Development*, *136*(16), 2675-2688.

Petrášek, J., Mravec, J., Bouchard, R., Blakeslee, J. J., Abas, M., Seifertová, D., ... & Friml, J. (2006). PIN proteins perform a rate-limiting function in cellular auxin efflux. *Science*, *312*(5775), 914-918.

Phillipson, B. A., Pimpl, P., daSilva, L., Crofts, A. J., Tayler, J. P., Movafeghi, A., Robinson, D. G. and Denecke, J. (2001). Secretory bulk flow of soluble proteins is efficient and COPII dependent. Plant Cell. 13, 2005–2020.

Pimpl, P., Hanton, S. L., Taylor, J. P., Pinto-daSilva, L. L., & Denecke, J. (2003). The GTPase ARF1p controls the sequence-specific vacuolar sorting route to the lytic vacuole. *The Plant Cell*, *15*(5), 1242-1256.

Pimpl, P., Movafeghi, A., Coughlan, S., Denecke, J., Hillmer, S., & Robinson, D. G. (2000). In situ localization and in vitro induction of plant COPI-coated vesicles. *The Plant Cell*, *12*(11), 2219-2235.

Pizarro, L., & Norambuena, L. (2014). Regulation of protein trafficking: Posttranslational mechanisms and the unexplored transcriptional control. *Plant Science*, *225*, 24-33.

Popescu, S. C. (2012). A model for the biosynthesis and transport of plasma membrane-associated signaling receptors to the cell surface. *Frontiers in plant science*, *3*.

Prasad, K., & Dhonukshe, P. (2013). Polar auxin transport: cell polarity to patterning. In *Polar Auxin Transport* (pp. 25-44). Springer Berlin Heidelberg.

Preuss, M. L., Schmitz, A. J., Thole, J. M., Bonner, H. K., Otegui, M. S., & Nielsen, E. (2006). A role for the RabA4b effector protein PI-4Kβ1 in polarized expansion of root hair cells in Arabidopsis thaliana. *The Journal of cell biology*, *172*(7), 991-998.

Preuss, M. L., Serna, J., Falbel, T. G., Bednarek, S. Y., & Nielsen, E. (2004). The Arabidopsis Rab GTPase RabA4b localizes to the tips of growing root hair cells. *The Plant Cell Online*, *16*(6), 1589-1603.

Qi, X., & Zheng, H. (2013). Rab-A1c GTPase defines a population of the trans-Golgi network that is sensitive to endosidin1 during cytokinesis in Arabidopsis.*Molecular plant*, *6*(3), 847-859.

Rashotte, A. M., Brady, S. R., Reed, R. C., Ante, S. J., & Muday, G. K. (2000). Basipetal auxin transport is required for gravitropism in roots of Arabidopsis.*Plant Physiology*, *122*(2), 481-490.

Reed, J. W. (2001). Roles and activities of Aux/IAA proteins in Arabidopsis. *Trends in plant science*, *6*(9), 420-425.

Reinhardt, D., Pesce, E. R., Stieger, P., Mandel, T., Baltensperger, K., Bennett, M., & Kuhlemeier, C. (2003). Regulation of phyllotaxis by polar auxin transport. *Nature*, *426*(6964), 255-260.

Renna, L., Stefano, G., Majeran, W., Micalella, C., Meinnel, T., Giglione, C., & Brandizzi, F. (2013). Golgi traffic and integrity depend on N-myristoyl transferase-1 in Arabidopsis. *The Plant Cell Online*, *25*(5), 1756-1773.

Reyes, F. C., Buono, R., & Otegui, M. S. (2011). Plant endosomal trafficking pathways. *Current opinion in plant biology*, *14*(6), 666-673.

Richter, S., Geldner, N., Schrader, J., Wolters, H., Stierhof, Y. D., Rios, G., ... & Jürgens, G. (2007). Functional diversification of closely related ARF-GEFs in protein secretion and recycling. *Nature*, *448*(7152), 488-492.

Richter, S., Kientz, M., Brumm, S., Nielsen, M. E., Park, M., Gavidia, R., ... & Jürgens, G. (2014). Delivery of endocytosed proteins to the cell–division plane requires change of pathway from recycling to secretion. *Elife*, *3*, e02131.

Richter, S., Müller, L. M., Stierhof, Y. D., Mayer, U., Takada, N., Kost, B., ... & Jürgens, G. (2012). Polarized cell growth in Arabidopsis requires endosomal recycling mediated by GBF1-related ARF exchange factors. *Nature cell biology*,*14*(1), 80-86.

Ritzenthaler, C., Nebenführ, A., Movafeghi, A., Stussi-Garaud, C., Behnia, L., Pimpl, P., ... & Robinson, D. G. (2002). Reevaluation of the effects of brefeldin A on

plant cells using tobacco Bright Yellow 2 cells expressing Golgi-targeted green fluorescent protein and COPI antisera. *The Plant Cell*, *14*(1), 237-261.

Robert, H. S., & Friml, J. (2009). Auxin and other signals on the move in plants.*Nature Chemical Biology*, *5*(5), 325-332.

Robinson, D. G., Scheuring, D., Naramoto, S., & Friml, J. (2011). ARF1 localizes to the golgi and the trans-golgi network. *The Plant cell*, *23*(3), 846-849.

Rosquete, M. R., Barbez, E., & Kleine-Vehn, J. (2012). Cellular auxin homeostasis: gatekeeping is housekeeping. *Molecular plant*, *5*(4), 772-786.

Roth-Nebelsick, A., Uhl, D., Mosbrugger, V., & Kerp, H. (2001). Evolution and function of leaf venation architecture: a review. *Annals of Botany*, *87*(5), 553-566.

Rozov, S. M., Zagorskaya, A. A., Deineko, E. V., & Shumny, V. K. (2013). Auxins: Biosynthesis, metabolism, and transport. *Biology Bulletin Reviews*, *3*(4), 286-295.

Ruegger, M., Dewey, E., Gray, W. M., Hobbie, L., Turner, J. and Estelle, M. (1998). The TIR1 protein of Arabidopsis functions in auxin response and is related to human SKP2 and yeast grr1p. *Genes Dev.* 12, 198-207.

Rutherford, S., & Moore, I. (2002). The Arabidopsis Rab GTPase family: another enigma variation. *Current opinion in plant biology*, *5*(6), 518-528.

Saarikangas, J., Zhao, H., & Lappalainen, P. (2010). Regulation of the actin cytoskeleton-plasma membrane interplay by phosphoinositides. *Physiological reviews*, *90*(1), 259-289.

Sachs, T. (1981). The control of the patterned differentiation of vascular tissues. *Adv. Bot. Res*, *9*, 151-262.

Sack, L., & Scoffoni, C. (2013). Leaf venation: structure, function, development, evolution, ecology and applications in the past, present and future. *New Phytologist*, *198*(4), 983-1000.

Sack, L., Scoffoni, C., McKown, A. D., Frole, K., Rawls, M., Havran, J. C., ... & Tran, T. (2012). Developmentally based scaling of leaf venation architecture explains global ecological patterns. *Nature Communications*, *3*, 837.

Saint□Jore, C. M., Evins, J., Batoko, H., Brandizzi, F., Moore, I., & Hawes, C. (2002). Redistribution of membrane proteins between the Golgi apparatus and endoplasmic reticulum in plants is reversible and not dependent on cytoskeletal networks. *The Plant Journal*, *29*(5), 661-678.

Saito, C., & Ueda, T. (2009). Functions of RAB and SNARE proteins in plant life. *International review of cell and molecular biology*, *274*, 183-233.

Šamaj, J., Baluška, F., Voigt, B., Schlicht, M., Volkmann, D., & Menzel, D. (2004). Endocytosis, actin cytoskeleton, and signaling. *Plant Physiology*,*135*(3), 1150-1161.

Šamaj, J., Read, N. D., Volkmann, D., Menzel, D., & Baluška, F. (2005). The endocytic network in plants. *Trends in cell biology*, *15*(8), 425-433.

Sanderfoot, A. A., Kovaleva, V., Bassham, D. C., & Raikhel, N. V. (2001). Interactions between syntaxins identify at least five SNARE complexes within the Golgi/prevacuolar system of the Arabidopsis cell. *Molecular Biology of the Cell*, *12*(12), 3733-3743.

Sauer, M., Balla, J., Luschnig, C., Wiśniewska, J., Reinöhl, V., Friml, J., & Benková, E. (2006). Canalization of auxin flow by Aux/IAA-ARF-dependent feedback regulation of PIN polarity. *Genes & development*, *20*(20), 2902-2911.

Sawchuk, M. G., Edgar, A., & Scarpella, E. (2013). Patterning of leaf vein networks by convergent auxin transport pathways. *PLoS Genet*, *9*(2), e1003294.

Scarpella, E., Francis, P., & Berleth, T. (2004). Stage-specific markers define early steps of procambium development in Arabidopsis leaves and correlate termination of vein formation with mesophyll differentiation. *Development*, *131*(14), 3445-3455.

Scarpella, E., Marcos, D., Friml, J., & Berleth, T. (2006). Control of leaf vascular patterning by polar auxin transport. *Genes & Development*, *20*(8), 1015-1027.

Sieburth, L. E., Muday, G. K., King, E. J., Benton, G., Kim, S., Metcalf, K. E., & Van Norman, J. M. (2006). SCARFACE encodes an ARF-GAP that is required for normal auxin efflux and vein patterning in Arabidopsis. *The Plant Cell Online*, *18*(6), 1396-1411.

Simon, M. L. A., Platre, M. P., Assil, S., Wijk, R., Chen, W. Y., Chory, J., & Jaillais, Y. (2014). A multi-colour/multi-affinity marker set to visualize phosphoinositide dynamics in Arabidopsis. *The Plant Journal*, *77*(2), 322-337.

Staehelin, L. A., & Kang, B. H. (2008). Nanoscale architecture of endoplasmic reticulum export sites and of Golgi membranes as determined by electron tomography. *Plant Physiology*, *147*(4), 1454-1468.

Stagg, S. M., Gurkan, C., Fowler, D. M., LaPointe, P., Foss, T. R., Potter, C. S., Carragher, B. and Balch, W. E. (2006). Structure of the Sec13/31 COPII coat cage. Nature. 439, 234-238.

Stefano, G., Renna, L., Chatre, L., Hanton, S. L., Moreau, P., Hawes, C., & Brandizzi, F. (2006). In tobacco leaf epidermal cells, the integrity of protein export from the endoplasmic reticulum and of ER export sites depends on active COPI machinery. *The Plant Journal*, *46*(1), 95-110.

Stefano, G., Renna, L., Rossi, M., Azzarello, E., Pollastri, S., Brandizzi, F., & Mancuso, S. (2010). AGD5 is a GTPase-activating protein at the trans-Golgi network. *The Plant Journal*, *64*(5), 790-799.

Steinmann, T., Geldner, N., Grebe, M., Mangold, S., Jackson, C. L., Paris, S., & Jürgens, G. (1999). Coordinated polar localization of auxin efflux carrier PIN1 by GNOM ARF GEF. *Science*, *286*(5438), 316-318.

Stenzel, I., Ischebeck, T., König, S., Hołubowska, A., Sporysz, M., Hause, B., & Heilmann, I. (2008). The type B phosphatidylinositol-4-phosphate 5-kinase 3 is essential for root hair formation in Arabidopsis thaliana. *The Plant Cell*, *20*(1), 124-141.

Stepanova, A. N., Robertson-Hoyt, J., Yun, J., Benavente, L. M., Xie, D. Y., Doležal, K., ... & Alonso, J. M. (2008). TAA1-Mediated Auxin Biosynthesis Is Essential for Hormone Crosstalk and Plant Development. *Cell*, *133*(1), 177-191.

Steynen, Q. J., & Schultz, E. A. (2003). The FORKED genes are essential for distal vein meeting in Arabidopsis. *Development*, *130*(19), 4695-4708.

Stierhof, Y. D., & El Kasmi, F. (2010). Strategies to improve the antigenicity, ultrastructure preservation and visibility of trafficking compartments in Arabidopsis tissue. *European journal of cell biology*, *89*(2), 285-297.

Swarup, R., & Péret, B. (2012). AUX/LAX family of auxin influx carriers—an overview. *Frontiers in plant science*, *3*.

Swarup, R., Kramer, E. M., Perry, P., Knox, K., Leyser, H. O., Haseloff, J., & Bennett, M. J. (2005). Root gravitropism requires lateral root cap and epidermal cells for transport and response to a mobile auxin signal. *Nature cell biology*,*7* (11), 1057-1065.

Takai, Y., Sasaki, T. and Matozaki, T. (2001). Small GTP-binding proteins. Physiol. Rev. 81, 153–208.

Takei, K., & Haucke, V. (2001). Clathrin-mediated endocytosis: membrane factors pull the trigger. *Trends in cell biology*, *11*(9), 385-391.

Takhtajan, A. (2009). *Flowering plants*. Springer Science & Business Media.

Tanaka, H., Dhonukshe, P., Brewer, P. B., & Friml, J. (2006). Spatiotemporal asymmetric auxin distribution: a means to coordinate plant development. *Cellular and Molecular Life Sciences CMLS*, *63*(23), 2738-2754.

Tanaka, H., Kitakura, S., De Rycke, R., De Groodt, R., & Friml, J. (2009). Fluorescence imaging-based screen identifies ARF GEF component of early endosomal trafficking. *Current Biology*, *19*(5), 391-397.

Tanaka, H., Kitakura, S., Rakusová, H., Uemura, T., Feraru, M. I., De Rycke, R., & Friml, J. (2013). Cell polarity and patterning by PIN trafficking through early endosomal compartments in Arabidopsis thaliana.

Tanaka, H., Nodzyński, T., Kitakura, S., Feraru, M. I., Sasabe, M., Ishikawa, T., & Friml, J. (2014). BEX1/ARF1A1C is required for BFA-sensitive recycling of PIN auxin transporters and auxin-mediated development in Arabidopsis. *Plant and Cell Physiology*, *55*(4), 737-749.

Teh, O. K., & Moore, I. (2007). An ARF-GEF acting at the Golgi and in selective endocytosis in polarized plant cells. *Nature*, *448*(7152), 493-496.

Tejos, R., Sauer, M., Vanneste, S., Palacios-Gomez, M., Li, H., Heilmann, M., ... & Friml, J. (2014). Bipolar plasma membrane distribution of phosphoinositides and their requirement for auxin-mediated cell polarity and patterning in Arabidopsis. *The Plant Cell Online*, *26*(5), 2114-2128.

Thole, J. M., & Nielsen, E. (2008). Phosphoinositides in plants: novel functions in membrane trafficking. *Current opinion in plant biology*, *11*(6), 620-631.

Thomas, P. W., Woodward, F. I., & Quick, W. P. (2003). Systemic irradiance signalling in tobacco. *New phytologist*, *161*(1), 193-198.

Tse, Y. C., Mo, B., Hillmer, S., Zhao, M., Lo, S. W., Robinson, D. G., & Jiang, L. (2004). Identification of multivesicular bodies as prevacuolar compartments in Nicotiana tabacum BY-2 cells. *The Plant Cell Online*, *16*(3), 672-693.

Ueda, T., Uemura, T., Sato, M. H., & Nakano, A. (2004). Functional differentiation of endosomes in Arabidopsis cells. *The Plant Journal*, *40*(5), 783-789.

Ungermann, C., and Langosch, D. (2005) Functions of SNAREs in intracellular membrane fusion and lipid bilayer mixing. J. Cell Sci. 118, 3819-3828.

van Berkel, K., de Boer, R. J., Scheres, B., & ten Tusscher, K. (2013). Polar auxin transport: models and mechanisms. *Development*, *140*(11), 2253-2268.

Vanneste, S., & Friml, J. (2009). Auxin: a trigger for change in plant development. *Cell*, *136*(6), 1005-1016.

Vermeer, J. E., Thole, J. M., Goedhart, J., Nielsen, E., Munnik, T., & Gadella Jr, T. W. (2009). Imaging phosphatidylinositol 4-phosphate dynamics in living plant cells. *The Plant Journal*, *57*(2), 356-372.

Vernoud, V., Horton A. C., Yang, Z. and Nielsen, E. (2003). Analysis of the small GTPase gene superfamily of Arabidopsis. Plant Physiol. 131, 1191–1208.

Vieten, A., Sauer, M., Brewer, P. B., & Friml, J. (2007). Molecular and cellular aspects of auxin-transport-mediated development. *Trends in plant science*, *12*(4), 160-168.

Vieten, A., Vanneste, S., Wiśniewska, J., Benková, E., Benjamins, R., Beeckman, T., & Friml, J. (2005). Functional redundancy of PIN proteins is accompanied by auxin-dependent cross-regulation of PIN expression. *Development*, *132*(20), 4521-4531.

Viotti, C., Bubeck, J., Stierhof, Y. D., Krebs, M., Langhans, M., van den Berg, W., & Schumacher, K. (2010). Endocytic and secretory traffic in Arabidopsis merge in the trans-Golgi network/early endosome, an independent and highly dynamic organelle. *The Plant Cell Online*, *22*(4), 1344-1357.

Voeltz, G. K., Rolls, M. M., and Rapoport, T. A. (2002). Structural organization of the endoplasmic reticulum. EMBO Rep. 3, 944–950

Vogler, H., & Kuhlemeier, C. (2003). Simple hormones but complex signalling. *Current opinion in plant biology*, *6*(1), 51-56.

Wee, E.G., Sherrier, D.J., Prime, T. A., and Dupree, P. (1998). Targeting of active sialyltransferase to the plant Golgi apparatus. *Plant Cell* 10, 1759–1768.

Weijers, D., Schlereth, A., Ehrismann, J. S., Schwank, G., Kientz, M., & Jürgens, G. (2006). Auxin Triggers Transient Local Signaling for Cell Specification in Arabidopsis Embryogenesis. *Developmental cell*, *10*(2), 265-270.

Wenzel, C. L., Schuetz, M., Yu, Q., & Mattsson, J. (2007). Dynamics of MONOPTEROS and PIN-FORMED1 expression during leaf vein pattern formation in Arabidopsis thaliana. *The Plant Journal*, *49*(3), 387-398.

Whyte, J. R., & Munro, S. (2002). Vesicle tethering complexes in membrane traffic. *Journal of cell science*, *115*(13), 2627-2637.

Wiśniewska, J., Xu, J., Seifertová, D., Brewer, P. B., Růžička, K., Blilou, I., & Friml, J. (2006). Polar PIN localization directs auxin flow in plants. *Science*, *312*(5775), 883-883.

Woodward, A. W., & Bartel, B. (2005). Auxin: regulation, action, and interaction. *Annals of botany*, *95*(5), 707-735.

Xu, J., & Scheres, B. (2005). Dissection of Arabidopsis ADP-RIBOSYLATION FACTOR 1 function in epidermal cell polarity. *The Plant Cell Online*, *17*(2), 525-536.

Xue, H., Chen, X., & Mei, Y. (2009). Function and regulation of phospholipid signalling in plants. *Biochem. J*, *421*, 145-156.

Yamada, K., Fuji, K., Shimada, T., Nishimura, M., & Hara□Nishimura, I. (2005). Endosomal proteases facilitate the fusion of endosomes with vacuoles at the final step of the endocytotic pathway. *The Plant Journal*, *41*(6), 888-898.

Yorimitsu, T., Sato, K., & Takeuchi, M. (2014). Molecular mechanisms of Sar/Arf GTPases in vesicular trafficking in yeast and plants. *Frontiers in plant science*, *5*.

Zažímalová, E., Murphy, A. S., Yang, H., Hoyerová, K., & Hošek, P. (2010). Auxin transporters—why so many?. *Cold Spring Harbor perspectives in biology*, *2*(3), a001552.

Zhang, C., Halsey, L. E., & Szymanski, D. B. (2011). The development and geometry of shape change in Arabidopsis thaliana cotyledon pavement cells. *BMC plant biology*, *11*(1), 27.

Zhang, N., Zeng, L., Shan, H., & Ma, H. (2012). Highly conserved low-copy nuclear genes as effective markers for phylogenetic analyses in angiosperms.*New Phytologist*, *195*(4), 923-937.

Zhao, H., Michelot, A., Koskela, E. V., Tkach, V., Stamou, D., Drubin, D. G., & Lappalainen, P. (2013). Membrane-sculpting BAR domains generate stable lipid microdomains. *Cell reports*, *4*(6), 1213-1223.

Zhao, Y. (2012). Auxin biosynthesis: a simple two-step pathway converts tryptophan to indole-3-acetic acid in plants. *Molecular plant*, *5*(2), 334-338.

Zheng, H., Rowland, O., & Kunst, L. (2005). Disruptions of the Arabidopsis enoyl-CoA reductase gene reveal an essential role for very-long-chain fatty acid synthesis in cell expansion during plant morphogenesis. *The Plant Cell*,*17*(5), 1467-1481.

Zwieniecki, M. A., Melcher, P. J., Boyce, C. K., Sack, L., & Holbrook, N. M. (2002). Hydraulic architecture of leaf venation in Laurus nobilis L. *Plant, Cell & Environment*, *25*(11), 1445-1450.

APPENDIX I

2xYT Media (1 Litre)
16g Bacto Tryptone.
10g Bacto Yeast Extract.
5g NaCl.
LB Agar (1 Litre)
10g Bacto-tryptone
5g Yeast extract
10g NaCl
SOC Media (1 Litre)
20g Bacto Tryptone
5g Bacto Yeast Extract
2ml of 5M NaCl
2.5ml of 1M KCl
10ml of 1M $MgCl_2$
10ml of 1M $MgSO_4$
20ml of 1M glucose
YEP medium
10 g yeast extract
10 g Bacto peptone
5 g NaCl
TBF I Buffer (pH 5.8)
30 mM KOAc
100 mM RbCl
50 mM $MnCl_2$
10 mM $CaCl_2$
TBF II Buffer (pH 7.0)
10 mM MOPS
10 mM RbCl
75 mM $CaCl_2$
15 % Glycerol
Infiltration buffer for Agrobacterium injection
20 mM trisodiumphosphate
500 mM 2-(N-morpholino) ethanesulfonic acid
200 mM acetosyringone in dimethyl sulfoxide
5 mg glucose/ml
Total DNA extraction buffer
1 Volume DNA extraction buffer
1 Volume nucleic lysis buffer
0.4 Volume 5% Sarkosyl
38mg/10ml-Na Bisulfite